Analytical solutions for the evolution of current carrying cosmic strings

Francisco Pimenta
Mestrado em Astronomia e Astrofísica
Departamento de Física e Astronomia
2023

Orientador
Dr. Carlos J A P Martins
Investigador FCT, Centro de Astrofísica de Universidade do Porto

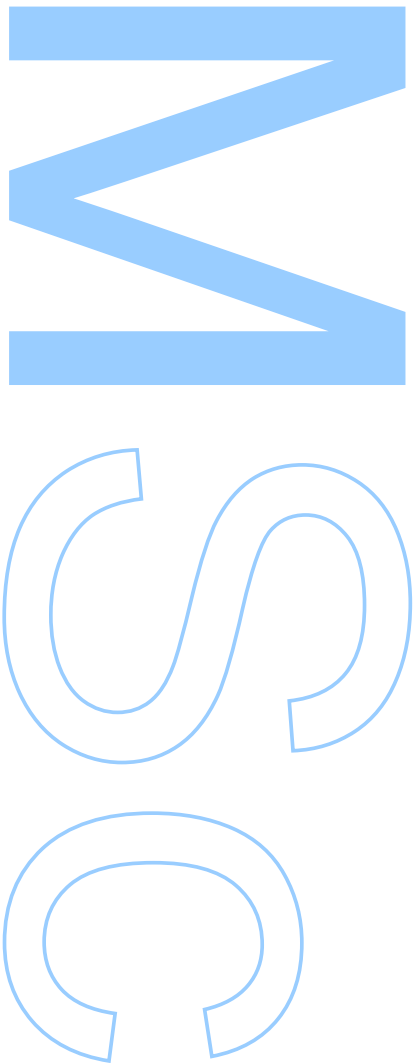

Acknowledgements

The journey that allowed to develop the work here presented would not have been possible without the support of all whose path I have been lucky enough to cross. In particular, I would like to express the most sincere acknowledgements:

- To Dr. Carlos Martins, for introducing me to the topological defects field, but mostly for his limitless patience and availability to discuss even the simplest of issues. Without his support this work would not be possible

- To José Ricardo Correia, for welcoming me into this research group and for the insightful discussions that we had. I would also like to acknowledge his role him producing the field theory numerical simulations that allowed to enrich this work.

- To all my colleagues and professors from the Masters degree in Astronomy and Astrophysics. All their teachings, in one way or another, certainly contributed to this thesis.

- Lastly, but certainly not least, to all my life long friends and family, and in particular to Ana Filipa, whose support is fundamental in every aspect of my life.

Abstract

Although cosmic strings arise naturally in both unifying theories and string theory inspired inflation models, no observational evidence of their existence has been found so far, implying that their study must rely on field theory numerical simulations. Since these simulations are still computationally demanding, alternative approaches based on analytical models that are able to characterise the evolution of the network based on a reduced number of macroscopic parameters are often used, with particular relevance for the velocity-dependent one scale model (VOS). Originally developed to explain the evolution of the simplest networks, its canonical version has already been extended to allow for strings with additional degrees of freedom, as small scale structure or charges and currents. In this work, its generalised version for current carrying strings is analysed and the compatible scaling solutions characterised. In particular, the expansion rates that allow for different qualitative behaviour of the strings charge and/or current are identified, as well as the impact on this evolution of the existence of energy and/or charge loss mechanisms, here included as model parameters. The identified solutions indicate that both charges and currents are more easily preserved for slower expansion rates, but full scaling can occur for specific values of the expansion rate. Finally, the analytical solutions predictions are compared with numerical simulations for different expansion rates. Although the qualitative behaviour is compatible with the analytical expectations, it was found that the details are not. In particular, the numerical simulations seem to suggest that the networks are loosing charge faster then expected and/or the strings velocity is higher than anticipated. It is left for future works to understand if this is due to a poor behaviour of some of the estimators associated with the numerical simulations, or if some more fundamental assumption of the analytical model is not valid for current-carrying strings.

Keywords: Cosmic strings, topological defects, analytical solutions, Cosmology

Resumo

Apesar de cordas cósmicas serem uma previsão de várias teorias de unificação ou modelos inflacionários baseados em teoria das cordas, não foram detetadas até hoje, pelo que o seu estudo depende de simulações numéricas avançadas. Sendo estas simulações computacionalmente exigentes, modelos analíticos em que a evolução da rede é caracterizada a partir de um número reduzido de parâmetros macroscópicos são comummente utilizados, e em particular o modelo *Velocity-dependent one scale* (VOS). Apesar de ter sido originalmente desenvolvido para estudar a evolução dos casos de redes de cordas mais simples. a sua versão canónica foi, entretanto, estendida para acomodar modelos de cordas com graus de liberdade adicionais, como estrutura de pequena escala ou cargas e correntes. Neste trabalho, é analisada a versão deste modelo desenvolvida para cordas com cargas generalizadas e as soluções em que as diferentes quantidades evoluem de acordo com leis bem definidas (*scaling*) caracterizadas. Em particular, as taxas de expansão que permitem diferentes comportamentos de um ponto vista qualitativo da carga e/ou corrente nas cordas são identificados. bem como o impacto da possível existência de mecanismos adicionais de perda de energia e/ou carga, aqui contemplados como parâmetros do modelo. As soluções encontradas sugerem que tanto cargas como correntes são mais facilmente conservadas para taxas de expansão mais baixas, apesar de regimes de *scaling* serem possíveis para valores específicos desta quantidade. Finalmente, as soluções analíticas são comparadas com os resultados de simulações numéricas para diferentes taxas de expansão. Apesar do comportamento ser qualitativamente semelhante às previsões analíticas, os seus detalhes não o são. Em particular, as simulações estudadas sugerem que as redes perdem carga mais rapidamente do que antecipado e/ou a velocidade característica das cordas é maior do que esperado. É deixado para trabalhos futuros perceber se estas diferenças se devem aos estimadores utilizados nas simulações numéricas, ou se alguma hipótese mais fundamental do modelo analítico não é válida para cordas cósmicas com cargas.

Palavras-chave: Cordas cósmicas, defeitos topológicos, soluções analíticas, Cosmologia

Contents

List of Figures

Chapter 1

Introduction

1.1 Modern Cosmology: the theoretical minimum

In the XXth century the physicist Lev Landau developed an exam based on everything a student was supposed to know in order to work with him called The Theoretical Minimum. Although the definition was slightly relaxed, this concept led to a series of courses, from Classical Mechanics to General Relativity and Quantum Mechanics, lectured by Stanford's Professor Leonard Susskind. In his idea, the theoretical minimum was "just what you need to know in order to proceed to the next level" [1]. Following the latter interpretation, our current understanding of the universe evolution in the context of modern Cosmology is mostly based on Einstein field equations, that can be expressed as: *

$$G_{\mu\nu} = R_{\mu\nu} - \frac{1}{2} g_{\mu\nu} R = 8\pi G T_{\mu\nu} \tag{1.1}$$

where $R_{\mu\nu}$ and R are the Ricci tensor and scalar (or scalar curvature) and can be computed for the metric tensor and its derivatives alone, here taken to be the Friedmann-Lemaître-Robertson-Walker (FLRW) metric, that may be written in spatial spherical coordinates as:

$$\begin{aligned} ds^2 &= -dt^2 + a(t)^2 \left[\frac{1}{1-kr^2} dr^2 + r^2 \left(d\theta^2 + \sin^2\theta d\phi^2 \right) \right] = \\ &= a(\tau)^2 \left[-d\tau^2 + \frac{1}{1-kr^2} dr^2 + r^2 \left(d\theta^2 + \sin^2\theta d\phi^2 \right) \right] \end{aligned} \tag{1.2}$$

*Here, for convenience, it has been set $c = 1$.

where $T_{\mu\nu}$ is the energy momentum tensor*, a is the scale factor, and t and τ are the cosmic and conformal time, respectively, that are related by:

$$dt = ad\tau \tag{1.3}$$

The curvature parameter, k, defines the nature of the space-time structure as flat ($k = 0$), hyperbolic/open ($k = -1$) or spherical/closed ($k = +1$).

Under this metric choice, the non vanishing components of the Einstein tensor can now be obtained as †:

$$G_{tt} = -3\frac{\ddot{a}}{a} + 3\left[\frac{\ddot{a}}{a} + \frac{\dot{a}^2 + k}{a^2}\right] = 3\frac{\dot{a}^2 + k}{a^2} \tag{1.4a}$$

$$G_{ij} = -\left(2\frac{\ddot{a}}{a} + \frac{\dot{a}^2 + k}{a^2}\right) a^2\gamma_{ij} \tag{1.4b}$$

where γ_{ij} is defined from the metric as:

$$\gamma_{ij}dx^i dx^j = \frac{1}{1 - kr^2}dr^2 + r^2\left(d\theta^2 + \sin^2\theta d\phi^2\right) \tag{1.5}$$

Making now use of the metric tensor for a perfect fluid ($T_{00} = T^{00} = \rho$ and $T_{ij} = pg_{ij} = pa^2\gamma_{ij}$), the time component of the Einstein equation and any of the spatial ones provide:

$$3\frac{\dot{a}^2 + k}{a^2} = 8\pi G\rho + \Lambda \longrightarrow \frac{\dot{a}^2 + k}{a^2} = \frac{8\pi G\rho + \Lambda}{3} \tag{1.6a}$$

$$-2\frac{\ddot{a}}{a} - \frac{\dot{a}^2 + k}{a^2} = 8\pi Gp - \Lambda \tag{1.6b}$$

where the cosmological constant as been made explicit and that are known as the **Friedmann equations**. Multiplying Equation 1.6b by 3 and adding Equation 1.6a, the **Raychaudhury equation** is finally obtained:

$$-6\frac{\ddot{a}}{a} = 8\pi G \cdot 3p - 2\Lambda + 8\pi G\rho \longrightarrow 3\frac{\ddot{a}}{a} = \Lambda - 4\pi G\left(\rho + 3p\right) \tag{1.7}$$

It should be noted that the relation between pressure (p) and density (ρ) can be written as an equation of state that differs for different components (non relativistic, relativistic or dark energy), but that may generally be written as:

$$p = wu = w\rho \tag{1.8}$$

*For convenience, the energy momentum tensor includes the effect of a cosmological constant or any other form of dark energy.

†The dot represents derivatives with respect to the physical time t, while the prime will represent derivatives with respect to conformal time τ.

where u is the energy density of the fluid. Assuming an adiabatic expansion of the universe, the first law of thermodynamics imply that:

$$dU = -dW \longrightarrow \frac{dU}{dt} = -p\frac{dV}{dt} \tag{1.9}$$

or, expressing the function from the scale factor, the fluid equation finally emerges:

$$\frac{d\left(a^3(t)\rho\right)}{dt} = -p\frac{d\left(a^3(t)\right)}{dt} \tag{1.10}$$

Substituting the equation of state in the form presented in Equation 1.8, and assuming w to be constant, results in the well known conservation law:

$$a^{3(1+w)}\rho = \rho_0 \tag{1.11}$$

where the equality follows from setting $a_0 = a(t=0) = 1$. It should be noted that:

1. For non-relativistic matter ($p \ll \rho$), $w = 0$ and the familiar mass conservation equation $a^3\rho = \rho_0$ is recovered, or $\rho \propto a^{-3}$.

2. For photons, as $p = u/3$, $w = 1/3$ and so $a^4\rho = \rho_0$ or, equivalently, $\rho \propto a^{-4}$

3. For the cosmological constant, and expressing $\rho_\Lambda = \Lambda/(8\pi G) = \rho_{\Lambda,0} = \text{constant}$, the equation of state is equivalent to $p_\lambda = -\rho_\Lambda$, or $w = -1$.

The contribution of different components to the right hand side of the Einstein equation can be explicitly written as the total pressure and densities $p = \sum_s p_s$ and $\rho = \sum_s \rho_s$ where the index s identifies the different types of particles, each with its own equation of state.

Finally, it is particularly useful to introduce the Hubble parameter, defined as $H = \dot{a}/a$, and the density parameter $\Omega_s = \rho_s/\rho_c$, being ρ_c the critical density associated to a flat universe. Here, the Friedmann equation can be alternatively expressed as:

$$\frac{H^2(t)}{H_0^2} = \sum_s \Omega_{s,0} a(t)^{-3(1+\omega_s)} \tag{1.12}$$

where the index 0 stands for the value of the quantities evaluated today. The properties expressed above combined imply that for very early times (small scale factor) radiation dominates leading to the so called **radiation era**, meaning:

$$H \propto a^{-2} \longrightarrow a \propto t^{1/2} \propto \tau \tag{1.13}$$

On the other end, for a sufficiently large scale factor, the dark energy will inevitably dominate, as it already does, leading to the **Λ era**:

$$H \propto \sqrt{\Omega_\lambda} \tag{1.14}$$

and the universe expands exponentially. Finally, and in between these two scenarios, non relativistic matter (both baryonic and dark) will govern the expansion of the universe during the **matter era**, in which case:

$$H \propto a^{-3/2} \longrightarrow a \propto t^{2/3} \propto \tau^2 \tag{1.15}$$

Although the theoretical framework of General Relativity applied to the universe evolution just described provides an unmatched level of understanding, there are still relevant aspects that are not fully understood.

Firstly, recent observations of high redshift have found that the universe is accelerating its expansion, implying that the cosmological constant must be positive and recent data from the Planck mission [2] constrain it to be such that $\Omega_\Lambda = 0.691 \pm 0.006$. Interestingly enough, this constant was not only firstly introduced by Einstein itself in order to make the universe stable, but later removed and considered as its "greatest mistake". However, the last word is always reserved for Nature itself and currently a non-vanishing value is accepted, in what is commonly referred to as dark energy.

On the other hand, observations of the rotation curve of galaxies reveal that the outer bodies exhibit higher velocities than the ones that could be foreseen from the observed matter in the galaxy. In order to keep the framework of General Relativity, it has been suggested that an important part of non-relativistic matter is in the form of what is commonly referred to, in the absence of a better name, as dark matter, as it hardly interacts, if at all, with the remaining forms of matter, expect for its gravitational influence. Recently additional evidences for this proposal have been found, in particular in the bullet cluster, where the mass distribution based on gravitational lensing and X-ray emissions can be seen to present different distributions [3, 4], as represented in Figure 1.1.

Finally, the Friedmann equation can be alternatively written as:

$$H^2 \left[1 - \frac{\rho}{\frac{3H^2}{8\pi G}} - \frac{\Lambda}{3H^2} \right] a^2 = H^2 \left[1 - \frac{\rho + \frac{\Lambda}{8\pi G}}{\frac{3H^2}{8\pi G}} \right] a^2 = -k \tag{1.16}$$

where our claim that the cosmological constant can be included in the stree-energy tensor becomes evident by defining the equivalent mass density for the cosmological constant as

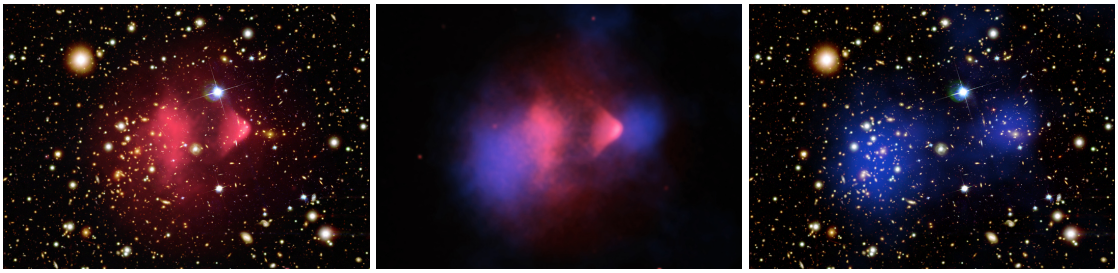

FIGURE 1.1: Identification of matter distribution in the bullet cluster from different sources. On the left panel, the X-ray emission associated with hot gas is superimposed on the visible matter. On the centre panel, the same X-ray emission is presented in pink, with the mass distribution based on gravitational lensing is coloured in blue. On the right panel, the visible matter is superimpose on the gravitational lensing estimates (Source: Chandra X-Ray Observatory: 1E 0657-56)

$\rho_\Lambda = \frac{\Lambda}{3H^2}$, in which case the expression above can be written as:

$$H^2 \left[1 - \frac{\rho + \rho_\Lambda}{\rho_c}\right] a^2 = H^2 \left[1 - \Omega_m - \Omega_\Lambda\right] a^2 = \left[1 - \Omega_m - \Omega_\Lambda\right] \dot{a}^2 = -k \tag{1.17}$$

where the critical density ρ_c has been defined and the density parameter Ω_i introduced as the ratio between the equivalent density and the critical density. From the expression above, it becomes clear that for a total density equal to the critical value, the universe if flat ($k = 0$). More importantly, since the right hand side is constant, so must be the left hand side. This apparently innocuous claim implies that to the universe being almost flat today (with maximum deviations at the percent level), it must have been much more so in the very early times. If this is not clear, it should be noted that for either a radiation or matter dominated expanding universe, $a(t)$ scales as t^λ, with $\lambda < 1$, implying that, for very early times, $\dot{a} \gg 1$ and the deviation from flatness (the term $1 - \Omega_m - \Omega_\Lambda$ on the left) must be very small. This is what is commonly identified as the **Flatness problem**. Additionally, the cosmic microwave background homogeneity at distances greater than allowed by causality is also not compatible with an universe that has been dominated by matter, and radiation before it, leading to the **Horizon problem**. These issues lead to the proposal of the inflationary cosmology scenario, where the universe experiences an exponential growth at the very early stages, before the onset of the radiation dominated epoch. It should be noted that a cosmological constant type of evolution can not be used to explain such epoch, although it also predicts an exponential expansion, since in this case it would not come to a stop. Although the details of inflation will not be addressed here, it should be mentioned that is also solves the so-called **Monopole problem**, by wiping out any traces of the magnetic monopoles that soon would come to dominate the universe expansion, which is strongly

contradicted by observations. Magnetic monopoles are the first example of a topological defect, although not the one of interest, introduced here and would have formed in many Grand Unified Theories (GUT). As will become clear, the formation of topological defects is a general prediction of any GUT where the universe experiences a phase transition, although no observational evidence exists so far.

1.2 Thesis objectives

Cosmic strings arise naturally in both unifying theories and superstring inspired inflation models. In the latter case, fundamental superstrings produced in the very early universe may have stretched to macroscopic scales, in which case they are known as cosmic superstrings. To better understand the underlying physical mechanisms and eventually constrain high-resolution experimental data defect fingerprints, analytical developments are needed. In this work, we have studied the asymptotic solutions of the generalised velocity-dependent one-scale model for current-carrying strings. This analysis, and the interpretation of the physical mechanisms that govern the evolution of such networks, also reveal the expansion rates that are compatible with each solution branch, namely under which conditions it would be possible to have charge and current solutions that are not erased through the universe expansion. Additionally, it is also important to understand, if a detection is made, what are the particular aspects of current carrying objects with respect to the remaining ones.

1.3 Organisation of the thesis

To answer the objectives above, this thesis is organised as follows. In Chapter 2 is discussed the theoretical background that justifies the quest for topological defects, in general, and strings, in particular, in a cosmological context. The discussion starts with some toy models that illustrate the formation of such elements and how they may arise in an expanding universe. Once this formation is properly understood, their evolution is studied, firstly from a microscopical point of view, where the field equations evolution are derived, and then characterised as a function of some macroscopic properties of the full network, namely energy, velocity, charge and current. Although this last step does simplify the problem at hand, the system of equations obtained is still mostly intractable for analytical purposes.

To solve this issue, Chapter 2 ends with the introduction of the scaling solutions, that will be characterised for the remaining of the work.

Having introduced the needed concepts, the solutions to the full system of equations, constrained to the power law behaviour discussed in Chapter 2, are presented. It should be noted, however, that not every single solution to the equations, from a mathematical point of view, is expected to be realisable due to additional, physics motivated, constraints (for instance, solutions where the network velocity equals the speed of light may be possible in purely mathematical grounds, but are clearly excluded as possible scaling solutions in the physical universe as we understand it today). To clearly separate between the two types of solutions, firstly the physical ones are presented in Chapter 3, while the purely mathematical ones are listed in Appendix A, with considerable less detail and discussion than their physical counterparts.

Having the solutions identified in analytical terms, it was considered relevant to make some preliminary comparison with full field numerical simulations. In Chapter 4 different approaches are used to try to quantify the evolution of the simulated network and use the constrained values to identify the branch of the analytical solutions that best explains this data. In particular, some introductory aspects related to Bayesian inference and Monte Carlo Markov Chain (MCMC) methods is provided.

Finally, Chapter 5 summarises the key findings of this work, as well as identifies some relevant limitations, proposing some research features to be further developed in future works.

Chapter 2

Topological defects

2.1 Introduction

Before proceeding to the possible evolutionary regimes of cosmic strings networks, it is fundamental to understand how these entities may have formed in a cosmological context and what equations govern their evolution. For that purpose, this Chapter starts by introducing some toy models where topological defects are formed spontaneously, that are then reinterpreted as oversimplifications of the actual scenario encountered in a cosmological framework. Here, also the observational implications of such a network are briefly presented.

After that, the equations that govern the simplest strings network evolution are derived and then extended to the more general cases, in particular to the current-carrying cosmic strings. This Chapter ends with the definition of the scaling solutions that this thesis aims at characterising, and that will be further explored in Chapter 3 and Appendix A.

2.2 Defects formation

2.2.1 Spontaneous symmetry breaking

The formation of topological defects is well established in condensed matter systems and clearly associated with some symmetry breaking transition that originates a non-trivial set of degenerate ground states, that may differ between different regions of the system. Although they are purely hypothetical in a cosmological context, it is thought that the different phase transitions that are expected in the framework of the current cosmological evolutionary model will also lead to formation of these type of structures. To gain some

additional insight into these processes, a simple toy model is useful, and in particular the one firstly studied by Goldstone [5], defined for a real field by the classical Lagrangian density:

$$\mathcal{L} = \frac{1}{2}\left(\partial_\mu \phi\right)^2 - \frac{1}{4}\lambda\left(\phi^2 - \eta^2\right)^2 \tag{2.1}$$

The Euler-Lagrange equations for ϕ can be obtained by simple variational principles and read:

$$\frac{\partial \mathcal{L}}{\partial \phi} - \partial_\mu\left(\frac{\partial \mathcal{L}}{\partial\left(\partial_\mu \phi\right)}\right) = \partial_\mu \partial^\mu \phi + \phi\lambda\left(\phi^2 - \eta^2\right) = 0 \tag{2.2}$$

The model just described can be used to better understand the formation of topological defects. From Equation 2.1, it is clear that true vacuum of the theory is associated with $|\phi| = \eta$, but there is another, unstable, equilibrium position for $\eta = 0$. It should be noted that the Lagrangian symmetry of the latter does not exist on the former. Expanding the potential around the $\phi = 0$ state leads to:

$$V(\phi = 0 + \delta\phi) = \frac{1}{4}\lambda\left(\delta\phi^2 - \eta^2\right)^2 \approx -\frac{1}{2}\lambda\delta\phi^2\eta^2 + C + \mathcal{O}(\delta\phi^4) \tag{2.3}$$

where C is a constant and the negative mass term is compatible with the previous identified instability of this state. On the other hand, to study the behaviour around the true vacuum state, it is convenient to extend the model above to allow for a complex scalar field, while still writing the perturbed state around a purely real state $\phi = \eta$:

$$\phi = \eta + \frac{1}{\sqrt{2}}\left(\phi_1 + i\phi_2\right) \tag{2.4}$$

Expanding the potential around it, now leads to:

$$V(\phi = \eta + \delta\phi) = \frac{1}{4}\lambda\left(\phi\phi^* - \eta^2\right)^2 = \frac{1}{2}\lambda\eta^2\phi_1^2 + V_{\text{int}} \tag{2.5}$$

where we can see that ϕ_1 can be interpreted as a massive particle with mas $m = \sqrt{\lambda}\eta$, while ϕ_2 is associated with a massless one. The physical meaning of such perturbations, and the corresponding mass/massless dichotomy can be made more clear by representing the potential in the plane defined by the real and imaginary parts of ϕ, as in Figure 2.1. Here, it becomes clear that ϕ_1 is associated with radial oscillations, and hence the positive mass term, while ϕ_2 is associated with oscillations over the phase angle.

Let now the field configuration at a given time be such that this unstable condition holds

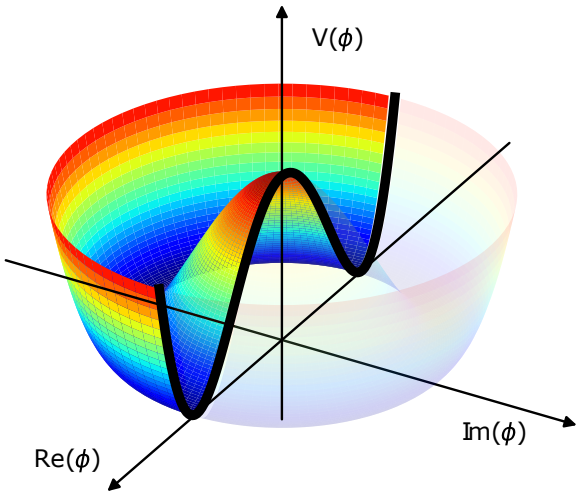

FIGURE 2.1: Typical mexican hat potential from the Goldstone model.

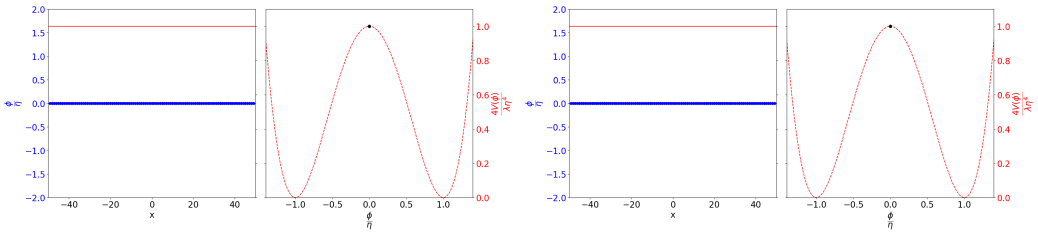

FIGURE 2.2: Time evolution of the field starting from the unstable condition for a single perturbation (on the left) or two independent perturbations (on the right).

and recover the real scalar field model. If a single point in spacetime is then perturbed, it will evolve towards its stable, true vacuum expected value $\phi = \eta e^{i\theta} = \pm\eta$, and this transition is then propagated to the all field, and no defect is formed. However, there is something in the reasoning above that makes us pause: what would be the effect of perturbations at different regions in space? In fact, the different regions will, in a sense, make an arbitrary choice of the field phase θ, each propagating with a finite speed. When the different regions meet, the only possibility to restore the field continuity is to have a point where $\phi = 0$, and the unstable, symmetric, state is recovered, with the associated energy density that is now trapped and a topological defect is formed. An example of the field evolution for a non stationary initial configuration obtained from a simple numerical evaluation of the field equation of motion is presented in Figure 2.2, while the overall field value as a function of time and position is represented in Figure 2.3.

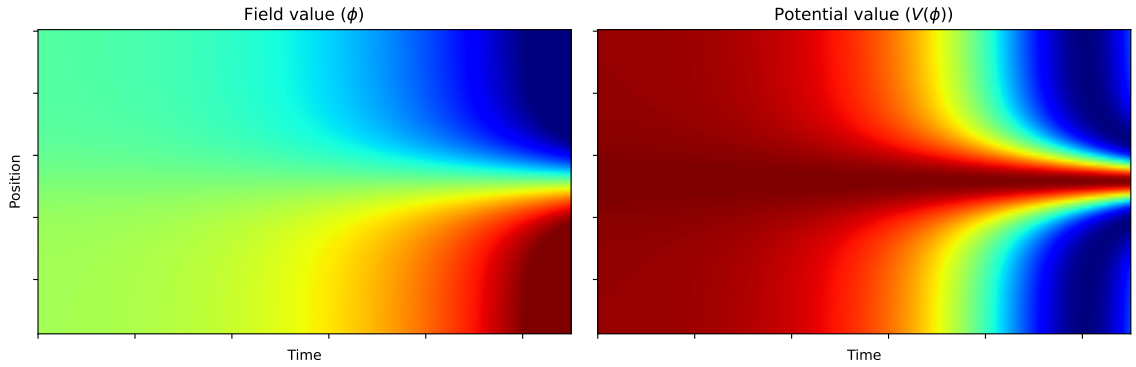

a

FIGURE 2.3: Full evolutionary portrait of the field value and corresponding potential for the case where a topological defect is formed.

2.2.2 Current carrying strings

If in the previous section attention was given to local symmetry breaking models, here local, gauge symmetries will be briefly analysed based on the abelian-Higgs model [6], since they are at the core of current carrying and superconducting strings. Following the same symmetry breaking arguments above, another 2-scalar complex field can be shown to give rise to superconducting solutions. Let now the Lagrangian be given by [7]:

$$\mathcal{L} = \left|\tilde{D}_\mu \phi\right|^2 + \left|D_\mu \sigma\right|^2 - \frac{1}{4}\tilde{F}_{\mu\nu}\tilde{F}^{\mu\nu} - \frac{1}{4}F_{\mu\nu}F^{\mu\nu} - V(\phi,\sigma) \tag{2.6}$$

where $\tilde{D}_\mu = \partial_\mu - ig\tilde{A}_\mu$ and $D_\mu = \partial_\mu - ieA_\mu$ are associated with the complex scalar fields ϕ and σ, respectively, and the potential takes the form:

$$V(\phi,\sigma) = \frac{1}{4}\lambda_\phi\left(|\phi|^2 - \eta_\phi^2\right)^2 + \frac{1}{4}\lambda_\sigma\left(|\sigma|^2 - \eta_\sigma^2\right)^2 + \beta\,|\phi|^2\,|\sigma|^2 \tag{2.7}$$

A representation of this potential for different values of β is plotted in Figure 2.4. It can be seen that, depending on the values of the coupling term β, both symmetries may, or may not, be broken simultaneously. In the case where the ϕ field symmetry is broken, this field will acquire its true vacuum value outside the string, and the σ field remains a symmetry of the theory. Inside the string, however, things are drastically different, since here $\phi = 0$ and the potential reduces to:

$$V(\sigma;\phi=0) = \frac{1}{4}\lambda_\phi\eta_\phi^4 + \frac{1}{4}\lambda_\sigma\left(|\sigma|^2 - \eta_\sigma^2\right)^2 \tag{2.8}$$

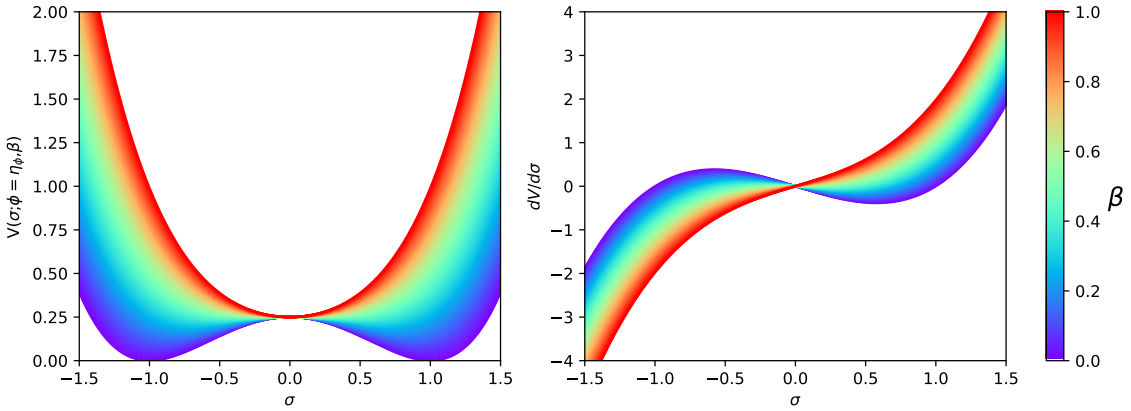

FIGURE 2.4: Potential and its derivative with respect to the field value characterisation for different values of β.

which reaches a minimum for $|\sigma| = |\eta| \neq 0$ and the σ field can **condensate** on the string core. For this field there is a locally conserved current given by:

$$\mathcal{J}_\mu = eJ_u = 2e\Im\left[\sigma^*\left(\partial_\mu - ieA_\mu\right)\sigma\right] = ie\left(\sigma^* D_\mu\sigma - \sigma D_\mu^*\sigma^*\right) \tag{2.9}$$

Since outside the string core $\sigma \to 0$, then its current is confined to the string itself. In particular, and taking an ansatz for the field configuration as $\sigma = \eta_\sigma e^{-i\alpha}$, where α is now an internal degree of freedom of the broken symmetry state, the total current can be easily identified as:

$$\mathcal{J}_\mu = 2e\eta_\sigma^2\left(\partial_\mu\alpha + eA_\mu\right) \tag{2.10}$$

while the corresponding charge may now be obtained as:

$$Q = \int dx^3\mathcal{J}_0 \tag{2.11}$$

Let now, for convenience, the string lay along the z axis. Since the field vanishes at scales larger than the condensate width, we must have $\alpha = \alpha(z)$ and the current above can be integrated across the string cross section to yield:

$$J = \int \mathcal{J}_z dxdy = 2e\left(\partial_z\alpha + eA_z\right)\int \eta_\sigma^2 dxdy \tag{2.12}$$

In particular, it should be noted that if eA_μ dominates the expression above, the current evolution is given by:

$$\partial_t J \approx \partial_t A_z\left(2e^2\int \eta_\sigma^2 dxdy\right) \tag{2.13}$$

which can be seen to be the London equations for the relation between a superconductor current and the external electric fields [8]. In fact, and taking derivatives in both sides and making use of Maxwell equations leads to:

$$\partial_t J \approx E_z \tag{2.14}$$

For a constant external electric the current grows linearly, which although is the expected behaviour for a superconductor [9], it is drastically different from the one encountered in a typical conducting wire, where Ohm's law would dictate:

$$J \propto E_z \tag{2.15}$$

In particular, it should be noted that Equation 2.14 allows for the onset of persistent currents, even in the absence of any applied external fields.

2.2.3 Phase transitions in Cosmology

If in the last section a reasonable mechanism to generate topological defects based on spontaneous symmetry breaking processes has been presented, its existence in a cosmological context is still unclear. In fact, the discussions above have implicitly relied on two major assumptions or conditions: if on one hand it has been required of the potential to have a configuration that would allow for non symmetric stable states, it has also been assumed that the field configuration had somehow started from the unstable symmetric configuration, and this may be easily questionable as a valid premise. The question that should be answered is whether cosmological evolution would be able to replicate these conditions.

To see how this may happen, its simpler to consider once more the Goldstone model previously introduced to illustrate the formation of defects. In this case, it can be shown that the effective potential at high temperatures is given by [10]:

$$V_{\text{eff}}(\phi, T) = V(\phi) + \frac{\lambda + 3e^2}{12} T^2 |\phi|^2 - \frac{2\pi}{45} T^4 = V(\phi) + \frac{\lambda + 3e^2}{12} T^2 |\phi|^2 - \frac{2\pi}{45} T^4 \tag{2.16}$$

with $e = 0$ and where $V(\phi)$ is the mexican hat potential for a single field represented in Figure 2.1. The expression above may be conveniently rewritten as:

$$V_{\text{eff}}(\phi, T) = \underbrace{\frac{\lambda}{12}\left(T^2 - 6\eta^2\right)}_{m^2(T;\lambda,\eta)} |\phi|^2 + \frac{\lambda}{4} |\phi|^4 + C(T;\lambda,\eta) \tag{2.17}$$

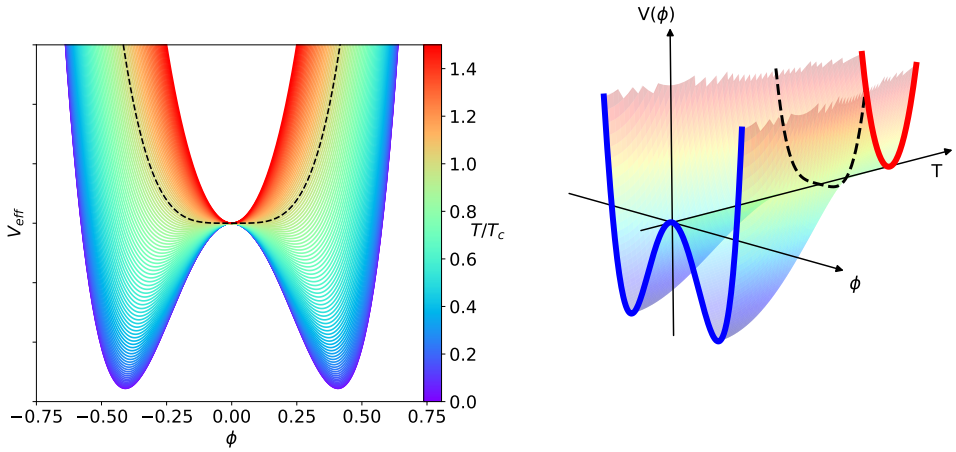

FIGURE 2.5: The effective potential evolution for different values of temperature.

where a temperature-dependent mass term has been defined as $m^2(T)$ and all the terms that do not depend on ϕ have been encapsulated in the constant C. The shape of this potential is presented in Figure 2.5 for different values of T. As can be seen, there is a critical temperature,obtained for $T = T_c = \sqrt{6}\eta$ (the black dashed lines on both plots) above which the potential minimum is found for $\phi = 0$. For $T < T_c$, however, a ground state with non-vanishing expected value is favoured and the symmetry is broken. The evident similarities between the plots in Figure 2.5 and in Figure 2.4 make the transposition of the discussion regarding topological defects formation there straightforward and hence a viable mechanism for the formation of these type of structures in a cosmological context is obtained.

2.3 Strings evolution

If in the previous section attention was dedicated to present the fundamental equations for cosmological evolution, strings themselves have not yet been properly considered. Here, this discussion will be made under the assumption that the string thickness is much smaller than its length, allowing to effectively treat the defect as a one-dimensional object whose motion can be written as:

$$x^\mu = x^\mu(\sigma^a) \tag{2.18}$$

where x^μ are the spacetime coordinates of the worldsheet while σ^a for $a = \{0, 1\}$ define the parameterisation on the worldsheet. The invariant spacetime interval may now be written as:

$$\mathrm{d}s^2 = g_{\mu\nu}\mathrm{d}x^\mu \mathrm{d}x^\nu = g_{\mu\nu}\partial_a x^\mu \partial_b x^\nu \mathrm{d}\sigma^a \mathrm{d}\sigma^b = g_{\mu\nu} x^\mu_{,a} x^\nu_{,b} \mathrm{d}\sigma^a \mathrm{d}\sigma^b = \gamma_{ab}\sigma^a \mathrm{d}\sigma^b \tag{2.19}$$

where the last equality defines the induced metric on the worldsheet.

As a point-like object trajectory over an arbitrary space-time is usually referred to as its wordline, a string sweeps a worldsheet, leading to an action of the form:

$$S = \int \mathcal{L}\sqrt{-\gamma}\mathrm{d}\sigma^2 \tag{2.20}$$

where γ is the determinant of the induced metric. Noting that the Lagrangian, $\mathcal{L}$, has units of mass squared, it may expanded in terms of the string curvature, κ, as:

$$\mathcal{L} = -\mu + \alpha\kappa + \beta\frac{\kappa^2}{\mu} + \ldots \tag{2.21}$$

where α and β are two numerical coefficients. Assuming the string curvature radius to be much larger than its thickness, which is equivalent to take the first term alone from the expansion presented in Equation 2.21, the Nambu-Goto action is recovered:

$$S = -\mu \int \sqrt{-\gamma}\mathrm{d}\sigma^2 \tag{2.22}$$

Having the Nambu-Goto action presented, the equations of motion follow directly by making it stationary against arbitrary variations of its coordinates:

$$x^{\mu;a}_{,a} + \Gamma^\mu_{\nu\sigma}\gamma^{ab}x^\nu_{,a}x^\sigma_{,b} = \frac{1}{\sqrt{-\gamma}}\partial_a\left(\sqrt{-\gamma}\gamma^{ab}x^\mu_{,b}\right) + \Gamma^\mu_{\nu\sigma}\gamma^{ab}x^\nu_{,a}x^\sigma_{,b} = 0 \tag{2.23}$$

2.3.1 Flat spacetime

The general equation of motion expressed in Equation 2.23 when applied to flat spacetime is significantly simplified, by the replacements $g_{\mu\nu} \to \eta_{\mu\nu}$ and $\Gamma^{\mu}_{\nu\sigma} = 0$. There is however still significant freedom in them, due to the action reparameterisation invariance that may be removed by making a particular identification of the worldsheet variables with the spacetime ones or, alternatively, by two gauge conditions. A particular convenient choice is to describe the string motion as a 3-vector, $\mathbf{x} = \mathbf{x}(t, \zeta)$, being t time and ζ a space like parameter, which can be made by using the conditions:

$$\dot{\mathbf{x}} \cdot \mathbf{x}' = 0 \tag{2.24a}$$

$$\dot{\mathbf{x}}^2 + \mathbf{x}'^2 = 1 \tag{2.24b}$$

$$\ddot{\mathbf{x}} - \mathbf{x}'' = 0 \tag{2.24c}$$

This particular choice is usually referred to as the transverse gauge, since as may become clear from Equation 2.24a, $\dot{\mathbf{x}}$ can now be interpreted as the transverse velocity as it is orthogonal to the string itself. On the other hand, Equation 2.24b can be used to write:

$$d\zeta = \frac{1}{\sqrt{1 - \dot{\mathbf{x}}^2}} |d\mathbf{x}| \tag{2.25}$$

It may now be seen that, under this particular gauge choice, the spacetime parameter that parameterises the string worldsheet can be understood as proportional to the energy per unit length of the string.

2.3.2 Curved spacetime

In a curved spacetime and considering an expanding universe described by the FLRW metric a particular convenient gauge choice, and perhaps the most natural one could make, is to identify the string spacetime parameter with the conformal time τ. Keeping the same spirit as before, a transversal velocity can still be identified by requiring:

$$\dot{\mathbf{x}} \cdot \mathbf{x}' = \mathbf{0} \tag{2.26}$$

where now dot and prime are derivatives with respect to conformal time and the spacelike parameter ζ. The equations of motion now read [11]:

$$\ddot{\mathbf{x}} + 2\frac{\dot{a}}{a}\left(1 - \dot{\mathbf{x}}^2\right)\dot{\mathbf{x}} = \frac{1}{\epsilon}\partial_\zeta\left(\frac{1}{\epsilon}\mathbf{x}'\right) \tag{2.27}$$

where ϵ can still be identified as an energy per unit length of the string defined as:

$$\epsilon \equiv \sqrt{\frac{\mathbf{x}'^2}{1-\dot{\mathbf{x}}^2}} \tag{2.28}$$

Note that from the evolution in a flat spacetime, the quantity above is unity. Combined with the gauge condition expressed by Equation 2.26, it can be shown that the time evolution of ϵ is governed by:

$$\dot{\epsilon} = -2\mathcal{H}\epsilon\dot{\mathbf{x}}^2 \tag{2.29}$$

where the conformal Hubble parameter $\mathcal{H} = \dot{a}/a$ has been introduced. The string total energy is given by:

$$E = a(\tau)\mu \int \epsilon \mathrm{d}\zeta \tag{2.30}$$

and its evolution dictated by:

$$\dot{E} = \dot{a}\mu \int \epsilon \mathrm{d}\zeta + a\mu \int \dot{\epsilon}\mathrm{d}\zeta = \mathcal{H}E - 2\mathcal{H}a\mu \int \epsilon\dot{\mathbf{x}}^2\mathrm{d}\zeta = \mathcal{H}E\left(1 - 2\left\langle v^2\right\rangle\right) \tag{2.31}$$

where the root mean square velocity that will play an important roll in the analytical models to be described has been introduced as:

$$\left\langle v^2\right\rangle = \frac{\int \epsilon\dot{\mathbf{x}}^2\mathrm{d}\zeta}{\int \epsilon\mathrm{d}\zeta} \tag{2.32}$$

From the definition above, it may be seen that the characteristic velocity value is nothing more than an weighted expected value, where the string energy has been used as weighting function. This concept may be generalised right away to any other quantity as:

$$\langle\mathcal{O}\rangle = \frac{\int \epsilon\mathcal{O}\mathrm{d}\zeta}{\int \epsilon\mathrm{d}\zeta} \tag{2.33}$$

2.3.3 VOS model

In the previous section the equations of motion of a string in an expanding universe have been derived, but if they are to be solvable analytically, further simplifications are needed. From now on whenever the velocity squared is mentioned it should be taken as the expected value as defined in Equation 2.32.

The Velocity-dependent One Scale model tries to provide this framework by providing differential equations for the evolution of the relevant macroscopic variables of a string network. In this sense, the evolution of the network total energy, if no additional degrees

of freedom are considered, coincides with the bare string one, can be obtained by assuming the network to be Brownian, meaning that inside an arbitrary volume with dimensions ξ^3, the average length of the strings is also ξ [12], hence motivating the name One-Scale. This is equivalent to defining the average energy density of the string network as:

$$\rho = \frac{\mu}{\xi^2} = \frac{E}{a^3} \tag{2.34}$$

The evolution equation of the energy density can now be used to write:

$$\frac{\dot{\rho}}{\rho} = \frac{a^3}{E}\frac{\mathrm{d}}{\mathrm{d}\tau}\left(\frac{E}{a^3}\right) = \frac{\dot{E}}{E} - 3\mathcal{H} = -2\mathcal{H}\left(1+v^2\right) \tag{2.35}$$

It can be easily seen that the Brownian network assumption allows to express the energy evolution of the network as a function of the correlation length, as is typically presented in the VOS model:

$$-\frac{\dot{\rho}}{\rho} = 2\frac{\dot{\xi}}{\xi} = 2\mathcal{H}\left(1+v^2\right) \tag{2.36}$$

The expression above constitutes the first fundamental equation of the VOS model, but it should be noted that by treating all the strings as infinite strings, it fails to properly account for the energy that is confined into smaller loops and for any energy loss mechanism. Under the VOS model framework, the former is considered by adding a term proportional to the network density and velocity and parameterised by the chop efficiency $\tilde{c}$, that essentially quantifies the energy fraction that is lost to loops*. On the other hand, external energy loss mechanisms may be accounted for by including a damping term, that in its most simple form may be taken as proportional to the velocity. With this additional phenomenological terms, the full equation for the characteristic length scale evolution now reads:

$$2\frac{\dot{\xi}}{\xi} = 2\mathcal{H}\left(1+v^2\right) + \frac{\xi v^2}{\ell_f} + \tilde{c}v_0 \tag{2.37}$$

The reasonable extensive derivation above was given to illustrate how the VOS model is able to provide overall differential equations for the evolution of characteristic macroscopic quantities, but also to make it explicit that in this process some information is inherently lost. In fact, and by averaging over the full network, one needs to add new phenomenological parameters that try to capture some of the details that a full network simulation would provide. Following a similar reasoning, and here the reader is referred to the detailed

*Note that while the energy lost to loops is positive, the network must lose energy, which is compatible with an additional increment of the characteristic length.

analysis conducted by Martins [13], the velocity equation can be written as:

$$\frac{dv}{dt} = (1-v^2)\left[\frac{k}{\xi} - v\left(2H + \frac{1}{\ell_f}\right)\right] \tag{2.38}$$

where the momentum parameter k has been introduced which quantifies the effect of small scale structure and may be taken as dependent on the velocity alone, the derivative has been made explicit since it is here with respect to cosmic time, and H is the Hubble parameter defined as da/adt. As a final remark, it should be mentioned that an additional assumption has been made to keep the One-Scale philosophy by taking the curvature radius to be well approximated by ξ. The velocity evolution equation can be written with respect to conformal time as:

$$\dot{v} = (1-v^2)\left[\frac{k}{\xi/a} - v\left(2\mathcal{H} + \frac{1}{\ell_f/a}\right)\right] \tag{2.39}$$

It should be still mentioned that the equations above have been presented in the usual form for the VOS model, but alternative representations may be used. One in particular that will be useful for the extended model that will be analysed is to express the energy equation from the comoving correlation length defined as:

$$\xi = a\xi_c \tag{2.40}$$

With this new definition, the VOS equations are now written as:

$$2\frac{\dot{\xi}_c}{\xi_c} = 2\mathcal{H}v^2 + \frac{\xi_c v^2}{\ell_{f_c}} + \tilde{c}v_0 \tag{2.41a}$$

$$\dot{v} = (1-v^2)\left[\frac{k}{\xi_c} - v\left(2\mathcal{H} + \frac{1}{\ell_{f_c}}\right)\right] \tag{2.41b}$$

where the friction length scale has also been redefined to its comoving counterpart.

2.3.4 Generalised VOS

The canonical VOS model just described can be seen to not be applicable when the strings network increases in complexity and possesses additional degrees of freedom, either in the form of small scale structure, commonly known as wiggles, or by the presence of charges and currents.

By simple qualitative analysis, it is clear that a single length scale representing both the network correlation length and the network energy can no longer be applied, since the

additional degrees of freedom can contribute themselves for the energy balance and the VOS equations must be generalised. A common approach is to keep the definition of the correlation length scale as the typical string separation, and hence related to the so-called bare string energy, while defining an additional length scale, L, that relates to the total energy of the network. If the wiggly case has already been explored by Almeida and Martins [14, 15] and calibrated with numerical simulations conducted by Correia and Martins [16], the current carrying case has only been explored in the chiral limit by Oliveira et al. [17]. Since this work aims at exploring the generalised cases where charges and currents may behave differently, only the generalised model provided by Martins et al. [18] will be presented.

Starting from the area swept by the string concept once more, where the current is assumed to live in, the Nambu-Goto action can be generalised to:

$$S = \int \mathrm{d}\sigma^2 \left(-\mu\sqrt{-\gamma} + \frac{1}{2}\sqrt{-\gamma}\gamma^{ab}\varphi_{,a}\varphi_{,b} - qA_\mu x^\mu_{,a}\epsilon^{ab}\varphi_{,b} \right) - \frac{1}{16\pi}\int \mathrm{d}^4x\sqrt{-g}F_{\mu\nu}F^{\mu\nu} \quad (2.42)$$

where use has been made of the fact that a conserved current in two dimensions can be written as the derivative of a scalar field, here taken to be φ. A physical interpretation of the different terms can be provided right away, since, from left to right, we can clearly identify the typical Nambu-Goto contribution, the worldsheet current correction, its coupling to the electromagnetic sector and the usual kinetic term associated with the external field. For the purpose of this work, it is convenient to rewrite the action above as [18]:

$$S = -\mu_0 \int f(\kappa)\sqrt{-\gamma}\mathrm{d}^2\sigma \quad (2.43)$$

where the Lagrangian has been written from a constant with units of mass squared, μ_0, and $f(\kappa)$, that depends on the so-called state parameter κ defined from a scalar field, ψ, as:

$$\kappa = \gamma^{ab}\varphi_{,a}\varphi_{,b} = q^2 - j^2 = \frac{\dot{\phi}^2}{a^2\left(1-\dot{\mathbf{x}}^2\right)} - \frac{\phi'^2}{a^2\mathbf{x}'^2} = \frac{1}{a^2\mathbf{x}'^2}\left(\varepsilon^2\dot{\phi}^2 - \phi'^2\right) \quad (2.44)$$

where the microscopic charge q^2 and current j^2 have been implicitly defined and the last equality above has been written to highlight the fact that the chiral limit studied by Oliveira et al. [17] corresponds, in this model, to the limit where $\kappa \to 0$.

Finally, the equations of motion of this system are better expressed by considering the dimensionless variables derived by Rybak et al. [19]:

$$\tilde{U} \equiv f - 2q^2 \frac{\mathrm{d}f}{\mathrm{d}\kappa} \tag{2.45a}$$

$$\tilde{T} \equiv f + 2j^2 \frac{\mathrm{d}f}{\mathrm{d}\kappa} \tag{2.45b}$$

$$\Phi \equiv -2qj \frac{\mathrm{d}f}{\mathrm{d}\kappa} \tag{2.45c}$$

which have been named in this way to reflect the fact that their dimensional counterparts are the the energy per unit length U, the string tension T and the scalar field representing the current φ.

Armed with these definitions, it is now clear that the total energy of the network is given by:

$$E = a\mu_0 \int \tilde{U} \varepsilon \mathrm{d}\sigma = a\mu_0 \int \left(f - 2q^2 \frac{\mathrm{d}f}{\mathrm{d}\kappa} \right) \varepsilon \mathrm{d}\sigma = a\mu_0 \int f \varepsilon \mathrm{d}\sigma - a\mu_0 \int 2q^2 \frac{\mathrm{d}f}{\mathrm{d}\kappa} \varepsilon \mathrm{d}\sigma \tag{2.46}$$

The first term above, up to a renormalisation factor, is just the bare string energy as defined in the canonical VOS model, which motivates the definition of the macroscopial ratio betweeen total energy and bare energy as:

$$\frac{E}{E_0} = \frac{\int f \varepsilon \mathrm{d}\sigma - \int 2q^2 \frac{\mathrm{d}f}{\mathrm{d}\kappa} \varepsilon \mathrm{d}\sigma}{\int \varepsilon \mathrm{d}\sigma} = \langle f \rangle - 2 \left\langle q^2 \frac{\mathrm{d}f}{\mathrm{d}\kappa} \right\rangle = F - 2Q^2 F' \tag{2.47}$$

where capital letters should be understood as the expected value of their microscopical counterpart and the variables have been assumed to be uncorrelated to obtain the last equality. Finally, and following the length scale approach spirit, one may rewrite the energy relation above by introducing an additional comoving length scale, L_c, that is related to the correlation length by:

$$L_c \sqrt{F - 2Q^2 F'} = \xi_c \tag{2.48}$$

where Q^2 has been defined as the expected value of the microscopic charge q^2. In similar fashion, one can define the macroscopic current, J^2, as the expected value of its microscopical counterpart, j^2. Under the VOS model these quantities evolve as:

$$\left(J^2\right)^{\bullet} = 2J^2 \left(\frac{v k_v}{L\sqrt{F - 2Q^2 F'}} - \mathcal{H} \right) = 2J^2 \left(\frac{v k_v}{LW} - \mathcal{H} \right) \tag{2.49a}$$

$$\left(Q^2\right)^{\bullet} = 2Q^2 \frac{F' + 2J^2 F''}{F' + 2Q^2 F''} \left(\frac{v k_v}{LW} - \mathcal{H} \right) \tag{2.49b}$$

where for convenience the relation between the two lengthscales, $W = \sqrt{F - 2Q^2F'}$, has been defined.

The full set of equations of the generalised VOS model for current carrying strings are then given by:

$$\dot{L}_c = \mathcal{H} L_c \left[v^2 - \left(1 - v^2\right) \frac{Q^2 + J^2}{W^2} F' \right] \tag{2.50a}$$

$$\dot{v} = \left(1 - v^2\right) \left[\frac{k_v}{W L_c} \left(1 + 2 \frac{Q^2 + J^2}{W^2} F' \right) - 2v\mathcal{H} \left(1 + \frac{Q^2 + J^2}{W^2} F' \right) \right] \tag{2.50b}$$

$$\left(J^2\right)^\bullet = 2J^2 \left(\frac{v k_v}{L_c W} - \mathcal{H} \right) \tag{2.50c}$$

$$\left(Q^2\right)^\bullet = 2Q^2 \frac{F' + 2J^2 F''}{F' + 2Q^2 F''} \left(\frac{v k_v}{L_c W} - \mathcal{H} \right) \tag{2.50d}$$

$$\dot{\xi}_c = \mathcal{H} \xi_c v^2 \left(1 + \frac{Q^2 + J^2}{W^2} F' \right) - v k_v \frac{J^2 + Q^2}{W^2} F' \tag{2.50e}$$

As in the canonical VOS model, the equations above do not properly account for additional energy loss mechanisms, a phenomenological concept that here should be extended to include charge losses. The additional terms to try to mimic these effects are:

$$\dot{L}_c = \cdots + \frac{g}{W} \frac{\tilde{c}}{2} v \tag{2.51a}$$

$$\left(J^2\right)^\bullet = \cdots + \rho \tilde{c} \frac{v}{L_c} \frac{(g-1)W}{F' - 2Q^2 F''} \tag{2.51b}$$

$$\left(Q^2\right)^\bullet = \cdots + (1 - \rho) \tilde{c} \frac{v}{L_c} \frac{(g-1)W}{F' + 2Q^2 F''} \tag{2.51c}$$

$$\dot{\xi}_c = \cdots + \frac{\tilde{c}}{2} v \tag{2.51d}$$

A final note should be made here regarding the charge loss parameters g. In the latest work by Rybak et al. [20], it is shown that the bias function dependence on the charge and current is given by:

$$g = 1 - g_Q \frac{F' + 2Q^2 F''}{F - 2Q^2 F'} Q^2 - g_J \frac{F' - 2Q^2 F''}{F - 2Q^2 F'} J^2 \tag{2.52}$$

from where it is clear that solutions with decaying charge and currents are asymptotically compatible with $g = 1$, while for constant charge and/or current solutions one may expect constant, but not necessarily unitary, values for g. Finally, the bias function asymptotic value for growing charges and/or currents depends on the nature of the microscopic model. Since in these cases, as will be discussed later, $F' \neq 0$, one may decouple between models

where $F'' = 0$ and models where $F'' \neq 0$. In the first cases, it follows that:

$$g = 1 + \frac{g_Q}{2} + \frac{g_J}{2}\frac{J^2}{Q^2} \tag{2.53}$$

and it should be noted that, if both charge and current exhibit the same behaviour, this is still a constant. On the other hand, if $F'' \neq 0$, it follows that:

$$g = 1 + g_Q \frac{F''}{F'} Q^2 - g_J \frac{F''}{F'} J^2 \tag{2.54}$$

and now the bias function exhibits a dependency on the charge and current values, that only vanishes if charge and currents exhibit similar behaviours and:

$$\frac{g_Q}{g_J} = \frac{J^2}{Q^2} = \frac{J_0^2}{Q_0^2} \tag{2.55}$$

in which case $g = 1$ once again. In any other case, g will have an implicit time dependency.

2.4 Scaling solutions

If the generalised VOS model equations are already a macroscopic description of the network evolution, they are still a formidable problem to solve analytically and further simplifications or assumptions are needed. This analysis is significantly simplified if power law solutions are assumed such that:

$$L_c = L_0 \tau^{\alpha} \quad , \quad \dot{L}_c = \alpha L_0 \tau^{\alpha-1} \tag{2.56a}$$

$$v = v_0 \tau^{\beta} \quad , \quad \dot{v} = \beta v_0 \tau^{\beta-1} \tag{2.56b}$$

$$J^2 = J_0^2 \tau^{\gamma} \quad , \quad \left(J^2\right)^{\bullet} = \gamma J_0^2 \tau^{\gamma-1} \tag{2.56c}$$

$$Q^2 = Q_0^2 \tau^{\delta} \quad , \quad \left(Q^2\right)^{\bullet} = \delta Q_0^2 \tau^{\delta-1} \tag{2.56d}$$

$$\xi_c = \xi_0 \tau^{\varepsilon} \quad , \quad \dot{\xi}_c = \varepsilon \xi_0 \tau^{\varepsilon-1} \tag{2.56e}$$

$$W = W_0 \tau^{\zeta} = \frac{\xi_0}{L_0} \tau^{\varepsilon-\alpha} \quad , \quad W^2 = \left(\frac{\xi_0}{L_0}\right)^2 \tau^{2(\varepsilon-\alpha)} \tag{2.56f}$$

where the physical solutions must be such that $\beta \leq 0$ and $\alpha \leq 1$. Under the same spirit, the scale factor also can be assumed to follow a scaling solution given by:

$$a = a_0 \tau^{\lambda} \longrightarrow \mathcal{H} = \frac{a'}{a} = \lambda \tau^{-1} \tag{2.57}$$

which is asymptotically equivalent to assume a scaling solution of the scale factor when expressed with respect to the cosmic time:

$$a(t) \propto t^{\frac{\lambda}{1+\lambda}} \tag{2.58}$$

Additionally, it should be noted that this representation as a function of conformal time and comoving length scales can be easily reinterpreted as a function of cosmic time and physical lengths. In fact, any quantity that is scaling with respect to conformal time as a power law of exponent ζ, will scale as a function of cosmic time as a power law with exponent $\zeta/(1+\lambda)$, while if a comoving length scales as τ^{κ} its physical counterpart will scale as $\tau^{\kappa+\lambda}$. In particular, and combining both conditions above, it is clear that linearly scaling comoving distances with respect to conformal time are fully equivalent to linearly scaling physical quantities with respect to cosmic time.

By assuming these power law solutions, the differential equations of the VOS model can be transformed into analytical ones by the adequate substitutions:

$$\alpha = \lambda\left[v_0^2\tau^{2\beta} - C\mathcal{K}\tau^{2(\alpha-\varepsilon)+\eta}\right] + \frac{g\tilde{c}}{2}\frac{v_0}{\xi_0}\tau^{1+\beta-\varepsilon} \tag{2.59a}$$

$$\beta = C\left[\frac{k_v}{v_0\xi_0}\tau^{1-\beta-\varepsilon}\left(1+2\mathcal{K}\tau^{2(\alpha-\varepsilon)+\eta}\right) - 2\lambda\left(1+\mathcal{K}\tau^{2(\alpha-\varepsilon)+\eta}\right)\right] \tag{2.59b}$$

$$\gamma = 2\left(\frac{v_0k_v}{\xi_0}\tau^{1+\beta-\varepsilon} - \lambda\right) - \rho\tilde{c}\frac{v_0}{\xi_0}\frac{\xi_0^2}{J_0^2L_0^2}\frac{1-g}{F'-2Q_0^2\tau^{\delta}F''}\tau^{1+\beta+\varepsilon-2\alpha-\gamma} \tag{2.59c}$$

$$\begin{aligned}\delta = {} & 2\frac{F'+2J_0^2\tau^{\gamma}F''}{F'+2Q_0^2\tau^{\delta}F''}\left(\frac{v_0k_v}{\xi_0}\tau^{1+\beta-\varepsilon} - \lambda\right) - \\ & - (1-\rho)\tilde{c}\frac{v_0}{\xi_0}\frac{\xi_0^2}{Q_0^2L_0^2}\frac{1-g}{F'+2Q_0^2\tau^{\delta}F''}\tau^{1+\beta+\varepsilon-2\alpha-\delta}\end{aligned} \tag{2.59d}$$

$$\varepsilon = \lambda v_0^2\tau^{2\beta}\left(1+\mathcal{K}\tau^{2(\alpha-\varepsilon)+\eta}\right) - \frac{v_0k_v}{\xi_0}\mathcal{K}\tau^{2(\alpha-\varepsilon)+\eta+1+\beta-\varepsilon} + \frac{\tilde{c}}{2}\frac{v_0}{\xi_0}\tau^{1+\beta-\varepsilon} \tag{2.59e}$$

where the following variables have been defined:

$$\mathcal{K} = \frac{L_0^2\mathcal{J}_0^2}{\xi_0^2}F' \tag{2.60a}$$

$$\mathcal{J}_0^2 = Q_0^2 + J_0^2 \text{ if } \delta = \gamma,\ \mathcal{J}_0^2 = J_0^2 \text{ if } \delta < \gamma \text{ or } \mathcal{J}_0^2 = Q_0^2 \text{ if } \delta > \gamma \tag{2.60b}$$

$$\eta = \gamma \text{ if } \delta \leq \gamma \text{ or } \eta = \delta \text{ if } \delta > \gamma \tag{2.60c}$$

$$C = 1 - v^2 \tag{2.60d}$$

The last definition above is reasonable since for $\beta = 0$, $1 - v_0^2$ is a constant, and for $\beta < 0$, $1 - v_0^2t^{2\beta} \sim 1$, which is also constant. Finally, it has been assumed that all the initial parameters $X_0 \neq 0$.

It should be noted that the equations above are valid as long as none of the power law exponents vanishes. If this is the case, the velocity, charge and current equations should be replaced by (in the charge equation it was already made the replacement $\alpha = \varepsilon$):

$$0 = \frac{k_v}{\xi_0}\left(1 + 2\mathcal{K}\tau^{2(\alpha-\varepsilon)+\eta}\right)\tau^{-\varepsilon} - 2v_0\lambda\tau^{-1}\left(1 + \mathcal{K}\tau^{2(\alpha-\varepsilon)+\eta}\right) \tag{2.61a}$$

$$0 = 2J_0^2\left(\frac{v_0 k_v}{\xi_0}\tau^{\beta-\varepsilon} - \lambda\tau^{-1}\right) + \rho\tilde{c}\frac{v_0}{\xi_0}\frac{(g-1)}{F' - 2Q_0^2F''\tau^{\delta}}\frac{\xi_0^2}{L_0^2}\tau^{\varepsilon-\alpha}\tau^{\beta-\alpha} \tag{2.61b}$$

$$0 = 2Q_0^2\frac{F' + 2J_0^2\tau^{\gamma}F''}{F' + 2Q_0^2F''}\left(\frac{v_0 k_v}{\xi_0}\tau^{\beta-\varepsilon} - \lambda\tau^{-1}\right) + (1-\rho)\tilde{c}\frac{v_0}{\xi_0}\frac{(g-1)}{F' + 2Q_0^2F''}\frac{\xi_0^2}{L_0^2}\tau^{\beta-\alpha} \tag{2.61c}$$

Although these equations are fully equivalent to the more general ones above, they may allow for less restrictive solutions. For instance, and assuming that both terms in between brackets in the velocity equation are constant (or at least not growing sufficiently fast), one would arrive at the following conclusions for the possibility of constant velocity solutions:

$$0 = \frac{k_v}{\xi_0}\left(1 + 2\mathcal{K}\right)\tau^{1-\varepsilon} - 2v_0\lambda\left(1 + \mathcal{K}\right) \tag{2.62a}$$

$$0 = \frac{k_v}{\xi_0}\left(1 + 2\mathcal{K}\right)\tau^{-\varepsilon} - 2v_0\lambda\tau^{-1}\left(1 + \mathcal{K}\right) \tag{2.62b}$$

It is clear that both solutions require $\varepsilon = 1$, but now comes the subtle point. As only asymptotic solutions are under analysis, it is assumed that $\tau \to \infty$, which actually makes that the two formulations above are not fully equivalent anymore. In fact, although in both cases it is still required $\varepsilon = 1$, the second formulation allows for a loophole worth searching for: since ε is clearly positive, one may allow for solutions where the correlation length does not scale linearly, but that for sufficient high τ is essentially indistinguishable from the true solutions for practical purposes. In the results that will be presented the more general formulation will be followed, with the caution to properly check for additional branches, hidden at first sight, whenever suitable.

A preliminary inspection of the different equations already identifies some of the relevant parameters that are most likely to play a central role in the analysis to come. In particular, the factor $2(\alpha - \varepsilon) + \eta$ that appears associated with F' is closely related to the relation defined by Equation 2.48 which in terms of the power law defined above yields:

$$L_0^2\tau^{2\alpha}\left(F - 2Q_0^2\tau^{\delta}F'\right) = \xi_0^2\tau^{2\varepsilon} \longrightarrow \frac{\xi_0^2}{L_0^2}\tau^{2(\varepsilon-\alpha)} = F - 2Q_0^2\tau^{\delta}F' \tag{2.63}$$

This is particular significant, since the presence of F on the right hand side above, that is not expected to vanish, fixes the relation between the 3 exponents. In particular, one can

easily see that for decaying or constant charge solutions ($\delta \leq 0$) both length-scales must evolve with a similar rate, $\alpha = \varepsilon$. On the other hand growing charge cases are only possible if the current length grows slower than the correlation length. Recovering the relation between the length scales and the corresponding energy densities one can easily see that these results are expected on purely physical grounds. In any case, it is not possible to have solutions where $\alpha > \varepsilon$, unless a rather unphysical behaviour is prescribed where $F = 0$.

As a final note, it should be mentioned that one may find mathematical solutions to the evolution equations that are not physical by different reasons:

- The network characteristic velocity must be lower than the speed of light, that in these units implies $v < 1$
- For an expanding universe, it is not expected the momentum parameter to vanish
- The correlation length cannot scale faster than t (or the comoving correlation length faster than τ), since it would violate causality

These physics motivated bounds naturally decouple the solutions between physical and mathematical solutions and these will be discussed in different chapters.

Chapter 3

Physical solutions

3.1 Introduction

The solutions will be presented in the following way. Firstly, energy and charge loss mechanisms will be neglected, in which case the network evolution is governed by the cosmic expansion alone. Once these solutions are properly presented and discussed, energy loss mechanisms will be introduced, but charge losses will still not be considered. This is easily accomplished by setting $g = 1$, which, following the discussion at the end of the last chapter, can also be interpreted as the asymptotic limit of any decaying charges and currents solution or growing solutions where $F'' \neq 0$ and Equation 2.55 is verified. Finally, charge losses will also be allowed to condition the network evolution. For simplicity, first the bias function will be assumed to be constant, but not unitary. This is compatible with constant charges and currents, or growing solutions where $F'' = 0$ and Q^2 and J^2 evolve in similar ways, meaning $\gamma = \delta = \eta$. Finally, in the last section of this chapter the remaining growing charge and current solutions will be presented, and in this case the bias function will be assumed to carry an explicit time dependency given by:

$$g = g_0 \tau^{\eta} \tag{3.1}$$

In order to aid with the visualisation of the different solutions found, but also to validate them, an application to solve numerically the system defined by Equation 2.50 was created. This application will be used when suitable to illustrate the findings. It was also decided to make the code available in a GitHub repo, that may be eventually populated with additional scripts in the future, and an user friendly interface made available through Streamlit.

3.2 Solutions without loss mechanisms

In this case, one may simply set $\tilde{c} = 0$. The current equation can be used to clearly see that in the absence of energy loss mechanisms any physical solution in an expanding universe must be such that $\varepsilon \geq 1 + \beta$. If one accepts the cases $\varepsilon > 1 + \beta$, then only decaying current solutions are possible, which is not the case if the perfect balance $\varepsilon = 1 + \beta \leq 1$ is assumed. In fact, further investigations regarding the former show that no solutions are consistent within that sub-branch and the macroscopical equations reduce to:

$$\alpha = \lambda \left[v_0^2 \tau^{2\beta} - C\mathcal{K}\tau^{2(\alpha-\varepsilon)+\eta} \right] \tag{3.2a}$$

$$\beta = C \left[\frac{k_v}{v_0 \xi_0} \tau^{-2\beta} \left(1 + 2\mathcal{K}\tau^{2(\alpha-\varepsilon)+\eta} \right) - 2\lambda \left(1 + \mathcal{K}\tau^{2(\alpha-\varepsilon)+\eta} \right) \right] \tag{3.2b}$$

$$\gamma = 2 \left(\frac{v_0 k_v}{\xi_0} - \lambda \right) \tag{3.2c}$$

$$\delta = 2 \frac{F' + 2J_0^2 \tau^\gamma F''}{F' + 2Q_0^2 \tau^\delta F''} \left(\frac{v_0 k_v}{\xi_0} - \lambda \right) \tag{3.2d}$$

$$\varepsilon = \lambda v_0^2 \tau^{2\beta} \left(1 + \mathcal{K}\tau^{2(\alpha-\varepsilon)+\eta} \right) - \frac{v_0 k_v}{\xi_0} \mathcal{K}\tau^{2(\alpha-\varepsilon)+\eta} \tag{3.2e}$$

From a physical point of view, this condition implies that the linear bare energy scaling with constant velocity that constitutes the canonical Nambu-Goto network evolution is still a possible solution. It is also clear that under these assumptions the quantity $\mathcal{K}\tau^{2(\alpha-\varepsilon)+\eta}$ plays a central role and that its value if completely fixed at $-\frac{1}{2}$ for decaying velocity solutions. In these cases, only solution A1 is possible.

Solution A1: Non decaying charge and current solution

1. Scaling solutions:

$$\boldsymbol{L_c = L_0 \tau^{\lambda/2}} \quad , \quad \boldsymbol{\xi_c = \xi_0 \tau^{1-\lambda}} \quad , \quad \boldsymbol{J^2 = J_0^2 \tau^{4-6\lambda}} \quad , \quad \boldsymbol{v = v_0 \tau^{-\lambda}}$$
$$\boldsymbol{L = L_0 \tau^{3\lambda/2}} \quad , \quad \boldsymbol{\xi = \xi_0 \tau} \quad , \quad \boldsymbol{Q^2 = Q_0^2 \tau^{4-6\lambda}}$$

2. Additional constraints:

$$\boldsymbol{\lambda = \frac{v_0 k_v}{\xi_0} = \frac{2}{3}} \quad , \quad \boldsymbol{\mathcal{K} = -\frac{1}{2}}$$

Although this solution is obtained here for a single expansion rate, it is actually compatible with the slow expansion rate branch identified by Oliveira et al. [17], in the particular case where $s = 0$. Although this may not be clear at first sight, it should be noted that for $s = 0$ one of the constraints of the mentioned work fixes the charge value at $Q_0 = 1$ and the velocity equation there will asymptotically be reduced to:

$$\dot{v} = -\frac{1-v^2}{2}(2Hv) \approx -Hv \longrightarrow v_0\beta t^{\beta-1} = -\lambda v_0 t^{\beta-1} \longrightarrow \lambda = -\beta \tag{3.3}$$

While this relation is similar to the one just identified, although expressed with respect to the cosmic time, it should be noted that another constraint is identified making $\beta = 1-\alpha = 1-\frac{3\lambda}{2}$, which when combined with the condition above yields:

$$\lambda = \frac{3\lambda}{2} - 1 \longrightarrow \lambda = \frac{2}{5} \tag{3.4}$$

and a single expansion rate is allowed. Furthermore, it can still be noted that an expansion rate of $2/5$ when expressed with respect to cosmic time is equivalent to an expansion rate of:

$$\lambda_t = \frac{\lambda_\tau}{\lambda_\tau + 1} = \frac{2}{5} \longrightarrow \lambda_\tau = \frac{2}{3} \tag{3.5}$$

which is exactly the same as in A1. If this solution is seen to be equivalent to the chiral limit one, here it is not needed that $Q_0^2 = J_0^2$, but it is required that:

$$\mathcal{K} = \frac{L_0^2}{\xi_0^2}\left(Q_0^2 + J_0^2\right)F' = \frac{Q_0^2 + J_0^2}{F - 2Q_0^2F'}F' = -\frac{1}{2} \longrightarrow J_0^2 = -\frac{F}{2F'} \tag{3.6}$$

If the reasoning above was valid for decaying velocity solutions, it does not hold for constant velocity ones, and these complete the set of physical solutions in the absence of energy loss mechanisms. Firstly, it should be noted that all the solutions here must have a comoving correlation length that scales linearly with conformal time (or, as mentioned before, physical correlation length that scale linearly with physical time).

A particular set of solutions, valid for expansion rates such that $v_0^2 = 1/\lambda$, is found in the particular case where $F' = 0$ and is given by A2. It should be noted that the condition above implies that there is a lower bound for λ at $\lambda > 1$, and hence these solutions are not realisable in the radiation era. Still within the sub-branch where $F' = 0$, there is another possible solution, A3, but that is only realisable for fast expansion rates ($\lambda > 2$), where the current will still decay, but now the charge is allowed to persist. A final comment is needed within these sub branch of solutions though, since some of them imply $Q_0^2 = J_0^2$,

which is compatible with the chiral limit, but also $F' = 0$, which is not the expected value that would make the system of equations fully equivalent to the one studied by Oliveira et al. [17].

Solution A2: General current and charge solution

1. Scaling solutions:

$$L_c = L_0\tau \quad , \quad \xi_c = \xi_0\tau \quad , \quad J^2 = J_0^2\tau^{4-2\lambda} \quad , \quad v = v_0$$
$$L = L_0 t \quad , \quad \xi = \xi_0 t \quad , \quad Q^2 = Q_0^2\tau^{4-2\lambda}$$

2. Additional constraints:

$$\lambda = \frac{1}{v_0^2} > 1 \quad , \quad \frac{v_0 k_v}{\xi_0} = 2 \qquad F' = 0 \quad , \quad \left(Q_0^2 = J_0^2\right)^{(*)}$$

* Not applicable for $\lambda = 2$, or $\gamma = \delta = 0$.

Solution A3: Decaying current and constant charge solution

1. Scaling solutions:

$$L_c = L_0\tau \quad , \quad \xi_c = \xi_0\tau \quad , \quad J^2 = J_0^2\tau^{4-2\lambda} \quad , \quad v = v_0$$
$$L = L_0 t \quad , \quad \xi = \xi_0 t \quad , \quad Q^2 = Q_0^2$$

2. Additional constraints:

$$\lambda = \frac{1}{v_0^2} > 2 \quad , \quad \frac{v_0 k_v}{\xi_0} = 2 \qquad F' = 0 \quad ,$$

A numerical simulation of the network evolution for different expansion rates and $F' = 0$ is presented in Figure 3.1. For simulations S1 to S3, the initial network charge and current for $\tau = 1$, which should not be read as the asymptotic solution scale parameter, Q_0 and J_0, were taken to be 0.2 and 0.1, respectively, and the constant charge solution is found. On the other hand, simulation S4 was carried out from starting conditions with charge and current equal to 0.1, and in this case the network evolves towards the decaying charge and current sub-branch. Finally, and for completeness, it should still be mentioned that although solution S1 started with a charge to current ratio of 2, the asymptotic solutions presented as dashed lines are such that $Q_0 = J_0$, while the same does not happen for simulation S2, where $Q_0 \neq J_0$. This can be easily understood by noting that the growing

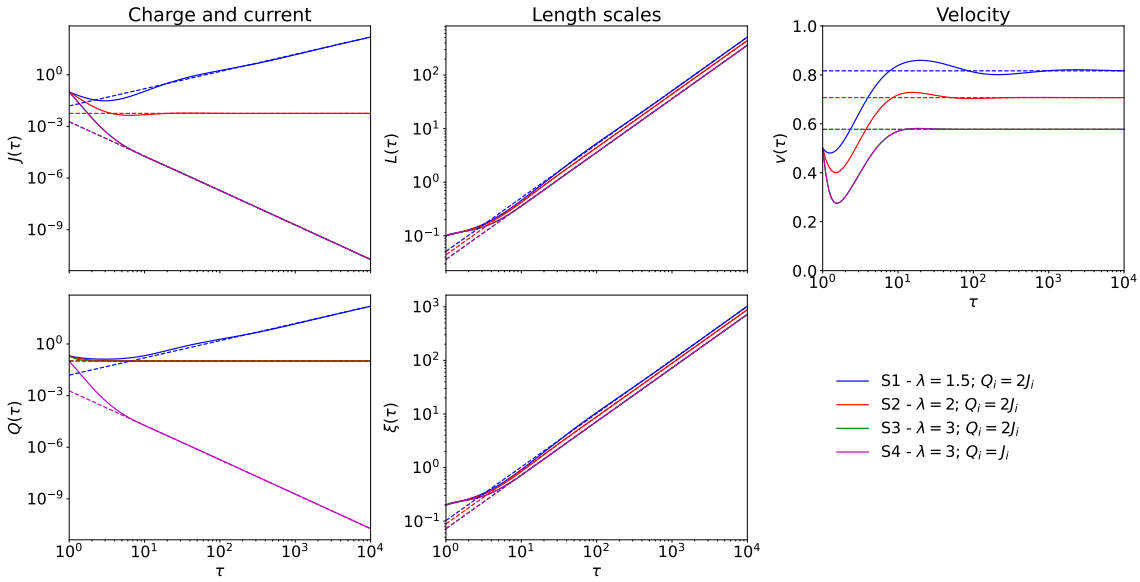

FIGURE 3.1: Network evolution as obtained by numerically solving the generalised VOS differential equations without charge or energy loss mechanisms and considering $F' = 0$, for different initial conditions and expansion rates (see Appendix B for details).

current sub-branch is only possible if $Q_0 = J_0$, and so the network finds its way into this state.

Leaving aside the cases where $F' = 0$, one can still identify solution A4, which is very similar to A2. Here, however, the chiral condition does not have to hold and arbitrary current and charge values are possible. Comparing both solutions, it can be seen that fast expansion rates associated with decaying charges and currents are asymptotically equivalent to the canonical Nambu-Goto case, but only the chiral limit is allowed when $F' = 0$.

Solution A4: Decaying current and charge solution

1. Scaling solutions:

$$L_c = L_0\tau \quad , \quad \xi_c = \xi_0\tau \quad , \quad J^2 = J_0^2\tau^{4-2\lambda} \quad , \quad v = v_0$$
$$L = L_0 t \quad , \quad \xi = \xi_0 t \quad , \quad Q^2 = Q_0^2\tau^{4-2\lambda}$$

2. Additional constraints:

$$\lambda = \frac{1}{v_0^2} > 2 \quad , \quad \frac{v_0 k_v}{\xi_0} = 2 \quad , \quad ,$$

Solution A5: Constant current and charge solution

1. Scaling solutions:

$$L_c = L_0\tau \quad , \quad \xi_c = \xi_0\tau \quad , \quad J^2 = J_0^2\tau^{4-2\lambda} \quad , \quad v = v_0$$
$$L = L_0 t \quad , \quad \xi = \xi_0 t \quad , \quad Q^2 = Q_0^2\tau^{4-2\lambda}$$

2. Additional constraints:

$$\lambda = 2 \quad , \quad \frac{v_0 k_v}{\xi_0} = 2 \quad , \quad v_0^2 = \frac{1+2\mathcal{K}}{2+2\mathcal{K}} = 1 - \frac{1}{2+2\mathcal{K}} \quad ,$$

Finally, a persisting charge and current solution is also found here for arbitrary values of current and charge, as given by solution A5. It can be noted that both solutions are similar to the ones obtained by Almeida and Martins [14] and by Oliveira et al. [17], in the appropriate branch. Once more, a numerical example starting from arbitrary initial conditions and different expansion rates is presented in Figure 3.2. For the lowest expansion rate, the decaying velocity solution from A1 is obtained.

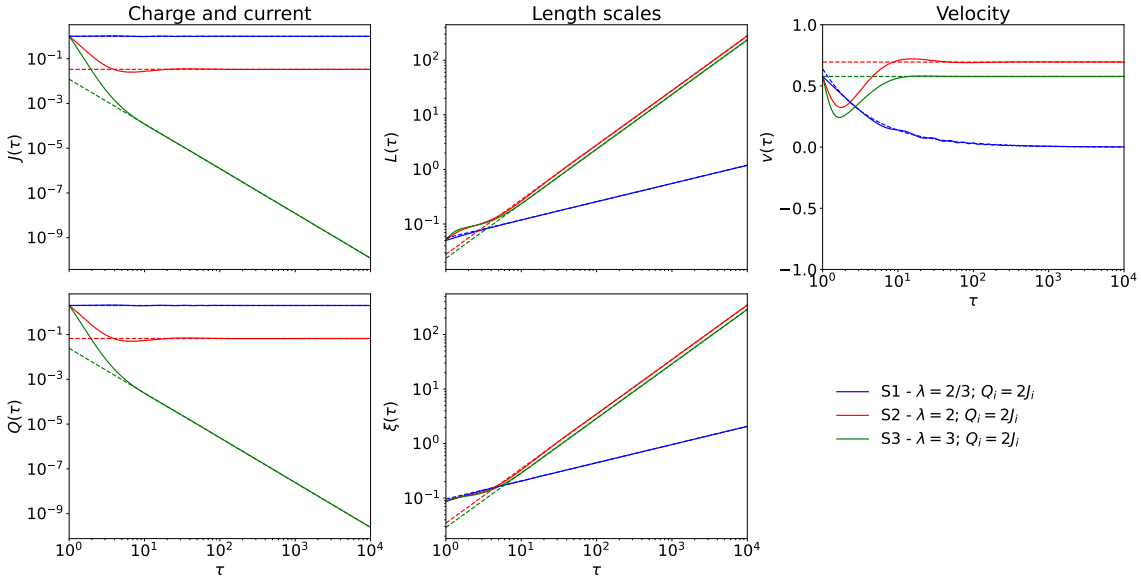

FIGURE 3.2: Network evolution as obtained by numerically solving the generalised VOS differential equations without charge or energy loss mechanisms and considering $F' \neq 0$, for different initial conditions and expansion rates (see Appendix B for details).

3.3 Solutions without charge loss mechanisms

If in the previous section both energy and charge losses have been neglected, by setting $\tilde{c} = 0$, here solutions with energy loss mechanisms are explored, which can be easily accomplished by setting $\tilde{c} \neq 0$ and $g = 1$. Following the discussion on the value of g, these solutions should also be interpreted as possible solutions for networks with charge loss mechanisms, but where the charge and current decay away. Additionally, setting $g = 1$ also has the consequence of keeping the velocity, charge and current equations the same as before, while the current and correlation length now read:

$$\alpha = \lambda \left[v_0^2 \tau^{2\beta} - C\mathcal{K}\tau^{2(\alpha-\varepsilon)+\eta} \right] + \frac{\tilde{c}}{2}\frac{v_0}{\xi_0}\tau^{1+\beta-\varepsilon} \tag{3.7a}$$

$$\varepsilon = \lambda v_0^2 \tau^{2\beta} \left(1 + \mathcal{K}\tau^{2(\alpha-\varepsilon)+\eta} \right) - \frac{v_0 k_v}{\xi_0}\mathcal{K}\tau^{2(\alpha-\varepsilon)+\eta+1+\beta-\varepsilon} + \frac{\tilde{c}}{2}\frac{v_0}{\xi_0}\tau^{1+\beta-\varepsilon} \tag{3.7b}$$

One thing that is already clear is that imposing $1 + \beta - \varepsilon < 0$ will reduce the system of equations to the previous cases, where no physical solutions were found. This means that the full set of equations, subjected to the constraint $1 + \beta = \varepsilon$, is given by:

$$\alpha = \lambda \left[v_0^2 \tau^{2\beta} - C\mathcal{K}\tau^{2(\alpha-\varepsilon)+\eta} \right] + \frac{\tilde{c}}{2}\frac{v_0}{\xi_0} \tag{3.8a}$$

$$\beta = C \left[\frac{k_v}{v_0 \xi_0}\tau^{-2\beta} \left(1 + 2\mathcal{K}\tau^{2(\alpha-\varepsilon)+\eta} \right) - 2\lambda \left(1 + \mathcal{K}\tau^{2(\alpha-\varepsilon)+\eta} \right) \right] \tag{3.8b}$$

$$\gamma = 2\left(\frac{v_0 k_v}{\xi_0} - \lambda \right) \tag{3.8c}$$

$$\delta = 2\frac{F' + 2J_0^2\tau^\gamma F''}{F' + 2Q_0^2\tau^\delta F''} \left(\frac{v_0 k_v}{\xi_0} - \lambda \right) \tag{3.8d}$$

$$\varepsilon = \lambda v_0^2 \tau^{2\beta} \left(1 + \mathcal{K}\tau^{2(\alpha-\varepsilon)+\eta} \right) - \frac{v_0 k_v}{\xi_0}\mathcal{K}\tau^{2(\alpha-\varepsilon)+\eta} + \frac{\tilde{c}}{2}\frac{v_0}{\xi_0} \tag{3.8e}$$

Once more, it can be easily seen that decaying velocity solutions are only possible if $\mathcal{K}\tau^{2(\alpha-\varepsilon)+\eta} = -\frac{1}{2}$, which is the same condition as before. This can be easily understood, since this constraint is obtained from the velocity equation alone, which is unaffected. Proceeding in a similar way as in the no losses cases, one can conclude that the only realisable solution is the one expressed by solution B1, with constant charge and currents. The subtle difference is that the allowed expansion rate is now found at:

$$\lambda = \frac{2}{3} - \frac{\tilde{c}}{3}\frac{v_0}{\xi_0} = \frac{2}{3 + \tilde{c}/k_v} = \lambda_{\text{nl}} - \frac{\tilde{c}}{3}\frac{v_0}{\xi_0} \tag{3.9}$$

where λ_{nl} identifies the expansion rate found in the no loss regimes. Once more, if one wants to express the corresponding expansion rate power law with respect to cosmic time

will find:

$$\lambda_t = \frac{\lambda_\tau}{\lambda_\tau + 1} = \frac{2}{5 + \tilde{c}/k_v} \tag{3.10}$$

which is the same as the one found by Oliveira et al. [17] in the limit $s \to 0$.

Solution B1: Non decaying charge and current solution

1. Scaling solutions:

$$L_c = L_0\tau^{1-\lambda} \quad , \quad \xi_c = \xi_0\tau^{1-\lambda} \quad , \quad J^2 = J_0^2 \quad , \quad v = v_0\tau^{-\lambda}$$
$$L = L_0\tau \quad , \quad \xi = \xi_0\tau \quad , \quad Q^2 = Q_0^2$$

2. Additional constraints:

$$\lambda = \frac{2}{3} - \frac{\tilde{c}}{3}\frac{v_0}{\xi_0} = \frac{2}{3 + \tilde{c}/k_v} \quad , \quad \mathcal{K} = -\frac{1}{2} \quad , \quad \frac{v_0 k_v}{\xi_0} = \lambda$$

Solution B2: General current and charge solution

1. Scaling solutions:

$$L_c = L_0\tau \quad , \quad \xi_c = \xi_0\tau \quad , \quad J^2 = J_0^2\tau^{4\lambda v_0^2 - 2\lambda} \quad , \quad v = v_0$$
$$L = L_0 t \quad , \quad \xi = \xi_0 t \quad , \quad Q^2 = Q_0^2\tau^{4\lambda v_0^2 - 2\lambda}$$

2. Additional constraints:

$$\lambda = \frac{1/v_0^2}{1 + \tilde{c}/k_v} \quad , \quad \frac{k_v}{\xi_0} = 2\lambda v_0 \qquad F' = 0 \quad , \quad \left(Q_0^2 = J_0^2\right)^{(*)}$$

* Not applicable for $\gamma = \delta = 0$.

Solution B3: Decaying current and constant charge solution

1. Scaling solutions:

$$L_c = L_0\tau \quad , \quad \xi_c = \xi_0\tau \quad , \quad J^2 = J_0^2\tau^{4\lambda v_0^2 - 2\lambda} \quad , \quad v = v_0$$
$$L = L_0 t \quad , \quad \xi = \xi_0 t \quad , \quad Q^2 = Q_0^2$$

2. Additional constraints:

$$\lambda = \frac{1/v_0^2}{1 + \tilde{c}/k_v} > \frac{2}{1 + \tilde{c}/k_v} \quad , \quad \frac{k_v}{\xi_0} = 2\lambda v_0 \qquad F' = 0 \quad , \quad v_0^2 < \frac{1}{2}$$

Looking now for the constant velocity solutions, one finds once more that they can only be realisable in regimes with linear scaling of the comoving lengths when expressed with respect to conformal time. The solutions found here are given by B2 and B3, which can be seen to be the natural extension of A2 and A3, respectively. For the general solution B2, one can easily identify a critical velocity that dictates the fate of current and charges at $v_c^2 = 1/2$. Once more, the expansion rate can be related to its no loss counterpart by:

$$\lambda = \frac{1}{v_0^2}\frac{1}{1+\tilde{c}/k_v} = \frac{\lambda_{\rm nl}}{1+\tilde{c}/k_v} \tag{3.11}$$

Combining this with the critical velocity, one finds a critical expansion rate at:

$$\lambda_c = \frac{2}{1+\tilde{c}/k_v} \tag{3.12}$$

One the other hand, the constant charge solution is only compatible with decaying currents, or $v_0 < v_c$. It should be noted that the relation between the asymptotic velocity and the expansion rate presented in both B2 and B3 can be inverted to yield:

$$v_0 = \sqrt{\frac{k_v}{\lambda\,(k_v + c)}} \tag{3.13}$$

which conveniently reduces to the no loss cases for $\tilde{c} = 0$. As before, a numerical simulation of the evolution governed by the full set of equations is presented in Figure 3.3, where in all cases the same initial conditions used to produce the plots in Figure 3.1 have been

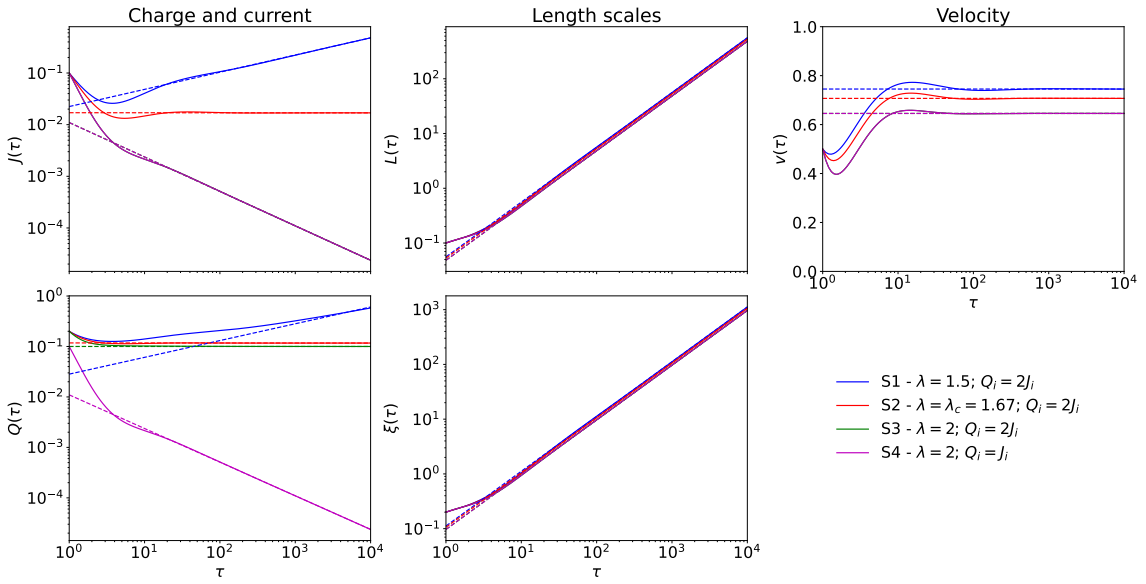

FIGURE 3.3: Network evolution as obtained by numerically solving the generalised VOS differential equations with energy loss mechanisms only and considering $F' = 0$, for different initial conditions and expansion rates (see Appendix B for details).

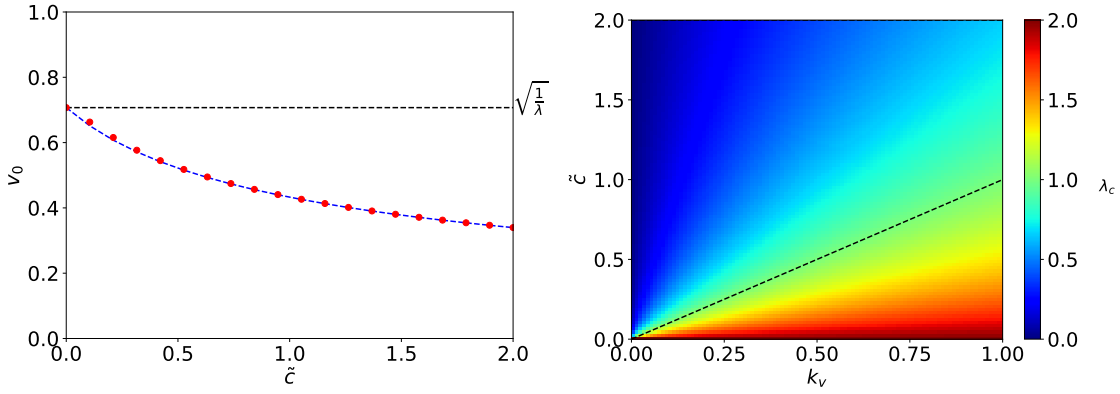

FIGURE 3.4: On the left, a representation of the impact of the energy loss parameter on the asymptotic velocity of the network. On the right, the critical expansion rate as a function of both the energy loss parameter and the momentum parameter.

used, but it has been assumed that $\tilde{c} = 0.05$. Clearly, for equivalent expansion rates, the asymptotic velocities obtained are lower than in the case of no charge loss (or, in a different perspective, the expansion rate compatible with a given network velocity is lower than before). This effect may be more simply highlighted by performing a set of simulations for varying values of the energy loss parameter $\tilde{c}$, while keeping the same expansion rate. In Figure 3.4 are presented the asymptotic velocities obtained for $\tilde{c} \in [0, 2]$ and $\lambda = 2$, as well as the expected values as computed from Equation 3.13 and the no loss limit ($v = \sqrt{\lambda^{-1}}$). Additionally, it should also be noted that the critical expansion rate is now found below the matter era threshold, and solutions in this epoch exhibit the same behaviour of the fast expansion rates from the no loss cases. Finally, the deviation of the critical expansion rate as a function of the energy loss and momentum parameter is also presented in Figure 3.4.

If solutions A2 and A3 have been properly generalised to B2 and B3, respectively, the same happens for the cases A4 and A5, which find their counterpart in B4 and B5. It may may be seen that the critical velocity is still the same as before, at $v_c^2 = 1/2$, and is associated with an expansion rate given by $\lambda_c = v_c k_v / \xi_0$, which can also be rewritten as:

$$\lambda_c v_c^2 = 1 - \frac{\tilde{c}}{2}\frac{v_c}{\xi_0} = 1 - \frac{\tilde{c}}{2}\frac{\lambda_c}{k_v} \longrightarrow \lambda_c = \frac{2}{2v_c^2 + \tilde{c}/k_v} = \frac{2}{1 + \tilde{c}/k_v} \tag{3.14}$$

The expansion rate above is exactly the same as the expansion rate that allows current and charges to be preserved, and lower than the value found in the absence of energy loss mechanisms. Once more, a numerical solution is presented for different expansion rates in Figure 3.5 for the conditions required by B1, B4 and B5, considering the same initial conditions as in the no loss case and $\tilde{c} = 0.05$. By comparison with the results presented in Figure 3.2, one can easily see that the asymptotic velocities are now found at lower values.

Solution B4: Decaying current and charge solution

1. Scaling solutions:

$$L_c = L_0\tau \quad , \quad \xi_c = \xi_0\tau \quad , \quad J^2 = J_0^2\tau^{4\lambda v_0^2-2\lambda} \quad , \quad v = v_0$$
$$L = L_0 t \quad , \quad \xi = \xi_0 t \quad , \quad Q^2 = Q_0^2\tau^{4\lambda v_0^2-2\lambda}$$

2. Additional constraints:

$$\lambda = \frac{1/v_0^2}{1+\tilde{c}/k_v} > \frac{2}{1+\tilde{c}/k_v} \quad , \quad F' \neq 0 \quad , \quad v_0^2 < \frac{1}{2} \quad ,$$

Solution B5: Constant current and charge solution

1. Scaling solutions:

$$L_c = L_0\tau \quad , \quad \xi_c = \xi_0\tau \quad , \quad J^2 = J_0^2 \quad , \quad v = v_0$$
$$L = L_0 t \quad , \quad \xi = \xi_0 t \quad , \quad Q^2 = Q_0^2$$

2. Additional constraints:

$$\lambda = 2 - \tilde{c}\frac{v_0}{\xi_0} = \frac{2}{1+\tilde{c}/k_v} \quad , \quad \lambda = \frac{v_0 k_v}{\xi_0} \quad , \quad v_0^2 = 1 - \frac{1}{2+2\mathcal{K}} \quad ,$$

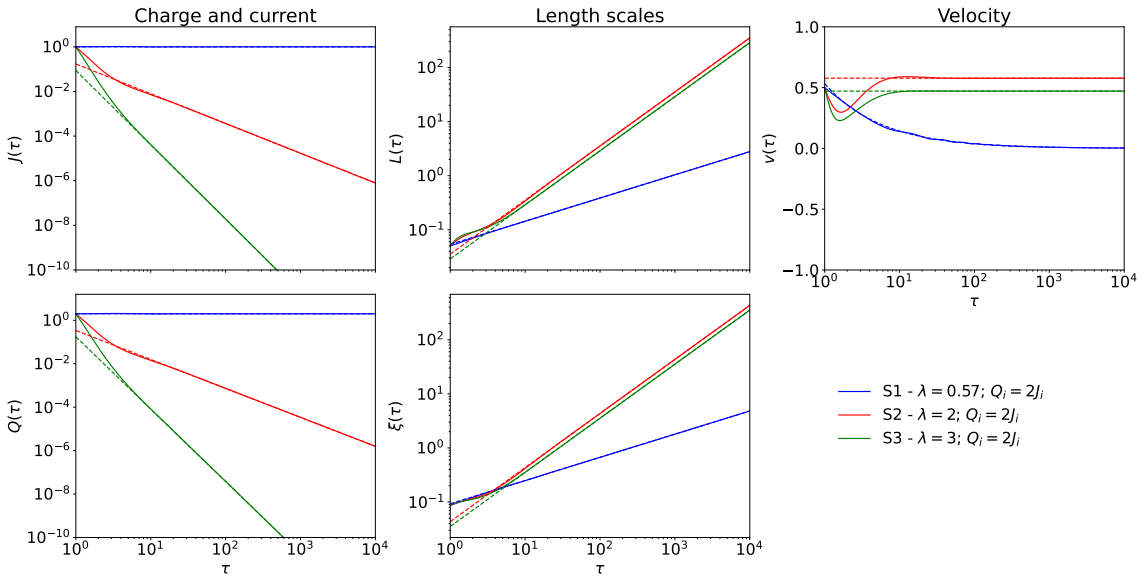

FIGURE 3.5: Network evolution as obtained by numerically solving the generalised VOS differential equations with energy loss mechanisms only and considering $F' \neq 0$, for different initial conditions and expansion rates (see Appendix B for details).

3.4 Solutions with constant bias function

Having explored the branches with and without energy losses, it is now time to complete the analysis by explicitly incorporating the charge loss mechanisms. It should be recalled, however, that a network where such mechanisms exist, but with decaying charge and currents, is compatible with the already studied solutions with $g = 1$, meaning that the charge loss possibilities are not strictly confined to this section. Starting once again from the current equation, it can be seen that another possibility emerges where solutions with $1 + \beta - \varepsilon > 0$ may be realisable, as long as it is verified that $2\varepsilon - 2\alpha - \gamma - \cdots = 0$, where the dots stand for some particular dependence on δ, depending on its value and on F' and F''. This condition will make the first and last terms perfectly balance each other. However, further investigating the cases where $1 + \beta - \varepsilon \neq 0$ reveals that they are not compatible with the full set of equations and hence it must be that $\varepsilon = 1 + \beta$. Making the adequate substitutions, the equations now read:

$$\alpha = \lambda\left[v_0^2\tau^{2\beta} - C\mathcal{K}\tau^{2(\alpha-\varepsilon)+\eta}\right] + g\frac{\tilde{c}}{2}\frac{v_0}{\xi_0} \tag{3.15a}$$

$$\beta = C\left[\frac{k_v}{v_0\xi_0}\tau^{-2\beta}\left(1 + 2\mathcal{K}\tau^{2(\alpha-\varepsilon)+\eta}\right) - 2\lambda\left(1 + \mathcal{K}\tau^{2(\alpha-\varepsilon)+\eta}\right)\right] \tag{3.15b}$$

$$\gamma = 2\left(\frac{v_0k_v}{\xi_0} - \lambda\right) - \rho\tilde{c}\frac{v_0\xi_0}{J_0^2L_0^2}\frac{1-g}{F' - 2Q_0^2\tau^\delta F''}\tau^{-\left[2(\alpha-\varepsilon)+\gamma\right]} \tag{3.15c}$$

$$\delta = 2\frac{F' + 2J_0^2\tau^\gamma F''}{F' + 2Q_0^2\tau^\delta F''}\left(\frac{v_0k_v}{\xi_0} - \lambda\right) - (1-\rho)\tilde{c}\frac{v_0\xi_0}{Q_0^2L_0^2}\frac{1-g}{F' + 2Q_0^2\tau^\delta F''}\tau^{-\left[2(\alpha-\varepsilon)+\delta\right]} \tag{3.15d}$$

$$\varepsilon = \lambda v_0^2\tau^{2\beta}\left(1 + \mathcal{K}\tau^{2(\alpha-\varepsilon)+\eta}\right) - \frac{v_0k_v}{\xi_0}\mathcal{K}\tau^{2(\alpha-\varepsilon)+\eta} + \frac{\tilde{c}}{2}\frac{v_0}{\xi_0} \tag{3.15e}$$

Although it may not be apparent at first sight, the inclusion of the charge loss mechanisms effectively prevents the solutions with constant velocity and $F' = 0$ from forming. This can be seen by noting that, were this to be true, then one would have from the characteristic length equations that:

$$\alpha = \lambda v_0^2\tau^{2\beta} + g\frac{\tilde{c}}{2}\frac{v_0}{\xi_0} \tag{3.16a}$$

$$\varepsilon = \lambda v_0^2\tau^{2\beta} + \frac{\tilde{c}}{2}\frac{v_0}{\xi_0} \tag{3.16b}$$

For constant values of g (but still considering $g \neq 1$), the expressions above implies $\alpha \neq \varepsilon$, while the consistency relation would also yield $L_cW = L_c\sqrt{F - 2Q^2F'} = L_c\sqrt{F} = \xi_c$ and $\alpha = \varepsilon$. This is clearly incompatible and hence all solutions must be such that $F' \neq 0$.

The decaying velocity solutions must still respect the same conditions as before, but now the presence of the charge loss mechanisms allows for different predicted behaviour as dictated by both the current and charge equations. Perhaps the most relevant case is the existence of a solution branch given by C1 where both quantities are allowed to grow over time, as long as the expansion rate is sufficiently low such that:

$$\lambda < \frac{2}{3 + g\tilde{c}/k_v} \tag{3.17}$$

which one can easily see that reduces to the critical expansion rate already identified in the previous sections by making the replacements $g \to 1$ or $\tilde{c} \to 0$ to recover the critical expansion rate from Section 3.3 or Section 3.2, respectively.

If solution C1 is not a clear generalisation of the decaying velocity solutions previously found, the upper bound for the expansion rate is also based on the $2/3$ value and in fact a constant charge and current solution that generalises solution B1 is given by solution C2. The constraint on ρ is particularly interesting since in the limit where $Q_0^2 = J_0^2$ it reduces to:

$$\rho = \frac{F' - 2Q_0^2 F''}{2F'} \tag{3.18}$$

which can easily be seen to be compatible with the chiral limit if one further imposes $F'' = 0$, yielding $\rho = 1/2$.

Solution C1: Growing charge and current solution

1. Scaling solutions:

$$L_c = L_0\tau^{\alpha} \quad , \quad \xi_c = \xi_0\tau^{1-\lambda} \quad , \quad J^2 = J_0^2\tau^{\eta} \quad , \quad v = v_0\tau^{-\lambda}$$
$$L = L_0\tau^{\lambda+\alpha} \quad , \quad \xi = \xi_0\tau \quad , \quad Q^2 = Q_0^2\tau^{\eta}$$

2. Additional constraints:

$$\lambda < \frac{2}{3 + g\tilde{c}/k_v} \quad , \quad \mathcal{K} = -\frac{1}{2} \quad , \quad \eta = 2 - 3\lambda - g\tilde{c}\frac{v_0}{\xi_0} > 0$$
$$\alpha = \frac{\lambda}{2} + \frac{g\tilde{c}}{2}\frac{v_0}{\xi_0} \quad , \quad \frac{v_0}{\xi_0} = \frac{2-\lambda}{2k_v + g\tilde{c}} \quad , \quad \left(\frac{\rho}{1-\rho} = \frac{J_0^2}{Q_0^2}\right)^{(*)}$$

* Only for $F'' = 0$.

Solution C2: Constant charge and current solution

1. Scaling solutions:

$$L_c = L_0\tau^{1-\lambda} \quad , \quad \xi_c = \xi_0\tau^{1-\lambda} \quad , \quad J^2 = J_0^2 \quad , \quad v = v_0\tau^{-\lambda}$$
$$L = L_0\tau \quad , \quad \xi = \xi_0\tau \quad , \quad Q^2 = Q_0^2$$

2. Additional constraints:

$$\lambda = \frac{2 + 2\left(1-g\right)c/k_v}{3 + \left(3-2g\right)c/k_v} \quad , \quad \mathcal{K} = -\frac{1}{2} \quad , \quad \rho \neq 0$$

$$4\left(Q_0^2 - J_0^2\right)\frac{Q_0^2 L_0^2}{\xi_0^2}F'' = 1 - \rho\left(\frac{F'\left(Q_0^2 + J_0^2\right) + 2Q_0^2F''\left(Q_0^2 - J_0^2\right)}{J_0^2(F' - 2Q_0^2F'')}\right)$$

A word of caution should be placed here, though, since this solution is only realisable if $\rho \neq 0$ and different solutions emerges if $\rho = 0$ or $\rho = 1$, given by C3 and C4, respectively. Here, the charge, or current, is still preserved, just like in C2, but now the current, or charge, decays away. This effect can seen in Figure 3.6, where the same initial conditions evolve towards different asymptotic solutions depending one the value of ρ. Finally, it should also be noted that solution C2 is closely related to solution B1, and in fact reducing to it in the limit $g = 1$.

Solution C3: Constant charge and decaying current solution

1. Scaling solutions:

$$L_c = L_0\tau^{1-\lambda} \quad , \quad \xi_c = \xi_0\tau^{1-\lambda} \quad , \quad J^2 = J_0^2\tau^{\gamma} \quad , \quad v = v_0\tau^{-\lambda}$$
$$L = L_0\tau \quad , \quad \xi = \xi_0\tau \quad , \quad Q^2 = Q_0^2$$

2. Additional constraints:

$$\lambda = \frac{2 + 2\left(1-g\right)c/k_v}{3 + \left(3-2g\right)c/k_v} \quad , \quad \mathcal{K} = -\frac{1}{2} \quad , \quad \rho = 0$$

$$\gamma = -\frac{2(1-g)\tilde{c}}{k_v + (1-g)\tilde{c}} = -\frac{4(1-g)\tilde{c}}{3k_v + (3-2g)\tilde{c}} < 0$$

Solution C4: Constant current and decaying charge solution

1. Scaling solutions:

$$L_c = L_0\tau^{1-\lambda} \quad , \quad \xi_c = \xi_0\tau^{1-\lambda} \quad , \quad J^2 = J_0^2 \quad , \quad v = v_0\tau^{-\lambda}$$
$$L = L_0\tau \quad , \quad \xi = \xi_0\tau \quad , \quad Q^2 = Q_0^2\tau^{\delta}$$

2. Additional constraints:

$$\lambda = \frac{2+2\,(1-g)\,c/k_v}{3+\,(3-2g)\,c/k_v} \quad , \quad \mathcal{K} = -\frac{1}{2} \quad , \quad \rho = 1$$

$$\delta = -\frac{2(1-g)\tilde{c}}{k_v+(1-g)\tilde{c}} = -\frac{4(1-g)\tilde{c}}{3k_v+(3-2g)\tilde{c}} < 0$$

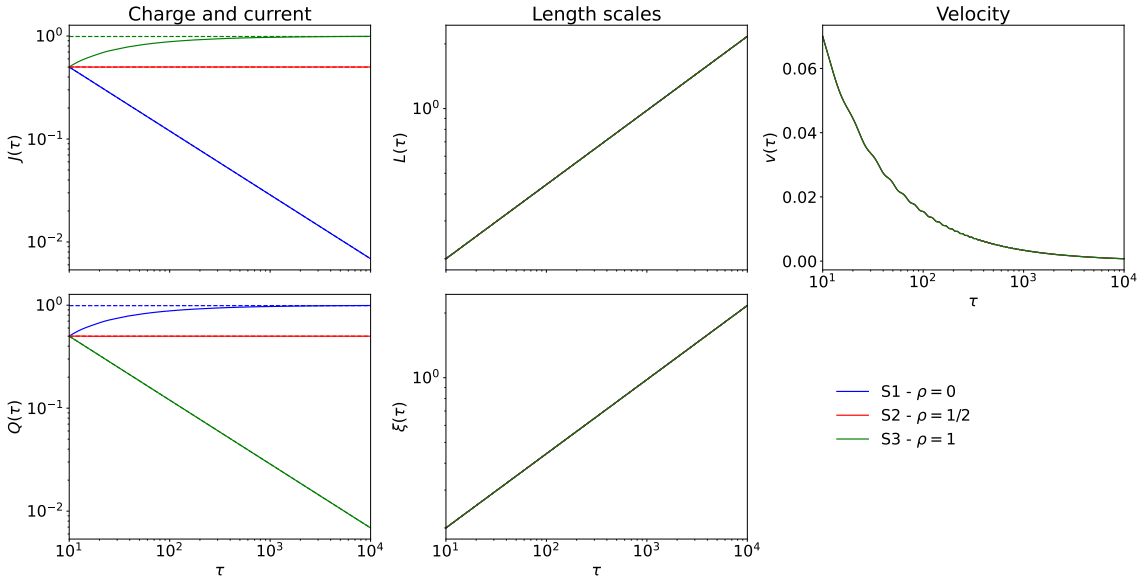

FIGURE 3.6: Network evolution as obtained by numerically solving the generalised VOS differential equations with energy and charge loss mechanisms considering the expansion rate compatible with decaying velocities (see Appendix B for details).

If there are also solutions with decaying velocities, there is also a branch of solutions where the network velocity is constant over the cosmological evolution. In these cases, it still useful to separate a sub-branch where charge and current evolve in a similar way ($\gamma = \delta$), a sub-branch where charge dominates ($\delta > \gamma$) and a sub-branch where current dominates ($\gamma > \delta$). In any case, all solutions are such that $\eta = 2(\varepsilon - \alpha) = 2(1-\alpha)$.

In the first sub-branch, there is a constant charge and current solutions, where the current length scales linearly with conformal time, as given by C6.

Solution C6: Constant charge and current solution

1. Scaling solutions:

$$L_c = L_0\tau \quad , \quad \xi_c = \xi_0\tau \quad , \quad J^2 = J_0^2 \quad , \quad v = v_0$$
$$L = L_0 t \quad , \quad \xi = \xi_0 t \quad , \quad Q^2 = Q_0^2$$

2. Additional constraints:

$$\lambda = \frac{2 - \tilde{c}/k_v\,(1-g)\,/\mathcal{K}}{1+\tilde{c}/k_v} \quad , \quad \rho = \frac{J_0^2}{Q_0^2+J_0^2}\frac{F' - 2Q_0^2F''}{F'}$$

$$2\frac{F''}{F'}\frac{Q_0^2 - J_0^2}{Q_0^2+J_0^2} = \rho\left(\frac{1}{Q_0^2} + \frac{1}{J_0^2}\frac{F'+2Q_0^2F''}{F'-2Q_0^2F''}\right) - \frac{1}{Q_0^2}$$

Solution C7: Growing charge and current solution

1. Scaling solutions:

$$L_c = L_0\tau^{\alpha} \quad , \quad \xi_c = \xi_0\tau \quad , \quad J^2 = J_0^2\tau^{2-2\alpha} \quad , \quad v = v_0$$
$$L = L_0\tau^{\alpha+\lambda} \quad , \quad \xi = \xi_0 t \quad , \quad Q^2 = Q_0^2\tau^{2-2\alpha}$$

2. Additional constraints:

$$\lambda < \frac{v_0k_v}{\xi_0} - \rho\tilde{c}\frac{v_0\xi_0}{J_0^2L_0^2}\frac{1-g}{2F'} \quad , \quad \frac{Q_0^2}{J_0^2} = \frac{1-\rho}{\rho} \quad , \quad F'' = 0$$
$$\alpha = \lambda\left(v_0^2 - C\mathcal{K}\right) + \frac{g\tilde{c}}{2}\frac{v_0}{\xi_0} \quad , \quad \frac{v_0k_v}{\xi_0} = 2\lambda v_0^2\frac{1+\mathcal{K}}{1+2\mathcal{K}}$$
$$\eta = 2\left(\frac{v_0k_v}{\xi_0} - \lambda\right) - \rho\tilde{c}\frac{v_0\xi_0}{J_0^2L_0^2}\frac{1-g}{F'} \quad , \quad 1 = \frac{v_0k_v}{2\xi_0} + \frac{\tilde{c}}{2}\frac{v_0}{\xi_0}$$

Additionally, there are also two solutions where both current and charge grow over time, as given by C7 and C8, which only differ on the value of F'' that is also reflected in the applicable constraints. It should be noted that there are two important constraints that lead to the definition of the critical expansion rate whenever either charge or current are constant, given by:

$$2\left(\frac{v_0k_v}{\xi_0} - \lambda\right) = \frac{\tilde{c}}{\mathcal{K}}\frac{v_0}{\xi_0}(1-g) \tag{3.19a}$$
$$1 = \frac{v_0k_v}{2\xi_0} + \frac{\tilde{c}}{2\xi_0} \tag{3.19b}$$

Solution C8: Growing charge and current solution

1. Scaling solutions:

$$L_c = L_0\tau^{\alpha} \quad , \quad \xi_c = \xi_0\tau \quad , \quad J^2 = J_0^2\tau^{2-2\alpha} \quad , \quad v = v_0$$
$$L = L_0\tau^{\alpha+\lambda} \quad , \quad \xi = \xi_0 t \quad , \quad Q^2 = Q_0^2\tau^{2-2\alpha}$$

2. Additional constraints:

$$\lambda < \frac{v_0 k_v}{\xi_0} \quad , \quad Q_0^2 = J_0^2 \quad , \quad F'' \neq 0$$
$$\alpha = \lambda\left(v_0^2 - C\mathcal{K}\right) + \frac{g\tilde{c}}{2}\frac{v_0}{\xi_0} \quad , \quad \frac{v_0 k_v}{\xi_0} = 2\lambda v_0^2\frac{1+\mathcal{K}}{1+2\mathcal{K}}$$
$$\eta = 2 - 2\alpha = 2\left(\frac{v_0 k_v}{\xi_0} - \lambda\right) \quad , \quad 1 = \frac{v_0 k_v}{2\xi_0} + \frac{\tilde{c}}{2}\frac{v_0}{\xi_0}$$
$$1 = \lambda v_0^2\left(1+\mathcal{K}\right) - \frac{v_0 k_v}{\xi_0}\mathcal{K} + \frac{\tilde{c}}{2}\frac{v_0}{\xi_0}$$

Solution C9: Constant charge and current solution

1. Scaling solutions:

$$L_c = L_0\tau \quad , \quad \xi_c = \xi_0\tau \quad , \quad J^2 = J_0^2 \quad , \quad v = v_0$$
$$L = L_0 t \quad , \quad \xi = \xi_0 t \quad , \quad Q^2 = Q_0^2\tau^{\delta}$$

2. Additional constraints:

$$2\left(\frac{v_0 k_v}{\xi_0} - \lambda\right) = \frac{\tilde{c}v_0}{\xi_0}\frac{1-g}{\mathcal{K}} \quad , \quad \frac{v_0 k_v}{\xi_0} = 2\lambda v_0^2\frac{1+\mathcal{K}}{1+2\mathcal{K}}$$
$$\delta = \frac{F' + 2J_0^2F''}{F'}\frac{\tilde{c}v_0}{\xi_0}\frac{1-g}{\mathcal{K}} < 0 \quad , \quad 1 = \frac{v_0 k_v}{2\xi_0} + \frac{\tilde{c}}{2}\frac{v_0}{\xi_0}$$
$$\lambda v_0^2\frac{1+\mathcal{K}}{1+2\mathcal{K}} = 1 - \frac{\tilde{c}}{2}\frac{v_0}{\xi_0} \quad , \quad \lambda = 2 - \tilde{c}\frac{v_0}{\xi_0}\left(1 - \frac{1-g}{2\mathcal{K}}\right)$$
$$\lambda = \frac{2 - \tilde{c}/k_v\left(1-g\right)/\mathcal{K}}{1+\tilde{c}/k_v} \quad , \quad \rho = 1$$

If these, or equivalent expressions, hold, then the compatible expansion rate must be such that:

$$\lambda = \frac{2 - \tilde{c}/k_v\left(1-g\right)/\mathcal{K}}{1+\tilde{c}/k_v} \tag{3.20}$$

It can be easily checked that for $g = 1$ the expansion rate from B5 is recovered.

The sub-branch where current eventually dominates the evolution is simpler, in the sense that in this case, a single solution is possible, as given by C9. In this case, ρ is required to be unity, while the current is constant, the charge decays, and the current length scales linearly. These restrictions remove the role of F'' in further distinguishing between different solutions.

Finally, the last sub-branch that is yet to be explored is dominated by charge over currents. In this case, the value of F'' is relevant once more, since it effectively decouples between C10 and C11.

Solution C10: Constant charge and current solution

1. Scaling solutions:

$$L_c = L_0\tau \quad , \quad \xi_c = \xi_0\tau \quad , \quad J^2 = J_0^2\tau^\gamma \quad , \quad v = v_0$$
$$L = L_0 t \quad , \quad \xi = \xi_0 t \quad , \quad Q^2 = Q_0^2$$

2. Additional constraints:

$$\lambda = \frac{2 - \tilde{c}/k_v\,(1-g)\,/\mathcal{K}}{1 + \tilde{c}/k_v} > \frac{v_0 k_v}{\xi_0}$$
$$\gamma = 2\left(\frac{v_0 k_v}{\xi_0} - \lambda\right) < 0 \quad , \quad F'' \neq 0 \quad , \quad \rho = 0$$

Solution C11: Constant charge and current solution

1. Scaling solutions:

$$L_c = L_0\tau^\alpha \quad , \quad \xi_c = \xi_0\tau \quad , \quad J^2 = J_0^2\tau^\gamma \quad , \quad v = v_0$$
$$L = L_0\tau^{\alpha+\lambda} \quad , \quad \xi = \xi_0 t \quad , \quad Q^2 = Q_0^2\tau^\delta$$

2. Additional constraints:

$$\frac{\tilde{c}v_0}{\xi_0}\frac{1-g}{\mathcal{K}} < 0 \quad , \quad \rho = 0 \quad , \quad F'' = 0$$
$$\gamma = 2\left(\frac{v_0 k_v}{\xi_0} - \lambda\right) \quad , \quad \delta = \gamma - \frac{\tilde{c}v_0}{\xi_0}\frac{1-g}{\mathcal{K}}$$
$$\alpha = \lambda\left(v_0^2 - C\mathcal{K}\right) + \frac{g\tilde{c}}{2}\frac{v_0}{\xi_0} \quad , \quad \delta = 2 - 2\alpha > 0$$

In both cases, it must be that $\rho = 0$, which can be read as the opposite limit of C9. If $F'' \neq 0$, then charge is not allowed to grow and must remain constant, while currents must decay and the current length scales linearly, as given by C10. On the other hand, if $F'' = 0$, a more general solutions is found as given by C11. A numerical comparison of the different possibilities is presented in Figure 3.7. A final comparison between two similar simulations, but with different values for $\tilde{c}$ and g is presented in Figure 3.8, where the distinct scaling of the current and correlation length can be easily seen. Note that the selected parameters have the particularity of ensuring that:

$$\lambda_1 = \frac{2 + 2\left(1 - g_1\right) c_1/k_v}{3 + \left(3 - 2g_1\right) c_1/k_v} \tag{3.21a}$$

$$\lambda_2 = \frac{2 - \tilde{c}_2/k_v \left(1 - g_2\right)/\mathcal{K}}{1 + \tilde{c}_2/k_v} \tag{3.21b}$$

or, assuming $\mathcal{K} = -1/2$ and k_v to be the same in both situations:

$$\frac{2 + 2\left(1 - g_1\right) c_1/k_v}{3 + \left(3 - 2g_1\right) c_1/k_v} = \frac{2 + 2\tilde{c}_2/k_v \left(1 - g_2\right)}{1 + \tilde{c}_2/k_v} \tag{3.22}$$

The condition above ensures that the same expansion rate will be identifiable with the compatible value with either decaying or constant velocities.

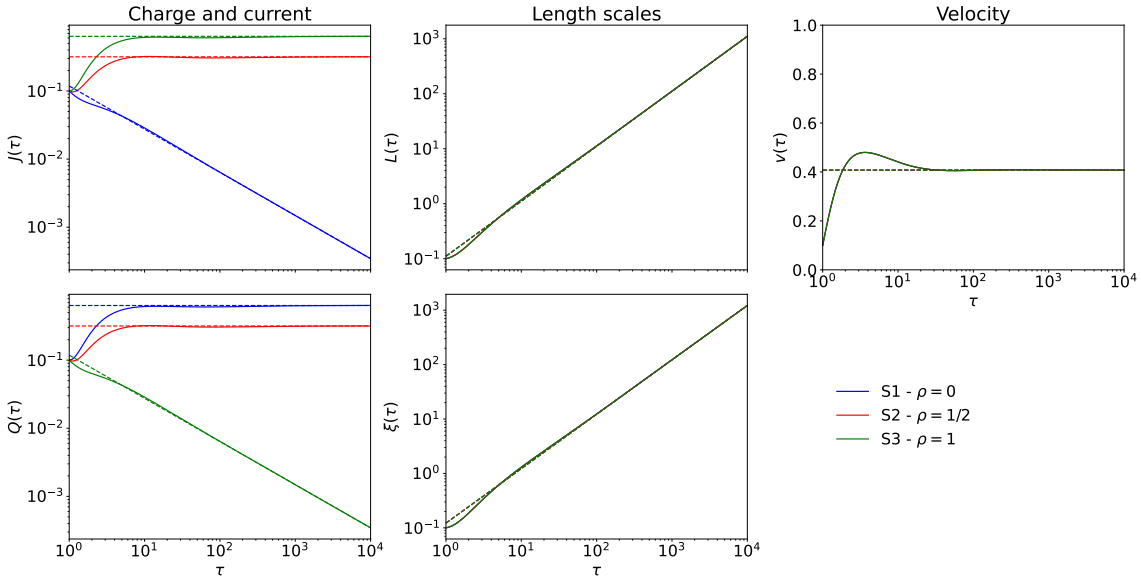

FIGURE 3.7: Network evolution as obtained by numerically solving the generalised VOS differential equations with energy and charge loss mechanisms considering expansion rates compatible with constant velocities, but different charge and/or current behaviour (see Appendix B for details).

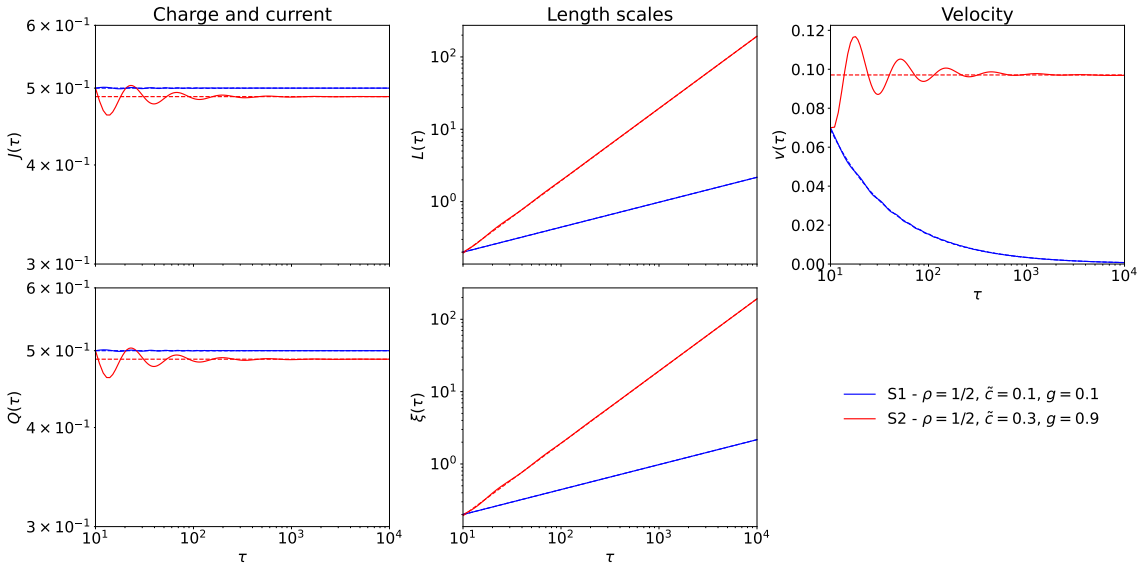

FIGURE 3.8: Network evolution as obtained by numerically solving the generalised VOS differential equations considering different energy and charge loss parameters (see Appendix B for details).

3.5 Solutions with dynamical bias function

Having explored the branches with and without energy losses, it is now time to complete the analysis by explicitly incorporating the bias function on charge and currents and hence on conformal time.

Starting once again from the current equation, it can be seen that another possibility emerges where solutions with $1+\beta-\varepsilon>0$ may be realisable, as long as it is verified that $2\varepsilon-2\alpha-\gamma-\cdots=0$, where the dots stand for some particular dependence on δ, depending on the its value and on F' and F''. This condition will make the first and last terms to perfectly balance each other. However, further investigating the cases where $1+\beta-\varepsilon\neq 0$ reveal that they are not compatible with the full set of equations and hence it must be that $\varepsilon=1+\beta$. Making the adequate substitutions, the equations now read:

$$\alpha = \lambda \left[v_0^2 \tau^{2\beta} - C\mathcal{K}\tau^{2(\alpha-\varepsilon)+\eta} \right] + g_0 \frac{\tilde{c}}{2} \frac{v_0}{\xi_0} \tau^{\eta} \tag{3.23a}$$

$$\beta = C \left[\frac{k_v}{v_0 \xi_0} \tau^{-2\beta} \left(1 + 2\mathcal{K}\tau^{2(\alpha-\varepsilon)+\eta} \right) - 2\lambda \left(1 + \mathcal{K}\tau^{2(\alpha-\varepsilon)+\eta} \right) \right] \tag{3.23b}$$

$$\gamma = 2 \left(\frac{v_0 k_v}{\xi_0} - \lambda \right) + \rho\tilde{c} \frac{v_0 \xi_0}{J_0^2 L_0^2} \frac{g_0}{F' - 2Q_0^2 \tau^{\delta} F''} \tau^{\eta - \left[2(\alpha-\varepsilon)+\gamma \right]} \tag{3.23c}$$

$$\delta = 2 \frac{F' + 2J_0^2 \tau^{\gamma} F''}{F' + 2Q_0^2 \tau^{\delta} F''} \left(\frac{v_0 k_v}{\xi_0} - \lambda \right) + (1-\rho)\tilde{c} \frac{v_0 \xi_0}{Q_0^2 L_0^2} \frac{g_0}{F' + 2Q_0^2 \tau^{\delta} F''} \tau^{\eta - \left[2(\alpha-\varepsilon)+\delta \right]} \tag{3.23d}$$

$$\varepsilon = \lambda v_0^2 \tau^{2\beta} \left(1 + \mathcal{K}\tau^{2(\alpha-\varepsilon)+\eta} \right) - \frac{v_0 k_v}{\xi_0} \mathcal{K}\tau^{2(\alpha-\varepsilon)+\eta} + \frac{\tilde{c}}{2} \frac{v_0}{\xi_0} \tag{3.23e}$$

In fact, looking more closely to the equations, it is clear that the characteristic length equation can only be fulfilled if:

$$\alpha = \varepsilon \tag{3.24a}$$

$$\lambda C \mathcal{K} = g_0 \frac{\tilde{c}}{2} \frac{v_0}{\xi_0} \tag{3.24b}$$

since in any other case the diverging term on the right will always dominate. Although this could not be an issue, the first constraint when used together with the correlation length equation yields:

$$\mathcal{K}\tau^{\eta} \left(\lambda v_0^2 \tau^{2\beta} - \frac{v_0 k_v}{\xi_0} \right) + \frac{\tilde{c}}{2} \frac{v_0}{\xi_0} = 0 \tag{3.25}$$

which clearly cannot be fulfilled for $\eta > 0$, as is being assumed here.

Chapter 4

Comparison with numerical simulations

4.1 Introduction

After studying the possible scaling solutions from an analytical point of view, it was considered adequate to provide some preliminary comparison against field theory numerical simulations, which is the goal of this Chapter. The main objective is to characterise the parameters that govern the evolution of the different parameters of interest, with particular attention given to the power law exponent of the scaling solutions. Additionally, the branch of the analytical solutions that is currently being spanned by the simulations will be identified. However, and because numerical simulations of cosmic strings networks is a topic on its own, with inherent challenging topics, not only related to the simulation itself, but also to the best diagnosis to characterise the results, a brief introduction is needed.

4.2 Numerical simulations of cosmic strings networks

Field theory numerical simulations present significant challenges and the reader is referred to the work by Correia and Martins [21] and Correia [22] for extensive details on this matter.

Firstly, it should be mentioned that there are essentially two ways of simulating the evolution of networks of strings. On one hand, in what may be read as a more macroscopic approach, Nambu-Goto types of simulations are based on filament-like elements. Although this approach may be justified as long as the string thickness is much smaller than its length and has already been used by different and independent research groups [23–27], it

also inevitably leaves out some important physical aspects of the microscopic physics at play, such as a loop formation. On the other hand, strings may not be directly simulated, but rather the fields whose configurations constitute the strings themselves. In this case, the full microscopic physics is properly considered, but this comes at a much greater computational cost, which manifests itself as lower dynamic range and/or spatial resolution. In any case, and since the microscopic physics content is preserved, these type of simulations can be easily generalised from simple abelian-Higgs models (see, for instance, [28]) to multiple fields simulations [21], a task clearly hardly realisable in Nambu-Goto simulations. The results that will be analysed here were obtained following the latter approach and conducted by José Ricardo Correia, the main author of many of the references above.

It is important to note that while in Nambu-Goto simulations the relevant macroscopic properties of the network can be easily estimated since the strings are well defined at all time instants, the same does not happen for field theory simulations, where diagnosis criteria whose focus is the correct interpretation of the fields' configuration at a given time step and their translation into macroscopic quantities also play an important role. The correlation length, as measured by the typical string-to-string distance, for instance, can be estimated from the box volume ($\mathcal{V}$, for its physical size, or V, when expressed in number of cells used for the simulation) and the string length (ℓ). While the former is known, the latter must be estimated and this leads to two different approaches that are often applied [16]:

$$\hat{\xi}_{\mathcal{L}} = \sqrt{-\frac{\mu V}{\sum_x \mathcal{L}_x}} \tag{4.1a}$$

$$\hat{\xi}_{W} = \sqrt{\frac{\mathcal{V}}{\sum W_{ij}}} \tag{4.1b}$$

The first approach is founded on the fact that Lagrangian density evaluated at each lattice cell ($\mathcal{L}_x$) is negatively peaked at the strings and vanishes away from it [29], while the latter is obtained simply by computing the gauge-invariant winding (W_{ij}), that is non-null if a string is piercing that particular cell. A similar analysis can be made for the remaining quantities of interest and the reader is referred to the work by Correia and Martins [21], but it should be clear that different choices may yield different estimators.

Finally, an important point should be made regarding the generation of the initial conditions and their approach to the scaling regimes. As the defects width is typically constant, but simulations are carried out in a box representing an expanding universe, they would eventually become too short in comoving coordinates to ever be identified in the

simulations [30]. To solve this issue, the coupling terms are often modified to account for a dependence on the scale factor, hence allowing to properly resolve the defects. Another issue is related to initial conditions themselves, which are often associated to an highly excited state [31]. To help dissipate this energy excess, an artificial over-damped epoch with exponential expansion, or a sufficiently faster power law, is typically prescribed. Although this strategy does indeed allow for a faster approach to scaling, it also distorts the time counting of the simulation, critical to identify the scaling regime properties. The most relevant consequence for this work is that the different quantities of interest no longer scale as $\propto \tau^p$, but rather as:

$$A(\tau) = A_0 \left(\tau - \tau_0\right)^p \tag{4.2}$$

where τ_0 is a time offset that mimics the impact of the artificially over-damped period of the simulations. It should be noted that for sufficiently high dynamic ranges this would not be an issue, but as already mentioned, dynamic range is often a limitation of this type of simulations.

4.3 Data description and inspection

Having presented a brief overview of the main concerns when performing numerical simulations of cosmic strings, the results may now be analysed. In this work 12 independent simulations considering different initial conditions for 4 different expansion rates, making a total of 48 time series, will be considered. The generated time series of all simulations are presented in Figure 4.1 and Figure 4.2, grouped by initial conditions.

One can immediately see overall trends that are consistent between all simulations. Firstly, the faster the expansion rate considered, the lower the network asymptotic velocity and the charge. This comes with no surprise, as the highest expansion rates are expected to be more efficient at erasing the defects. Additionally, the charge to current ratio (last row in both figures) seem to be reasonably stable, specially for the lowest expansion rate, but is not unity. Finally, the step-like behaviour identifiable in both charge and current time series indicates that the simulations are on the verge of being able to properly track the evolution of these macroscopical quantities. This is particularly relevant since it may distort the results if one intends to combine the different "observations" into an expected value and uncertainty level. To mitigate this issue a pre-processment of the data was carried out where these plateaus were identified and smoothed out of the time series, leaving a

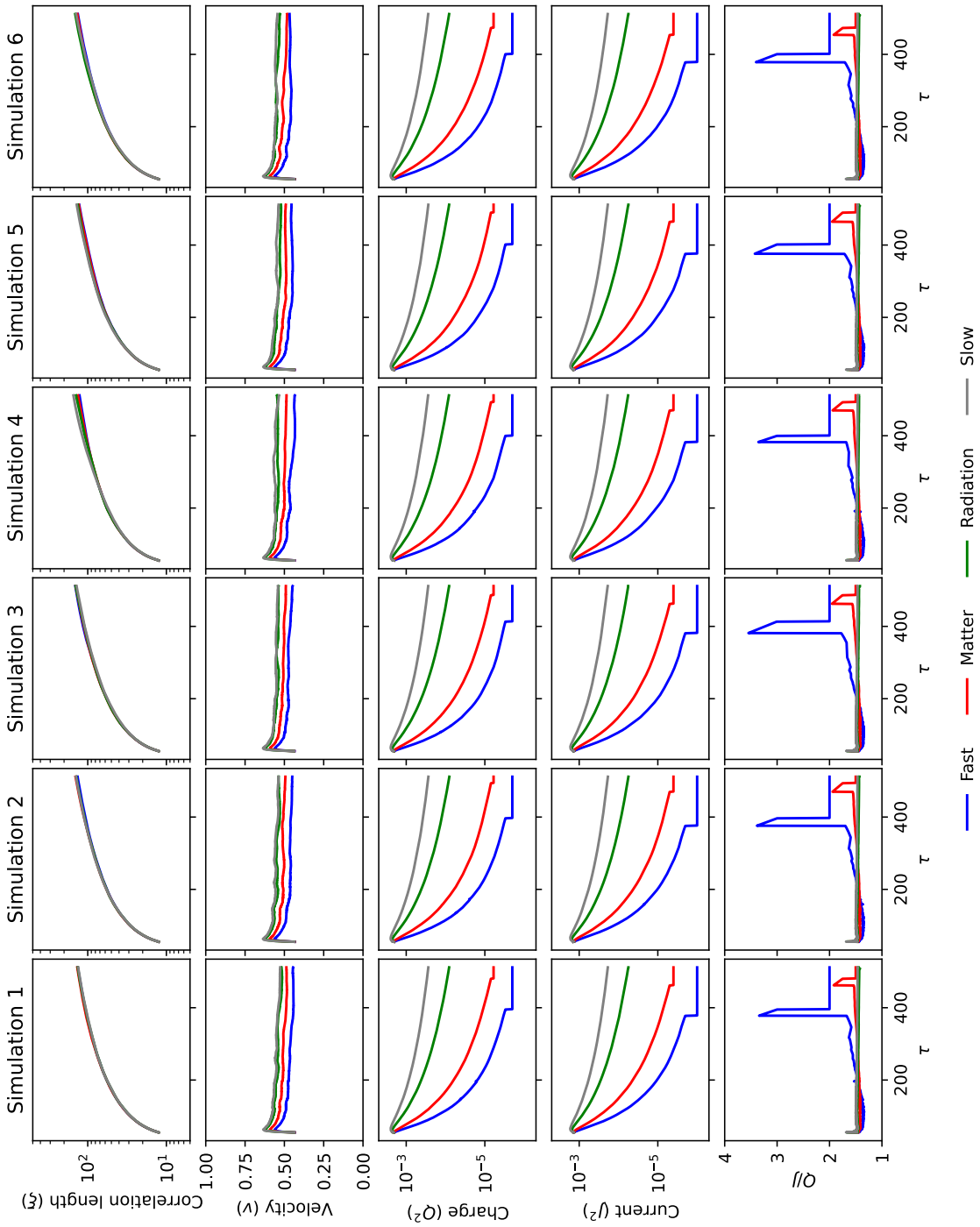

FIGURE 4.1: Time series estimated from the numerical simulations 1 to 6 grouped by initial conditions.

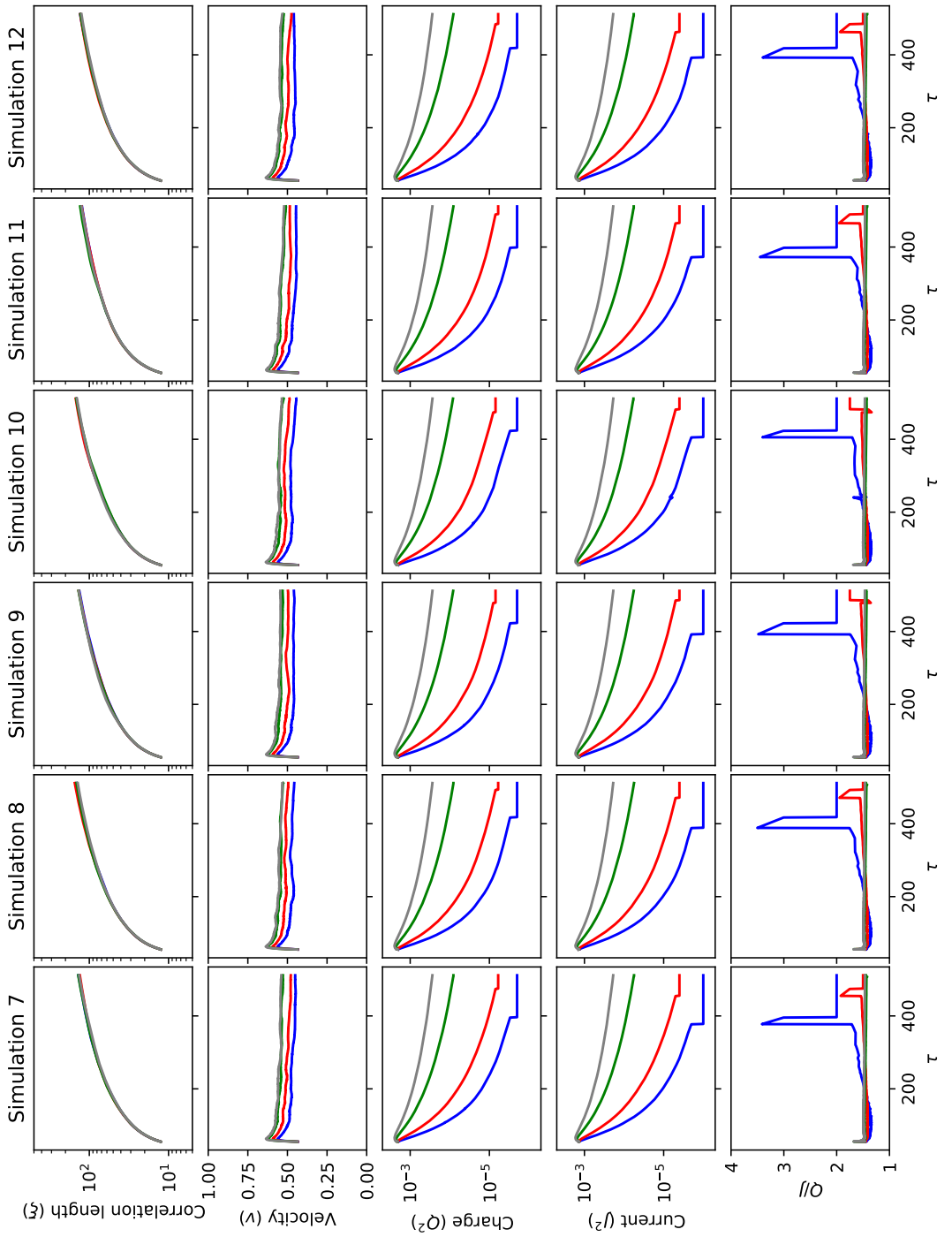

FIGURE 4.2: Time series estimated from the numerical simulations 7 to 12 grouped by initial conditions.

more well behaved response to analyse, up until the onset of the last identified plateau, which could not be properly accounted for. The results of all the simulations grouped by expansion rate, as well as its mean value and 1σ region, are presented in Figure 4.3, for the original data, and in Figure 4.4, for the smoothed data. For the remaining of this work, only the latter will be used.

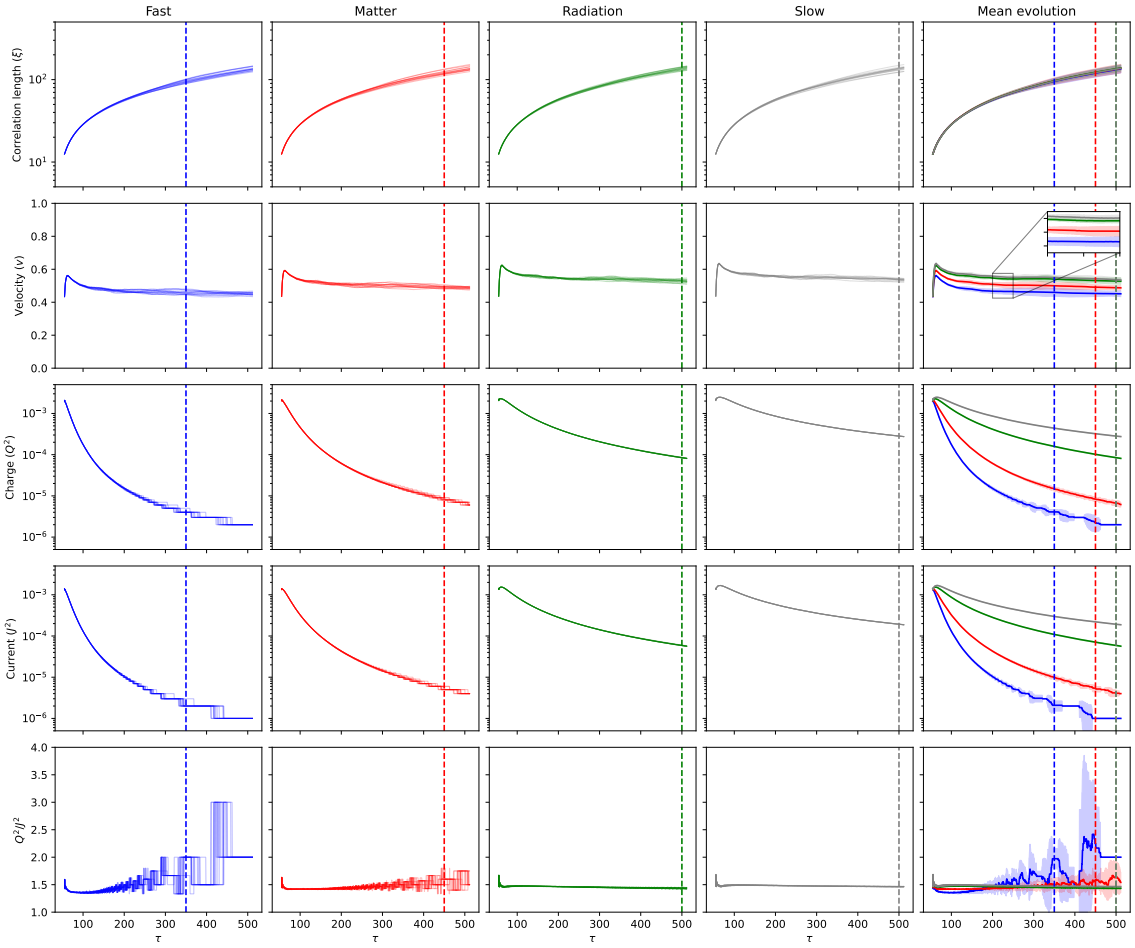

FIGURE 4.3: Raw time series estimated from the numerical simulations grouped by expansion rate.

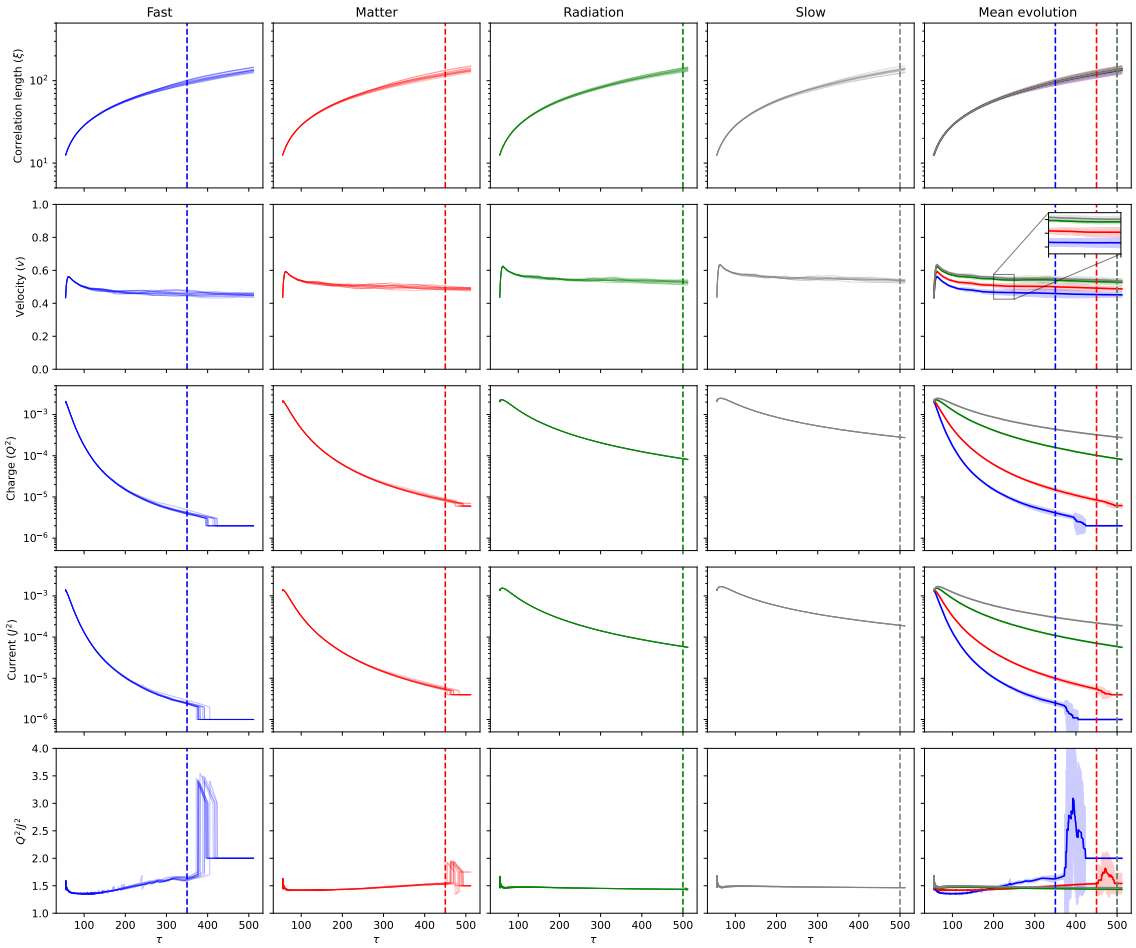

FIGURE 4.4: Smoothed time series estimated from the numerical simulations grouped by expansion rate. The vertical dashed lines define the dynamic range limit assumed for each simulation.

4.4 Preliminary parameters estimation

Having analysed and pre-processed the data series in the previous section, it is fundamental to be able to extract from them the relevant parameters that may be compared against the analytical solutions. In this section, this task will be handled by different approaches, starting from a direct least squares fit and ending with a full MCMC analysis to better constraint the parameters. In all cases, it should be recalled that the evolutionary model that will be assumed is of the type:

$$A(\tau) = A_0 \, (\tau - \tau_0)^p \tag{4.3}$$

where τ_0 is expected to be the same for all parameters within a given simulation, and even for all simulations that share a common expansion rate, provided the over-damped epoch is equivalent. The velocity is assumed to be constant and hence defined by a single parameter.

From a visual inspection of the results, it was considered adequate to consider the period starting at $\tau = 100$, up until the dashed lines in Figure 4.4, where the solutions appear to have reasonably converged.

The first approach was to simply fit a curve governed by Equation 4.3. There are, however, two distinct possibilities: either to fit each realisation separately, or to consider a single realisation from the mean evolution, where the dispersion around the mean value is considered as an uncertainty. The results from the latter approach are presented in Figure 4.5, while all the fitted parameters are presented in Figure 4.6. In this case, the fit to each simulation is represented by a dot, while the horizontal line and the shaded region were obtained from the overall fit.

It is interesting to note that fitting each realisation separately provides drastically different outcomes when compared to the overall fit. This can be at least partially explained by noting that as different orders can be spanned by the data to be fitted, a single fit that does not incorporate any uncertainty on the data points will tend to favour the highest values. This is particularly relevant for the charge and current decays, where in Figure 4.5 a poorer agreement between fitted and observed data is clearly visible in the latest part of the simulation. It should be noted that this may indicate that the network is not fully

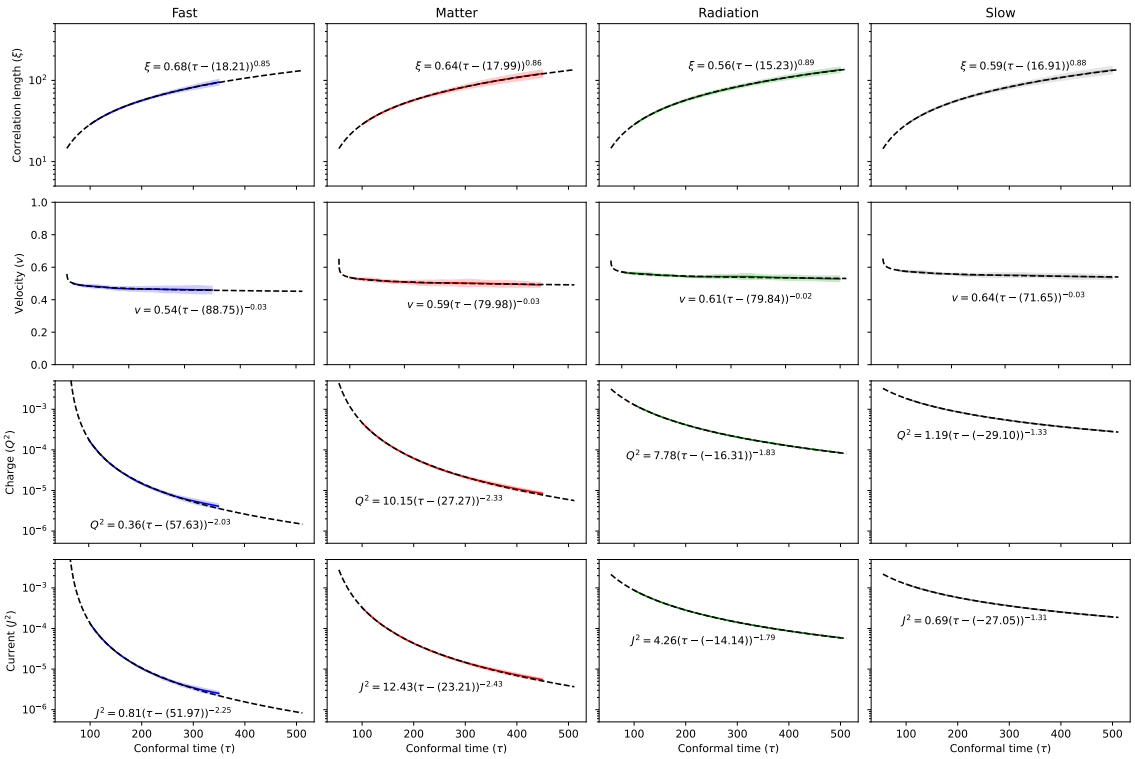

FIGURE 4.5: Estimated power laws considering the mean evolution time series.

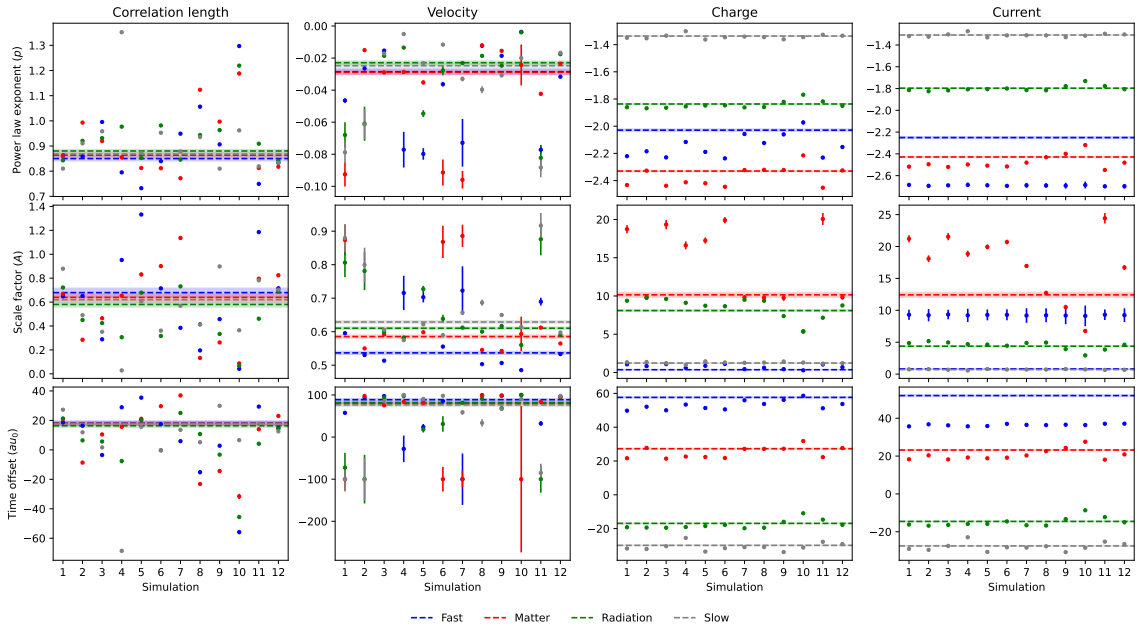

FIGURE 4.6: Power law exponent and scale factor for all expansion rates and initial conditions.

converged yet and that the scaling exponents are actually varying during the dynamic range under analysis. In any case, the time offset can be seen to be reasonably constant and lower then 50 for all cases, which allow us to make a log-log fit considering the last part of the simulations by making the approximation:

$$A(\tau) = A_0 \left(\tau - \tau_0\right)^p \approx A_0 \tau^p \longrightarrow \ln A \approx \ln A_0 + p \ln \tau \tag{4.4}$$

Simple error propagation under the Gaussian assumption can be easily used to estimate the uncertainty in the offset at the $x-$axis interception into uncertainties into the scale factor. The results are presented in Figure 4.7, where it can now be seen that the individual fits as well as the mean fit are now much more consistent.

The simple least square analysis conducted until now to provide a first grasp into the expected value of the power law exponent and scale factor of the different quantities of interest has shown that a critical point was the fact that the simulations may, in principle, exhibit a given offset in time. Here, we would like to have an alternative approach that does not depend on the proper identification of this time offset. We note that the corresponding quantity rate of change is given by:

$$\dot{A} = A_0 p \left(\tau - \tau_0\right)^{p-1} \tag{4.5}$$

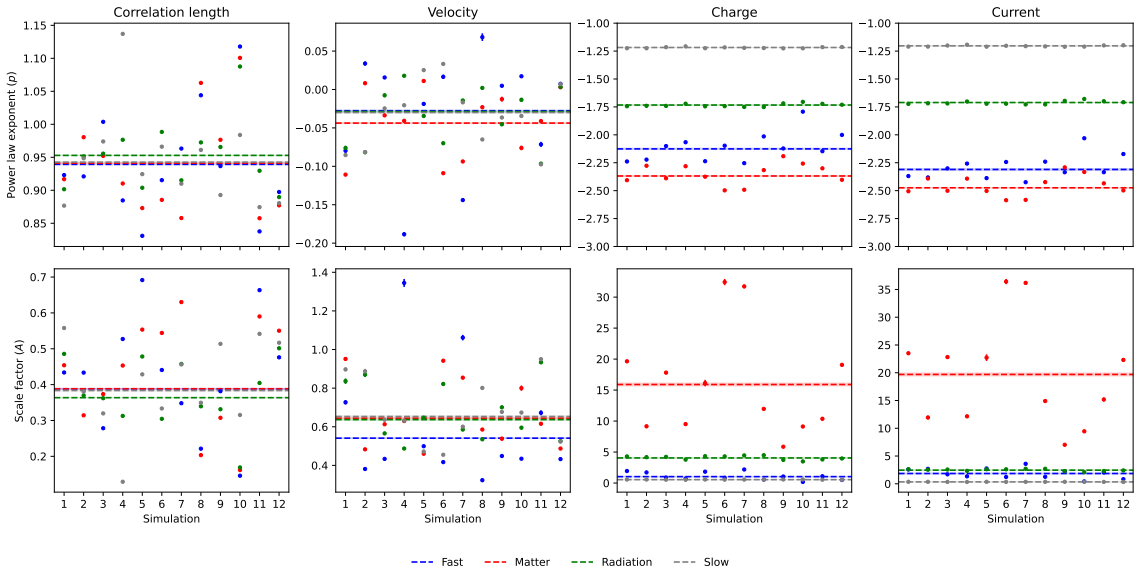

FIGURE 4.7: Power law exponent and scale factor for all expansion rates and initial conditions considering a log-log fit from $\tau = 250$ onward.

meaning that the degeneracy between the power law exponent and the, unknown, time offset, can be removed by writing:

$$\frac{A}{\dot{A}} = \frac{1}{p}\tau - \frac{\tau_0}{p} \tag{4.6}$$

Although the procedure above should, in principle, provide robust estimates, it does rely on the ability to properly estimate the time derivative of the different quantities of interest, which may introduce uncertainties in the process. However, and since this linear relation is expected to hold for any time offset and scaling exponent, the derivative may be computed between points with a given time delay to minimise the uncertainties. Additionally, this procedure allows us to analyse if the best fit power law exponent is actually evolving along the simulation or not.

The results for the mean simulation of all the steps above is presented in Figure 4.8 and Figure 4.9, where it has also been included a fit considering only the points for $\tau \geq 250$.

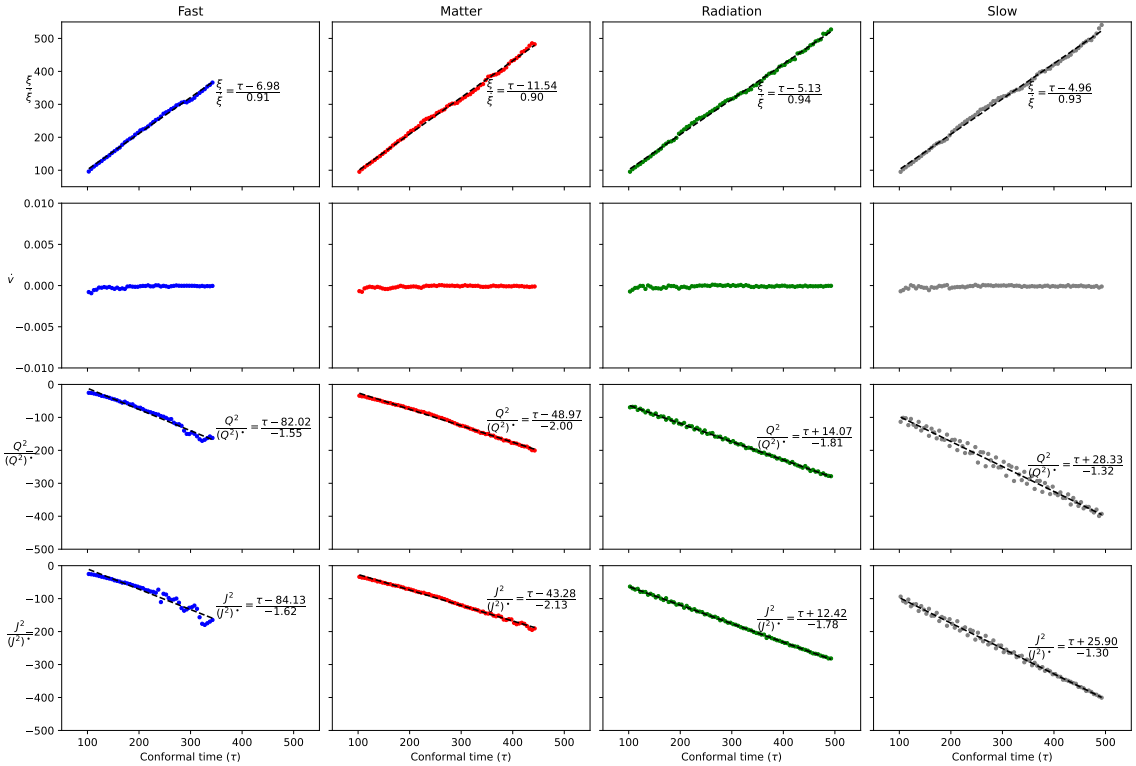

FIGURE 4.8: Fits to the derivative estimators considering all the points.

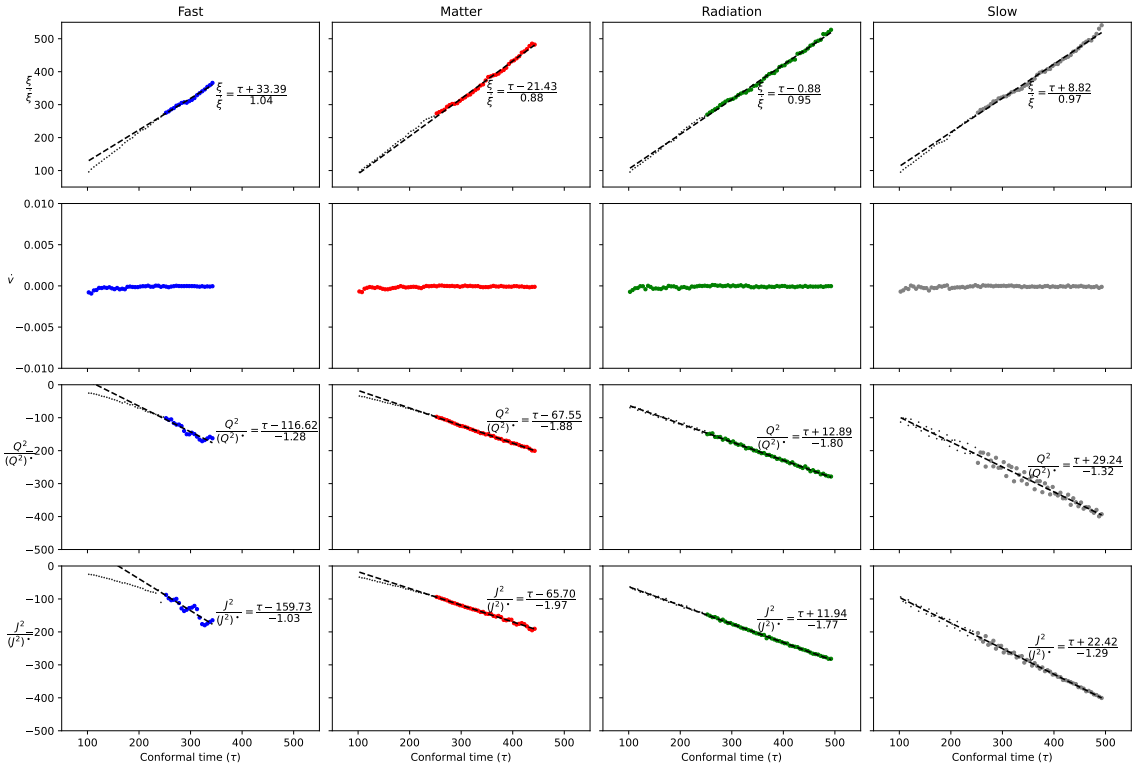

FIGURE 4.9: Fits to the derivative estimators considering only points where $\tau \geq 250$.

4.5 Markov Chain Monte Carlo methods

Finally, and to better understand the correlations between the different parameters of the power law evolution defined by Equation 4.3, a simple code to run a Markov Chain Monte Carlo (MCMC) analysis was developed. Since this is still unexplored in the present document, it was considered that a previous theoretical description was firstly needed, before presenting the results. It should ne noted that the description here is mostly adapted from the previous work by Pimenta et al. [32].

4.5.1 Theoretical background

The core definition of an MCMC analysis is the ability to sample a given probability distribution. In this case, the desired probability function is associated to a given hypothesis or model, H_i, conditioned to the observational data (or, in this case, numerical simulations outputs), D_{obs}, and some previous information, I. Using the product rule in probabilities, it can be shown that the probability density function of interest, $P(H_i|D_{obs} \cap I)$, is given by:

$$P(H_i|D_{obs} \cap I) = \frac{P(H_i|I) \times P(D_{obs}|H_i \cap I)}{P(D_{obs}|I)} \tag{4.7}$$

It is customary to identify the probabilities above as the prior distribution ($P(H_i|I)$), containing the previous belief that a particular hypothesis is true from some previous (not related to the data) information, the likelihood, containing the probability of obtaining the observed data from the hypothesis and previous information ($P(D_{obs}|H_i \cap I)$), usually represented as $\mathcal{L}(H_i)$, and the posterior distribution function, which essentially updates the prior information from the data. The prior and posterior names are easily understood as they represent the probability of the hypothesis being true, before and after considering the new data. Further extending this reasoning, the hypothesis can still depend on some model parameters, $\boldsymbol{\theta}$, in which case, the posterior distribution for the parameters is:

$$P(\boldsymbol{\theta}|D \cap I) = \frac{P(\boldsymbol{\theta}|I) \times P(D|\boldsymbol{\theta} \cap I)}{P(D|I)} \propto P(\boldsymbol{\theta}|I) \times P(D|\boldsymbol{\theta} \cap I) = P(\boldsymbol{\theta}|I) \times \mathcal{L}(\boldsymbol{\theta}) \tag{4.8}$$

where it has been tacitly assumed that the model chosen is, indeed, the true model. Under this assumption, the question is no longer what model best fits the data, but which are the most probable parameters to it (in this case, $\boldsymbol{\theta}$).

As the model parameter space size increases, the characterisation of the posterior distribution is more easily obtained by Markov Chain Monte Carlo (MCMC), rather then by

directly searching the parameter space. The main idea behind this method is to construct samples that respect a given distribution taking random walks over the parameter space, where the new sample (of parameters) $\boldsymbol{\theta}_{i+1}$ depends solely on the previous step, $\boldsymbol{\theta}_i$, and on the transition probability, formalised by $p(\boldsymbol{\theta}_{i+1}|\boldsymbol{\theta}_i)$. If the initial period, that is strongly affected by the particular initial conditions of the walk, is rejected, the samples obtained do follow the posterior distribution $p(\boldsymbol{\theta}|D \cap I)$. In this work, an algorithm based on the Metropolis-Hastings algorithm (MH) [33, 34] has been used, iterating over the following steps:

1. An initial value is chosen within the parameter space $\boldsymbol{\theta}_i = \boldsymbol{\theta}_1$
2. A proposed value for $\boldsymbol{\theta}_{i+1}$, $\boldsymbol{\Gamma}$, is generated from a proposal distribution, usually taken as a multivariate Gaussian function with prescribed mean and covariance function.
3. The metropolis ratio is computed, defined as $r = \dfrac{p(\boldsymbol{\Gamma}|I)}{p(\boldsymbol{\theta}_i|I)} \dfrac{\mathcal{L}(\boldsymbol{\Gamma})}{\mathcal{L}(\boldsymbol{\theta}_i)} \dfrac{q(\boldsymbol{\theta}_i|\boldsymbol{\Gamma})}{q(\boldsymbol{\Gamma}|\boldsymbol{\theta}_i)}$, being q the proposal distribution.
4. A random number U is generated from an uniform distribution in the interval 0 to 1.
5. If $r \geq U$, then the proposal is accepted and $\boldsymbol{\theta}_{i+1} = \boldsymbol{\Gamma}$, otherwise $\boldsymbol{\theta}_{i+1} = \boldsymbol{\theta}_i$.

4.5.2 Implementation

To properly implement the MH algorithm the likelihood function must be defined so that the Metropolis ratio may be computed. In this case, and taking into account all the available simulations, it may be written, for n data points assumed to be independent, as:

$$\mathcal{L}(\boldsymbol{\theta}) = \frac{1}{(2\pi)^{n/2}\left|\det \mathbf{C}\right|^{1/2}} \exp\left[-\frac{1}{2}\boldsymbol{\epsilon}\mathbf{C}^{-1}\boldsymbol{\epsilon}^{T}\right] \approx \frac{1}{(2\pi)^{n/2}\prod_i \sigma_i} \exp\left[-\frac{1}{2}\sum_i \left(\frac{\epsilon_i}{\sigma_i}\right)^2\right] \quad (4.9)$$

where $\boldsymbol{\theta}$ contains all the relevant model properties (in this case, scale factor, power law exponent and time offset), $\boldsymbol{\epsilon}$ is the error vector obtained as the difference between the predictions of Equation 4.3, when the model properties are $\boldsymbol{\theta}$, and simulated values, and $\mathbf{C}$ is the covariance matrix. The last equality follows from assuming the covariance matrix to be diagonal with non vanishing elements given by the standard deviation, σ_i, of the different realisations.

Having the likelihood function, only the prior distributions are required to implement the MH algorithm. In this work, these have been assumed to be uniform in a given range

for the power law exponent and time offset, while for the scale factor, a modified Jeffreys prior was defined as [35]:

$$p(\mathbf{\Phi}_{i,j}|I) \propto \frac{1}{\mathbf{\Phi}_{i,j} + \phi_{min}} \tag{4.10}$$

Note that while the Metropolis ratio reduces to the likelihood ratio for the time offset and power law exponent, it does not do so for the scale factor, where the prior distribution should be explicitly considered.

Additionally, fixed length chains have been constructed starting by a random value between predefined limit ranges for the different model, based on the results obtained in Section 4.4. It has also been assumed independent one dimensional Gaussian distributions for each parameter as proposal distributions, with a standard deviation that was updated for the first half of the chain at every U steps by the recursion relation:

$$\hat{\sigma}_i^k = \hat{\sigma}_i^{k-1} + (\hat{A}_r^k - A_r) \times 10^{\text{int}\left[\log \hat{\sigma}_i^k\right]} \tag{4.11}$$

where $\hat{\sigma}_i$ is the standard deviation associated with the proposal distribution of the model parameter i, $\hat{A}_r^k$ is the estimated acceptance rate from the U points and $\hat{A}_r$ is the intended acceptance rate, that has been defined as 0.3, in accordance with results obtained in [36]. After running steps 1 to 5 of the MH algorithm, the convergence of each model parameter chain should be tested. In this work, an adaptation of the Gelman and Rubin statistics [37] taken from the work by Brinckmann and Lesgourgues [38] was used, where each full chain is divided into 3 smaller ones that are then used to estimate the potential scale reduction factor.

4.5.3 Results

Having presented the main principles and the code properties developed, the MCMC analysis were performed taking into account the correlation, charge and current behaviours and the following model parameters:

- 3 power law exponents (one for each quantity of interest), with a corresponding uniform prior
- 3 scale factor (one for each quantity of interest), with a corresponding Jeffreys prior
- 1 time offset

The velocity evolution was not considered in this analysis, since it will be mostly insensitive to the time offset. In all the corner plots that will be presented, the quantities related to the correlation length, charge and current, will be displayed in blue, red and green, respectively.

Starting from the radiation epoch simulations, the results considering the full time series ($\tau \geq 100$) or only the last part of it ($\tau \geq 250$) are presented in Figure 4.10 and Figure 4.11. Although it can be seen that the correlation length power law exponent is constrained differently in both cases, it is also true that this does not seem to impact significantly on the decaying results for charge and current, but reflecting itself in the charge and current scale factor. Although ideally only the upper part of the time series would be used, in the faster expansion rates this is precisely the region that is poorly sampled by the simulations, but if it is assumed that the power law governing their evolution are mostly unaffected by the correlation length, then lower τ may be used. The results for the remaining expansion rates are presented in Figure 4.12 and Figure 4.13 (considering $\tau > 100$) and Figure 4.14 (considering $\tau > 250$).

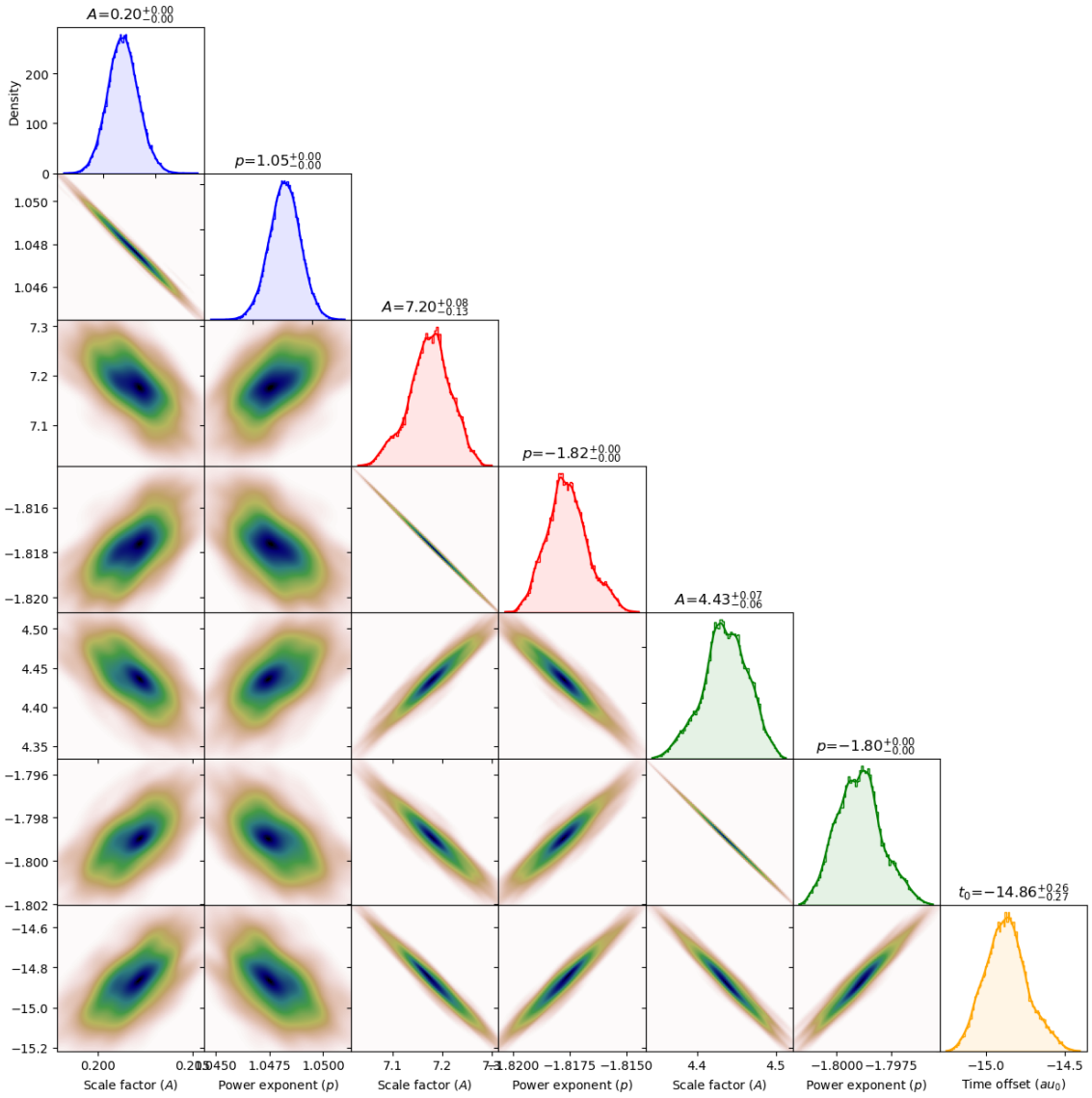

FIGURE 4.10: Corner plots for the radiation epoch simulations considering $\tau > 100$. From left to right, the proportionality factor and the power law exponent for the correlation length (in blue), charge (in red) and current (in green), and the time offset (in yellow).

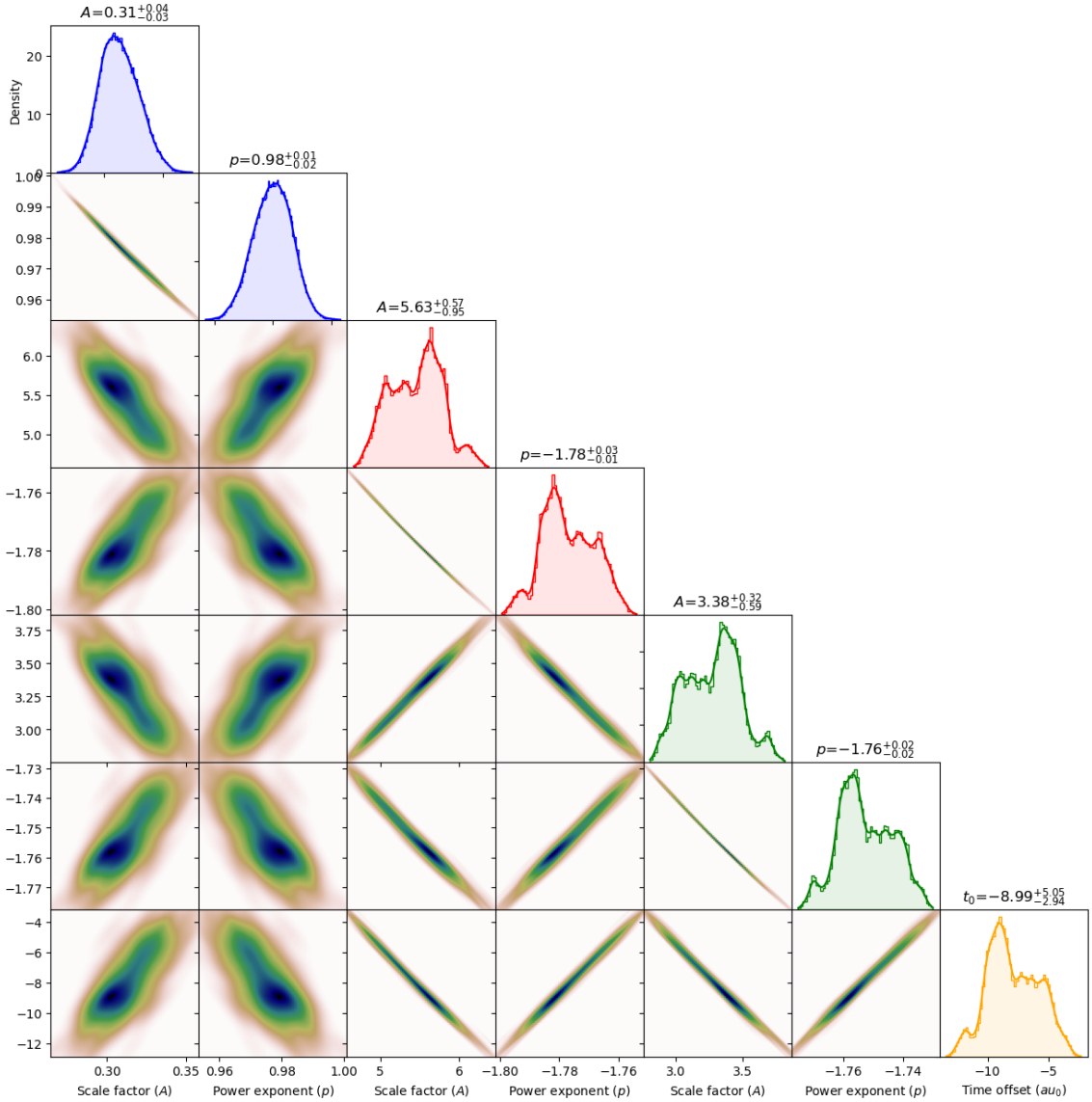

FIGURE 4.11: Corner plots for the radiation epoch simulations considering $\tau > 250$. From left to right, the proportionality factor and the power law exponent for the correlation length (in blue), charge (in red) and current (in green), and the time offset (in yellow).

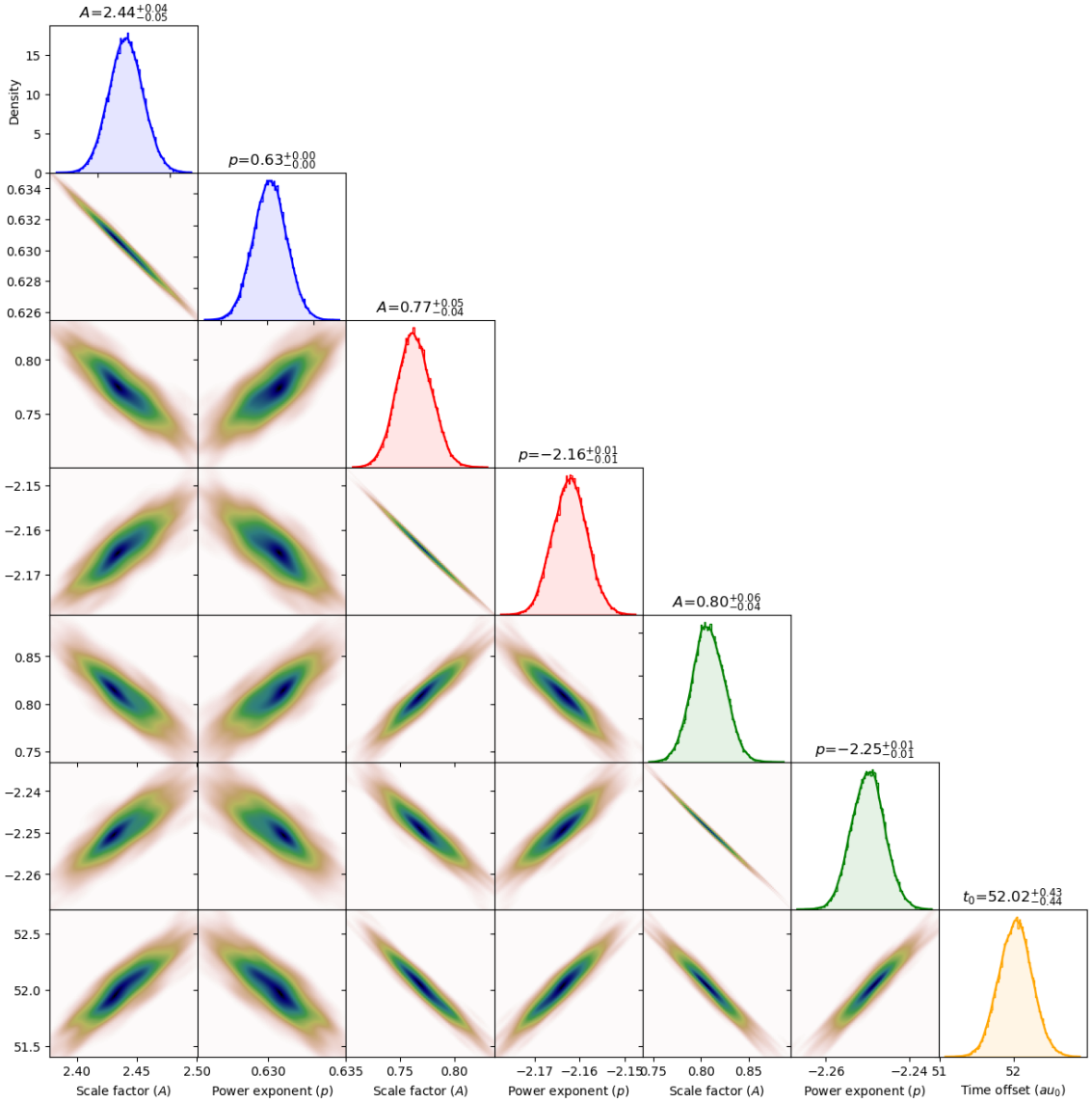

FIGURE 4.12: Corner plots for the fastest expansion rate simulations considering $\tau > 100$. From left to right, the proportionality factor and the power law exponent for the correlation length (in blue), charge (in red) and current (in green), and the time offset (in yellow).

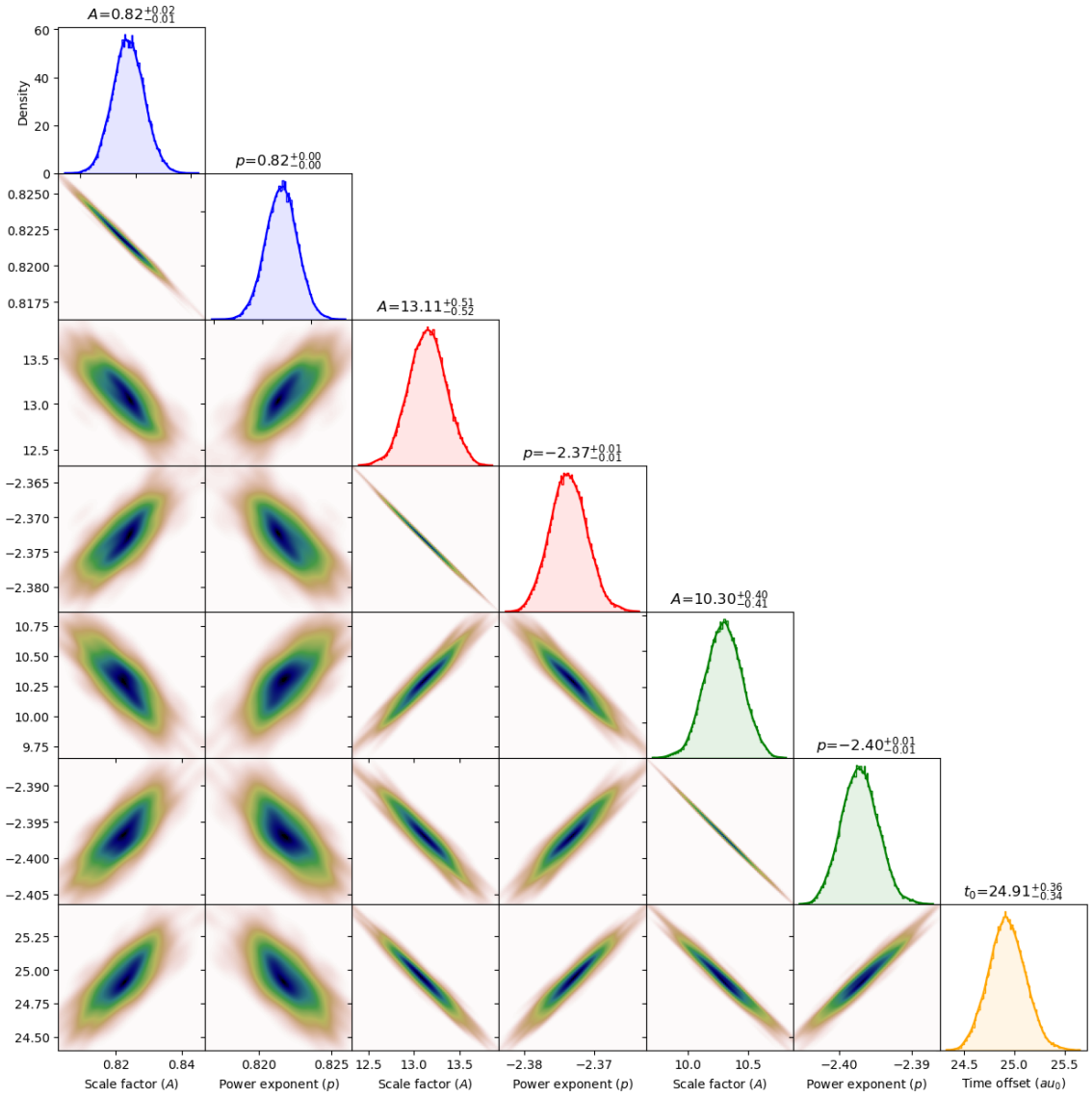

FIGURE 4.13: Corner plots for the matter epoch simulations considering $\tau > 100$. From left to right, the proportionality factor and the power law exponent for the correlation length (in blue), charge (in red) and current (in green), and the time offset (in yellow).

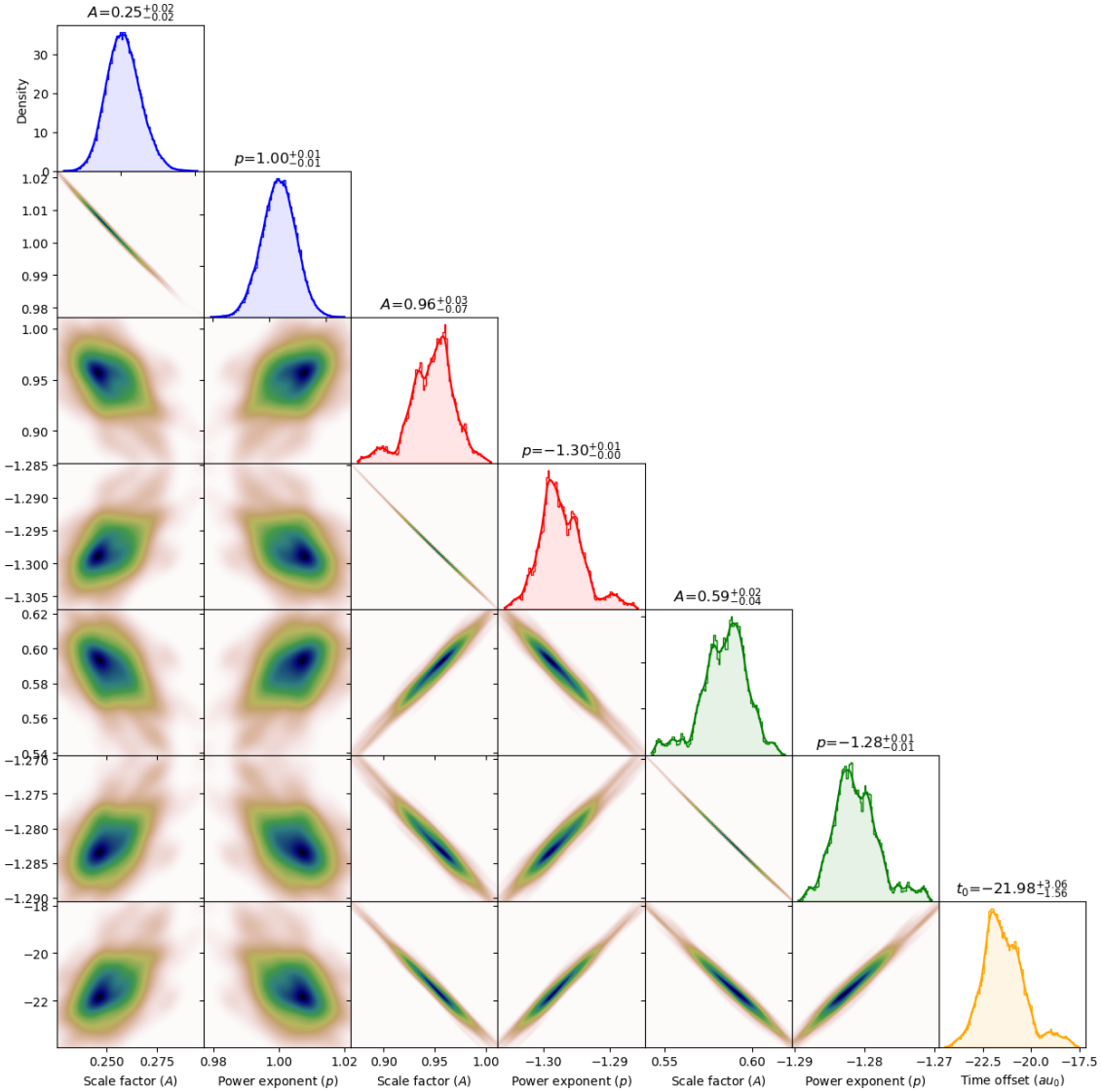

FIGURE 4.14: Corner plots for the slowest expansion rate simulations considering $\tau > 250$. From left to right, the proportionality factor and the power law exponent for the correlation length (in blue), charge (in red) and current (in green), and the time offset (in yellow).

4.6 Comparison with analytical solutions

Having tested different approaches to constrain the power laws that are compatible with the simulated results, it is now time to try to relate them to the previously identified from an analytical approach. Before doing so, it is convenient to summarise the results obtained until now. In Figure 4.15 and Table 4.1 are presented the estimates obtained from the different methods for the different expansion rates.

From these results, some major trends may be identified. Firstly, although some dispersion is found in the proportionality factors identified, the power law exponents for the different quantities are mostly compatible. Additionally, it seems clear that all the solutions are mostly consistent with a constant velocity and decaying charge and currents. This last aspect, in particular, implies a network that is asymptotically compatible with $g = 1$, leaving as possible analytical counterparts solutions B2 and B4. In these cases, it will always be that $\eta = 4\lambda v_0^2 - 2\lambda = \lambda\left(4v_0^2 - 2\right)$. It should be noted that although the velocity was seen to still exhibit some evolution over the explored dynamic range, an upper bound can be obtained from these solutions at:

$$v_0^2 = \frac{1}{\lambda\left(1 + \tilde{c}/k_v\right)} \leq \frac{1}{\lambda} \tag{4.12}$$

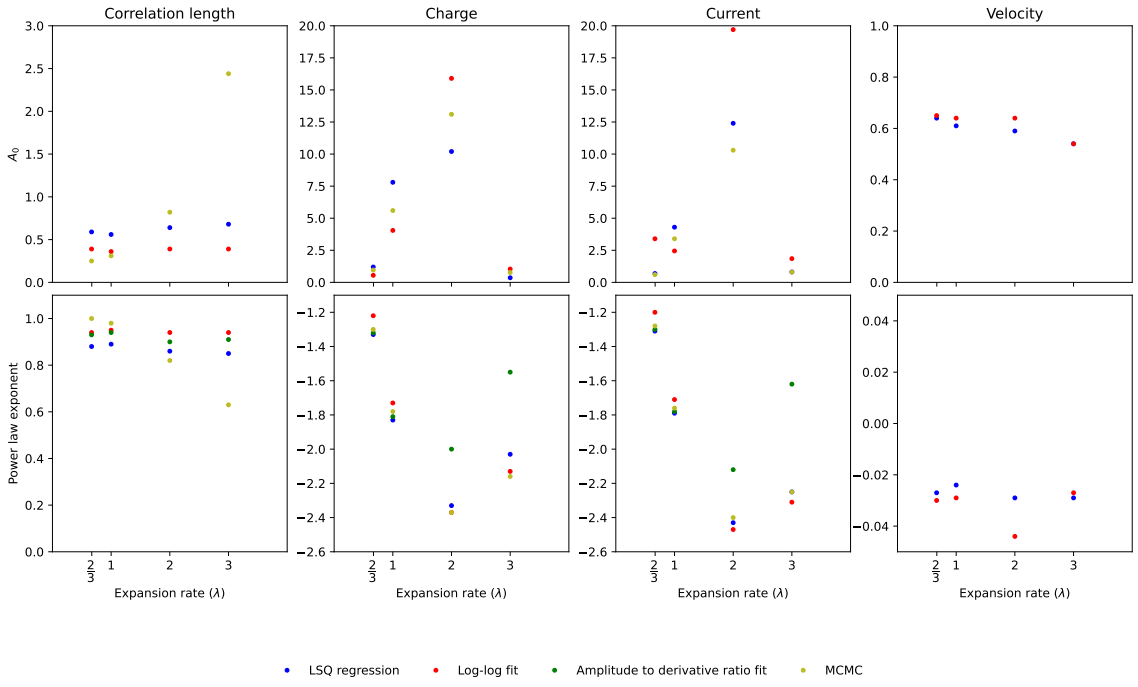

FIGURE 4.15: Results obtained for the power law parameters using different approaches (the time offsets have not been included).

TABLE 4.1: Fitted power law parameters for the different expansion rates and approaches.

	λ	Correlation length			Current			Charge			Velocity		
		ξ_0	ε	t_0	J_0^2	γ	t_0	Q_0^2	δ	t_0	v_0	β	t_0
Curve fit	3	$0.68^{+0.08}_{-0.08}$	$0.85^{+0.02}_{-0.02}$	$0.85^{+0.02}_{-0.02}$	$0.81^{+0.08}_{-0.08}$	$-2.25^{+0.02}_{-0.02}$	$52.0^{+0.8}_{-0.8}$	$0.36^{+0.03}_{-0.03}$	$-2.03^{+0.02}_{-0.02}$	$57.7^{+0.7}_{-0.7}$	$0.54^{+0.01}_{-0.01}$	$-0.029^{+0.004}_{-0.004}$	9^{+5}_{-5}
	2	$0.64^{+0.06}_{-0.06}$	$0.86^{+0.02}_{-0.02}$	$18.0^{+2.4}_{-2.4}$	$12.4^{+0.8}_{-0.8}$	$-2.43^{+0.02}_{-0.02}$	$23.2^{+0.6}_{-0.6}$	$10.2^{+0.7}_{-0.7}$	$-2.33^{+0.02}_{-0.02}$	$27.3^{+0.6}_{-0.6}$	$0.59^{+0.02}_{-0.02}$	$-0.029^{+0.004}_{-0.004}$	8^{+7}_{-7}
	1	$0.56^{+0.04}_{-0.04}$	$0.89^{+0.02}_{-0.02}$	$15.2^{+2.0}_{-2.0}$	$4.3^{+0.02}_{-0.02}$	$-1.79^{+0.01}_{-0.01}$	$-14.1^{+0.5}_{-0.5}$	$7.8^{+0.2}_{-0.2}$	$-1.83^{+0.01}_{-0.01}$	$-16.3^{+0.5}_{-0.5}$	$0.61^{+0.01}_{-0.01}$	$-0.024^{+0.003}_{-0.003}$	8^{+6}_{-6}
	2/3	$0.59^{+0.05}_{-0.05}$	$0.88^{+0.02}_{-0.02}$	$16.9^{+2.2}_{-2.2}$	$0.69^{+0.02}_{-0.02}$	$-1.31^{+0.01}_{-0.01}$	$-27.1^{+0.5}_{-0.5}$	$1.2^{+0.02}_{-0.02}$	$-1.33^{+0.01}_{-0.01}$	$-29.1^{+0.5}_{-0.5}$	$0.64^{+0.01}_{-0.01}$	$-0.027^{+0.003}_{-0.003}$	7^{+8}_{-8}
Log fit	3	$0.39^{+0.01}_{-0.01}$	$0.94^{+0.01}_{-0.01}$	-	$1.85^{+0.01}_{-0.01}$	$-2.31^{+0.01}_{-0.01}$	-	$1.04^{+0.04}_{-0.04}$	$-2.13^{+0.01}_{-0.01}$	-	$0.54^{+0.01}_{-0.01}$	$-0.027^{+0.001}_{-0.001}$	-
	2	$0.39^{+0.01}_{-0.01}$	$0.94^{+0.01}_{-0.01}$	-	$19.7^{+0.3}_{-0.3}$	$-2.47^{+0.01}_{-0.01}$	-	$15.9^{+0.3}_{-0.3}$	$-2.37^{+0.01}_{-0.01}$	-	$0.64^{+0.01}_{-0.01}$	$-0.044^{+0.001}_{-0.001}$	-
	1	$0.36^{+0.01}_{-0.01}$	$0.95^{+0.01}_{-0.01}$	-	$2.45^{+0.01}_{-0.01}$	$-1.71^{+0.01}_{-0.01}$	-	$4.05^{+0.01}_{-0.01}$	$-1.73^{+0.01}_{-0.01}$	-	$0.64^{+0.01}_{-0.01}$	$-0.029^{+0.001}_{-0.001}$	-
	2/3	$0.39^{+0.01}_{-0.01}$	$0.94^{+0.01}_{-0.01}$	-	$0.34^{+0.01}_{-0.01}$	$-1.20^{+0.01}_{-0.01}$	-	$0.55^{+0.01}_{-0.01}$	$-1.22^{+0.01}_{-0.01}$	-	$0.65^{+0.01}_{-0.01}$	$-0.030^{+0.001}_{-0.001}$	-
Derivative fit	3	-	$0.91^{+0.02}_{-0.02}$	7^{+5}_{-5}	-	$-1.62^{+0.02}_{-0.02}$	84^{+10}_{-10}	-	$-1.55^{+0.04}_{-0.04}$	82^{+6}_{-6}	-	-	-
	2	-	$0.90^{+0.01}_{-0.01}$	11^{+2}_{-2}	-	$-2.12^{+0.02}_{-0.02}$	44^{+3}_{-3}	-	$-2.00^{+0.02}_{-0.02}$	49^{+3}_{-3}	-	-	-
	1	-	$0.94^{+0.01}_{-0.01}$	5^{+2}_{-2}	-	$-1.78^{+0.01}_{-0.01}$	-12^{+2}_{-2}	-	$-1.81^{+0.01}_{-0.01}$	-14^{+2}_{-2}	-	-	-
	2/3	-	$0.93^{+0.01}_{-0.01}$	5^{+2}_{-2}	-	$-1.30^{+0.02}_{-0.02}$	-26^{+3}_{-3}	-	$-1.32^{+0.03}_{-0.03}$	28^{+6}_{-6}	-	-	-
MCMC	3	$2.44^{+0.05}_{-0.04}$	$0.63^{+0.01}_{-0.01}$	$52.0^{+0.5}_{-0.5}$	$0.80^{+0.05}_{-0.04}$	$-2.25^{+0.01}_{-0.01}$	$52.0^{+0.5}_{-0.5}$	$0.77^{+0.05}_{-0.04}$	$-2.16^{+0.01}_{-0.01}$	$52.0^{+0.5}_{-0.5}$	$0.45^{+0.03}_{-0.03}$	-	-
	2	$0.82^{+0.02}_{-0.01}$	$0.82^{+0.01}_{-0.01}$	$24.9^{+0.4}_{-0.4}$	$10.3^{+0.4}_{-0.4}$	$-2.40^{+0.01}_{-0.01}$	$24.9^{+0.4}_{-0.4}$	$13.1^{+0.5}_{-0.5}$	$-2.37^{+0.01}_{-0.01}$	$24.9^{+0.4}_{-0.4}$	$0.49^{+0.03}_{-0.02}$	-	-
	1	$0.31^{+0.04}_{-0.03}$	$0.98^{+0.01}_{-0.02}$	-9^{+5}_{-3}	$3.4^{+0.3}_{-0.6}$	$-1.76^{+0.02}_{-0.02}$	-9^{+5}_{-3}	$5.6^{+0.6}_{-1.0}$	$-1.78^{+0.03}_{-0.01}$	-9^{+5}_{-3}	$0.53^{+0.02}_{-0.03}$	-	-
	2/3	$0.25^{+0.02}_{-0.02}$	$1.00^{+0.01}_{-0.01}$	-22^{+3}_{-2}	$0.60^{+0.02}_{-0.04}$	$-1.28^{+0.01}_{-0.01}$	-22^{+3}_{-2}	$0.96^{+0.03}_{-0.07}$	$-1.30^{+0.01}_{-0.01}$	-22^{+3}_{-2}	$0.54^{+0.02}_{-0.03}$	-	-

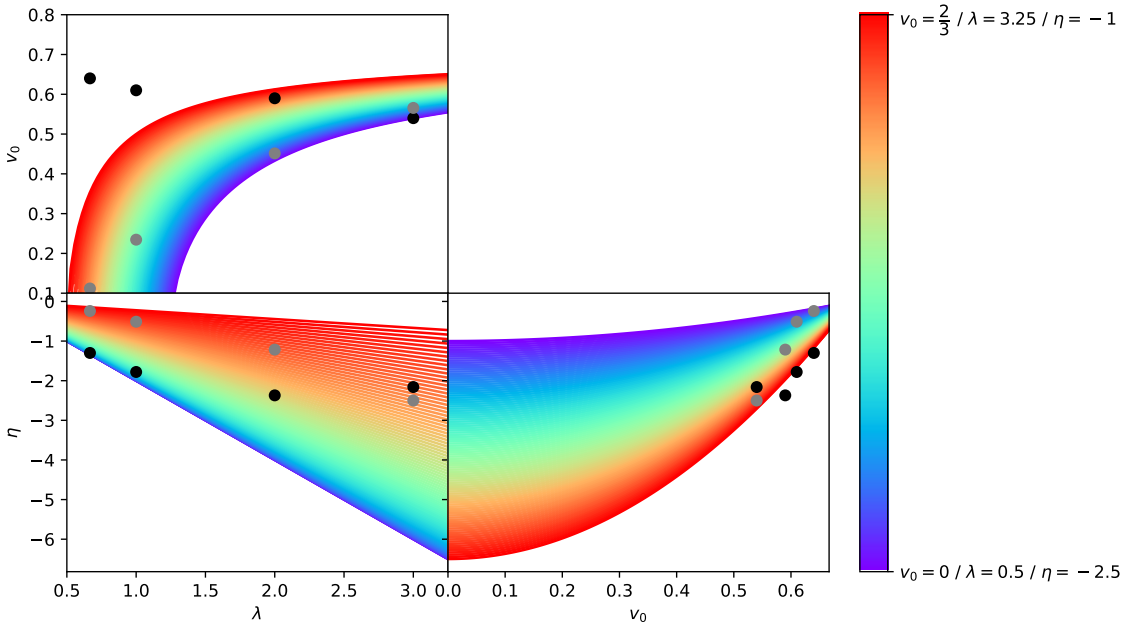

FIGURE 4.16: Representation of the different relations expected based on the analytical solutions. The black and grey points represent the fitted value of each quantity and the expected value based on the analytical solution. For the top left panel, the charge decay rate varies between -2.5 (blue limit) and -1 (red limit). For the bottom left panel, the asymptotic velocity varies between 0 (blue limit) and 2/3 (red limit). For the bottom right panel, the expansion rate varies between 0.5 (blue limit) and 3.25 (red limit).

where it has been assumed $\tilde{c} \geq 0$. It can immediately be seen that the critical case is the highest expansion rate, which would yield $v_0^2 \leq 1/3$, but this condition is verified in all simulations, even in the slowest ones.

If this upper bound is clearly respected, the relation between the network velocity, the charge (or current) decay rate and the expansion rate is not, as can be seen from Figure 4.16, where the relations have been expressed by successively fixing each of the parameters, while allowing the remaining ones to vary. The black and grey points represent the fitted value of each quantity and the expected value based on the analytical solution, respectively. As can be seen, the fitted values are not compatible with the analytical predictions, which may be stated either as a network where the strings have too high velocities, for the rate at which they are loosing charge and current (top left panel on Figure 4.16), or a network that is loosing charge and current just too fast, for the typical velocities it exhibits (bottom left panel on Figure 4.16).

It should be noted that these deviations may be hardly associated to the identification uncertainties, as these are also the best constraint parameters, but other sources of error may still be found, in particular:

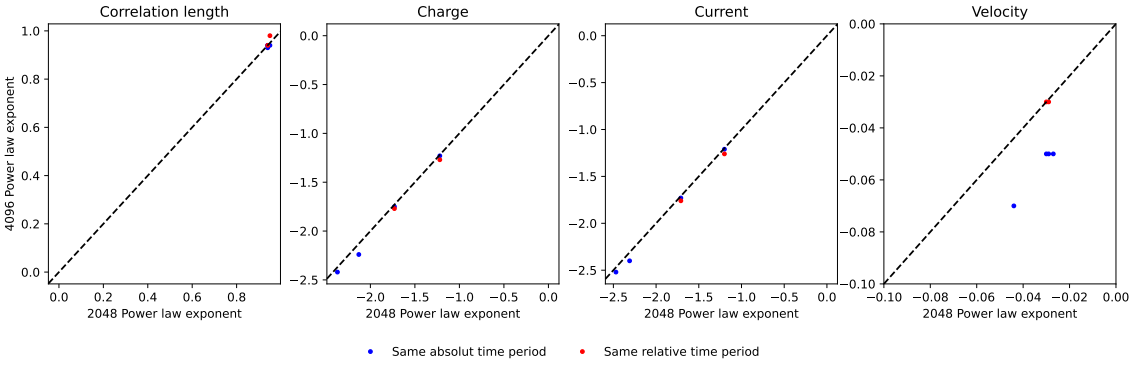

FIGURE 4.17: Comparison between the results obtained from a 2048^3 box and the results obtained considering the same time period and the same portion of the available data from a 4096^3 box.

- The solutions under analysis have still not reached the scaling regime, implying that higher dynamic ranges are needed
- Some of the hypothesis of the generalised VOS model are not adequate, in particular the exclusive dependence of the momentum parameter on the velocity
- The numerical estimators used to map the field simulations into the macroscopical quantities of interest exhibit some bias that carries an implicit time dependence

To check if the lack of dynamic range could be the source of the deviations, numerical simulations considering a 4096^3 box were analysed. The comparison of the estimates obtained are presented in Figure 4.17, where two different approaches have been followed. On one hand, the time period corresponding to the original 2048^3 box has been used (blue points). On the other hand, the red points were obtained by considering the same portion of the simulation, meaning the second half of the available points. This latter approach could not be used for the two fastest expansion rates, since it was no longer possible to detect any charge or current there. Since the results are mostly compatible in all analysis, the lack of dynamic range may be excluded as the source for the deviations, where it can play, at most, a sub-dominant role.

Taking now a closer look to the generalised VOS model assumptions, it can be seen that the energy loss parameter $\tilde{c}$ is assumed to be constant, while the momentum parameter was assumed to be dependent on the velocity only, which allowed us to treat it like a constant too. However, a first estimate for the ratio $\tilde{c}/k_v$ can be obtained from the fitted parameters

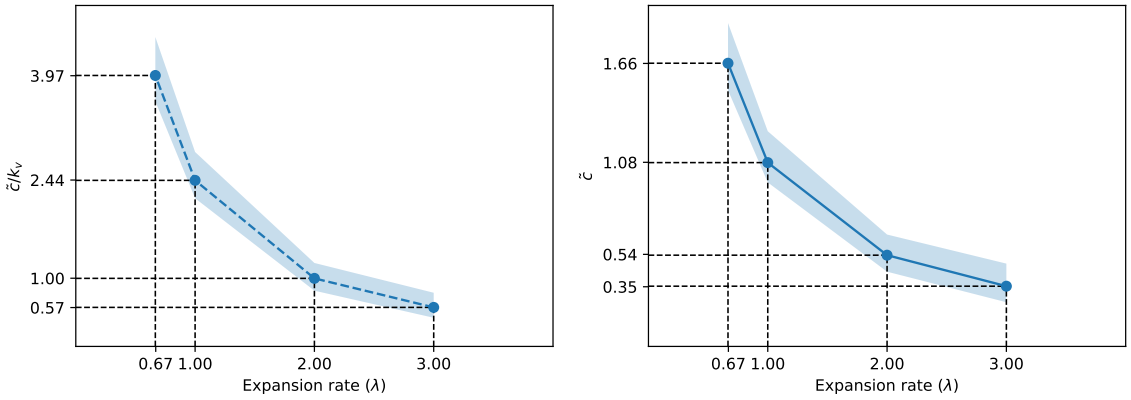

FIGURE 4.18: Estimates for $\tilde{c}/k_v$ (on the left) and, assuming the a Nambu-Goto type of behaviour for k_v, for $\tilde{c}$ (on the right).

as:

$$\tilde{c}/k_v = \frac{1}{\lambda v_0^2} - 1 = \frac{1 - \lambda v_0^2}{\lambda v_0^2} \tag{4.13}$$

If one further assumes the analytical solution for the Nambu-Goto strings momentum parameter given by [39]:

$$k_v = \frac{2\sqrt{2}}{\pi}\left(1 - v^2\right)\left(1 + 2\sqrt{2}v^3\right)\frac{1 - 8v^6}{1 + 8v^6} \tag{4.14}$$

then Equation 4.13 can even be used to place constraints on $\tilde{c}$ itself. The results for both estimates are presented in Figure 4.18, where the upper and lower bounds have been computed from the maximum and minimum velocity values within the dynamic range under analysis*. It is interesting to note that there appears to exist a relation between these parameters and the expansion rate, which may partially explain the different results. For this to explain the velocity excess (or charge decay rate excess), it must be that at least one out of $\tilde{c}$ and k_v has a dependency on the charge in the network.

*This choice was motivated by the previous realisation that the velocity may still have not fully converged, in which case taking the uncertainty as the time series standard deviation would be misleading.

Another possibility is that a near-scaling solutions was obtained. To better understand this claim, the equations for decaying charge are here recovered as:

$$\alpha = \lambda v_0^2 + \frac{\tilde{c}}{2}\frac{v_0}{\xi_0}\tau^{1-\varepsilon} \tag{4.15a}$$

$$0 = \frac{k_v v_0}{\xi_0}\tau^{-\varepsilon} - 2\lambda v_0^2 \tau^{-1} \tag{4.15b}$$

$$\gamma = 2\left(\frac{v_0 k_v}{\xi_0}\tau^{1-\varepsilon} - \lambda\right) \tag{4.15c}$$

$$\delta = 2\left(\frac{v_0 k_v}{\xi_0}\tau^{1-\varepsilon} - \lambda\right) \tag{4.15d}$$

$$\varepsilon = \lambda v_0^2 + \frac{\tilde{c}}{2}\frac{v_0}{\xi_0}\tau^{1-\varepsilon} \tag{4.15e}$$

where the adequate form for constant velocities has been used. A true solution must be such that $\varepsilon = 1$, but relaxing that slightly, it may be seen that we may have $\varepsilon > 0$, but not necessarily unity. On a different perspective, we may still have $\varepsilon = 1$, but drop the identification $k_v v_0/\xi_0 = 2\lambda v_0^2$ and assume that the velocity equation would be essentially satisfied still. In any case, it is still true that:

$$\delta = 2\left(\frac{v_0 k_v}{\xi_0} - \lambda\right) = 4\frac{k_v}{\tilde{c}}\left(\varepsilon - \lambda v_0^2\right) - 2\lambda \tag{4.16}$$

where we have made use of the correlation length equation to provide a relation for the asymptotic velocity and ξ_0:

$$\frac{k_v v_0}{\xi_0} = \frac{2k_v}{\tilde{c}}\left(\varepsilon - \lambda v_0^2\right) \tag{4.17}$$

implying:

$$\frac{\tilde{c}}{k_v} = 4\frac{1 - \lambda v_0^2}{\delta + 2\lambda} \tag{4.18}$$

Although this formulation shares most of the features from the true scaling regime, the relation $\delta = 4\lambda v_0^2 - 2\lambda$ does not need to be satisfied anymore and the network may essentially exhibit any asymptotic velocity, eventually more dependent on the initial conditions then on the network evolution.

Finally, as already discussed, as important as the simulations themselves are the diagnosis criteria. It may happen that either the velocity or the charge estimator, or even both, present some bias that translates itself into an additional time dependence. For instance, the charge estimator weighting functions depend on the fields value, and this may lead to

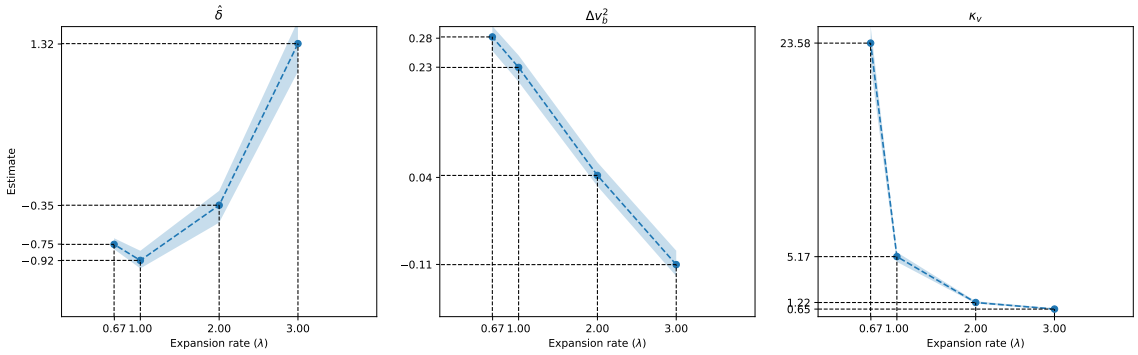

FIGURE 4.19: Characterisation of the identified possible bias sources. On the left, the estimate bias impact on the charge estimator, assuming the velocity estimator is correct. On the centre and right panels, the characterisation of the velocity excess, assuming the charge estimator to be correct, expressed as an additive constant or proportionality factor.

effectively include a bigger region around the strings for higher energy states, or lower simulation times. In this case, one could expect that the charge would appear to be decaying away faster then it really does, just by the fact that smaller and smaller portions of the box charge are being associated with the strings. This issue could be tackled by repeating the analysis considering different estimators and studying its influence in the response, but a first estimate of the expected bias may be obtained by computing what would this hidden temporal dependence has to look like, if this is to explain the deviations encountered. To evaluate this effect, two different analysis were conducted. Firstly, it was assumed the velocity estimator to be correct, while the charge could carry an hidden time dependence. In this case, the estimated decay ($\hat{\delta}$) rate would actually be such that:

$$\hat{\delta} = \delta + \delta_b \longrightarrow \delta_b = \hat{\delta} - \delta = \hat{\delta} - \left(4\lambda v_0^2 - 2\lambda\right) \tag{4.19}$$

where δ is the analytical solution, and has been replaced by its representation in terms of the expansion rate and the asymptotic velocity, and δ_b is the hidden time dependence due to the estimator bias. On a different perspective, it was assumed that the charge estimator is correct, but the estimated velocity ($\hat{v}_0$) contained an additional term, Δv_b, that may alternatively be written as a fraction (κ_v) of the true value:

$$\hat{v}_0^2 = v_0^2 + \Delta v_b^2 = \kappa_v v_0^2 = \kappa_v \frac{\delta + 2\lambda}{4\lambda} \tag{4.20}$$

In Figure 4.19 are presented the results for the different bias estimators. Although no definite answer may be given and only additional simulations may shed some light into the true nature of the bias, if it exists at all, it seems that the velocity excess is well related to the expansion rate.

Chapter 5

Conclusions

5.1 Summary

In this thesis the complex evolution of charged cosmic strings network have been studied. Although in a first approach this evolution was studied from a reduced order analytical model, it was later compared to the output of complex numerical simulations, kindly made available by José Ricardo Correia. Both these approaches, as well as the needed theoretical background to gained deeper insight into topological defects, defined the structure and organisation of this thesis.

In Chapter 2 topological defects formation and the processes that may allow to developed charged strings in a cosmological context from the symmetry breaking phase transition of complex fields were introduced and briefly illustrated with some toy models. Additionally, and because solving the full field theory equations is not feasible in purely analytical terms, the reduced order model that is generalised VOS model, where the network evolution properties are condensed in a relatively short number of macroscopic quantities, was also introduced. Finally, the so-called scaling solutions for the differential equations of the analytical models were defined, as well as a brief discussion regarding their physical interpretation.

Having the problem properly formalised, Chapter 3 is fully devoted to presenting the solutions branches with a clear physical interpretation (the purely mathematical ones are presented, for consistency, in Appendix A). Here, additional energy and/or charge loss mechanisms, that in the analytical model framework manifest themselves as additional parameters, are successively introduced, and the corresponding solutions discussed and compared to previous works by [14, 15] and [17]. To aid the visualisation of the identified

solutions, a user-friendly interface was also developed and used to produce the plots that illustrate the network evolution based on numerically solving the macroscopical differential equations for different conditions.

At this point, several solutions branches had already been identified, and it was considered appropriate to compare their predictions to the output of full field theory simulations, and this if the focus of Chapter 4. Since this topic had not been covered yet, a brief introduction to the simulation of strings network is provided, and only then the results properly explored. After a preliminary data evaluation and analysis, different approaches were used to characterise the different quantities evolution.

5.2 Main contributions

In the previous section a brief description of the contents of each chapter was provided, but some conclusions and analysis should be particularly highlighted here, in particular to the qualitative behaviour of the evolution for different conditions.

Firstly, when no energy loss mechanism were considered, it was clear that, assuming $F' \neq 0$ three distinct types of solutions emerged, that could be easily related to the ones identified by Almeida and Martins [14], provided one makes the adequate associations between charge and small-scale structure, and to the ones identified by Oliveira et al. [17] for the chiral limit, provided one takes the limit $s \to 0$ in these. This identification is presented in Table 5.1, where the power law exponents taken from [14, 17] were converted to express scaling solutions with respect to conformal time and comoving lengths, noting a general power law $\propto t^{\zeta_t}$, where $\zeta_t = a + b\lambda_t$, corresponds to:

$$\zeta_\tau = \frac{\zeta_t}{1-\lambda_t} = \frac{a+b\lambda_t}{1-\lambda_t} = \frac{a}{1-\lambda_t} + b\lambda_\tau = a\,(1+\lambda_\tau) + b\lambda_\tau = a + (a+b)\lambda_\tau \tag{5.1}$$

where the indexes t and τ have been used to clearly indicate if the corresponding parameter is evaluated with respect to physical or conformal time, respectively. It is interesting to note that the decaying velocity solution obtained by Almeida and Martins [14], although associated with a slightly different expansion rate, shows that the small scale structure plays the role of the charge in our model. In particular, it should be noted that while the small scale parameter, μ, evolves as $2-3\lambda$, its square would evolve as $4-6\lambda$, which is exactly the same dependence that we have found.

In fact, for fast expansion rates, it was found that the charge and current will always decay, while the network velocity is kept constant, a regime that finds its limit at the matter

TABLE 5.1: Comparison of the solutions obtained in Chapter 3 with those obtained by Oliveira et al. [17] and Almeida and Martins [14], for the chiral and wiggly models, respectively, without energy loss mechanism. The power law exponents have been expressed with respect to conformal time and comoving distances.

	Chapter 3						Oliveira [17]					Almeida [14]				
	λ	α	β	γ	δ	ε	λ	α	β	γ	ε	λ	α	β	γ	ε
A1	$\frac{2}{3}$	$\frac{\lambda}{2}$	$-\lambda$	$4-6\lambda$	$4-6\lambda$	$1-\lambda$	<2	$\frac{\lambda}{2}$	$\frac{\lambda-2}{2}$	0	$\frac{\lambda}{2}$	$<\frac{1}{2}$	$\frac{\lambda}{2}$	$-\lambda$	$2-3\lambda$	$1-\lambda$
A2	>1	1	0	$4-2\lambda$	$4-2\lambda$	1	2	1	0	0	1	2	1	0	0	1
							>2	1	0	$4-2\lambda$	1	>2	1	0	0	1
A3	>2	1	0	$4-2\lambda$	0	1	>2	1	0	$4-2\lambda$	1	>2	1	0	0	1
A4	>2	1	0	$4-2\lambda$	$4-2\lambda$	1	>2	1	0	$4-2\lambda$	1	>2	1	0	0	1
A5	2	1	0	0	0	1	2	1	0	0	1	2	1	0	0	1

epoch expansion rate, where charge and current are allowed to subsist. It was also possible to find subtle variations of these solutions, where charges are allowed to survive, or even grow, by imposing $F' = 0$*. It is interesting to note that a generalisation of the decaying velocity solutions found by Oliveira et al. [17] here is only found for a very particular expansion rate, lower than the radiation epoch one*. Finally, it should be noted that the universe expansion plays an important role here, since in its absence, and still assuming no additional energy loss mechanism, one would only find frozen network solutions.

Once the network is allowed to lose energy, here parameterised by $\tilde{c}$, even the non expanding universe solutions exhibit some evolution. There, and although charge, current and velocity are still constant, but the correlation length now increases over time, which is the natural manifestation of a network losing energy. On the other hand, the expanding universe solutions are also a generalised version from the ones previously identified. The most distinct features here are the lower asymptotic velocities that come with the increase of $\tilde{c}$ and the deviation of the critical expansion rate, previously compatible with the matter epoch, to lower values. Additionally, it should be noted that while these solutions are valid for networks with no charge losses (by setting $g = 1$), it was also argued, based on the work by Rybak et al. [20], that the decaying charge and current solutions are also a possible limit of any network, since these are asymptotically equivalent to a network with $g = 1$. Once more, one can easily relate these solutions to the ones obtained by Oliveira et al. [17] and Almeida and Martins [14], with the appropriate adaptations, as presented in Table 5.2 and Table 5.3. It should be noted that the charge decay law of Oliveira et al. [17] may not look

*See the limitations and future developments for further discussion on this matter.

TABLE 5.2: Comparison of the solutions obtained in Chapter 3 with those obtained by Oliveira et al. [17] for the chiral limit model, with energy loss mechanism. The power law exponents have been expressed with respect to conformal time and comoving distances.

	Chapter 3						Oliveira [17]				
	λ	α	β	γ	δ	ε	λ	α	β	γ	ε
B1	$\frac{2}{3+\tilde{c}/k_v}$	$1-\lambda$	$-\lambda$	0	0	$1-\lambda$	$< \frac{2}{1+c/k_v}$	$\frac{1+\tilde{c}/k_v}{2}\lambda$	$\frac{1+\tilde{c}/k_v}{2}\lambda - 1$	0	$\frac{1+\tilde{c}/k_v}{2}\lambda$
B2	$\frac{1/v_0^2}{1+\tilde{c}/k_v}$	1	0	$4\lambda v_0^2 - 2\lambda$	$4\lambda v_0^2 - 2\lambda$	1	$\frac{2}{1+c/k_v}$	1	0	0	1
							$> \frac{2}{1+c/k_v}$	1	0	$\frac{4}{1+c/k_v} - 2\lambda$	1
B3	$> \frac{2}{1+\tilde{c}/k_v}$	1	0	$4\lambda v_0^2 - 2\lambda$	0	1	$> \frac{2}{1+c/k_v}$	1	0	$\frac{4}{1+c/k_v} - 2\lambda$	1
B4	$> \frac{2}{1+\tilde{c}/k_v}$	1	0	$4\lambda v_0^2 - 2\lambda$	$4\lambda v_0^2 - 2\lambda$	1	$> \frac{2}{1+c/k_v}$	1	0	$\frac{4}{1+c/k_v} - 2\lambda$	1
B5	$\frac{2}{1+\tilde{c}/k_v}$	1	0	0	0	1	$\frac{2}{1+c/k_v}$	1	0	0	1

TABLE 5.3: Comparison of the solutions obtained in Chapter 3 with those obtained by Almeida and Martins [14] for the wiggly model, with energy loss mechanism. The power law exponents have been expressed with respect to conformal time and comoving distances.

	Chapter 3						Almeida [14]				
	λ	α	β	γ	δ	ε	λ	α	β	γ	ε
B1	$\frac{2}{3+\tilde{c}/k_v}$	$1-\lambda$	$-\lambda$	0	0	$1-\lambda$	$< \frac{1}{2+c_{eff}/k_{eff}}$	$\frac{c_{eff}/k_{eff}}{1+c_{eff}/k_{eff}} + \frac{1-c_{eff}/k_{eff}}{2+2c_{eff}/k_{eff}}\lambda$	$-\lambda$	$\frac{2-\left(3+c_{eff}/k_{eff}\right)\lambda}{1+c_{eff}/k_{eff}}$	$1-\lambda$
B2	$\frac{1/v_0^2}{1+\tilde{c}/k_v}$	1	0	$4\lambda v_0^2 - 2\lambda$	$4\lambda v_0^2 - 2\lambda$	1	$\frac{2}{1+c_{eff}/k_{eff}}$	1	0	0	1
							$> \frac{2}{1+c/k}$	1	0	0	1
B3	$> \frac{2}{1+\tilde{c}/k_v}$	1	0	$4\lambda v_0^2 - 2\lambda$	0	1	$> \frac{2}{1+c/k}$	1	0	0	1
B4	$> \frac{2}{1+\tilde{c}/k_v}$	1	0	$4\lambda v_0^2 - 2\lambda$	$4\lambda v_0^2 - 2\lambda$	1	$> \frac{2}{1+c/k}$	1	0	0	1
B5	$\frac{2}{1+\tilde{c}/k_v}$	1	0	0	0	1	$\frac{2}{1+c_{eff}/k_{eff}}$	1	0	0	1

the same as ours at first sight, but, referring back to B2 to B5, it can be seen that:

$$4\lambda v_0^2 - 2\lambda = \frac{4}{1+\tilde{c}/k_v} - 2\lambda \tag{5.2}$$

Finally, the full general model with arbitrary values for $\tilde{c}$ and g exhibited more complex solutions where, for adequate choice of parameters, the charge and/or current may actually exhibit very distinct behaviours. These solutions were typically associated with more and more complex constraints on the relations between the different model parameters. For a non expanding universe, however, solutions under these conditions are always associated with constant velocities, but may exhibit constant or growing charges, but not decaying ones, while still requiring $F' \neq 0$ and $F'' = 0$.

In parallel to the identification of the solutions themselves, there are also some relevant outputs that may be used in future works. On one hand, although the scripts specially developed to aid the visualisation of the network evolution based on the analytical model differential equations do not contain any particularly challenging feature, they may still be useful to illustrate and test some aspects of the generalised VOS model. On the other hand,

the different approaches used to study the output of the filed theory numerical simulations, and in particular the MCMC code adapted from the work by Pimenta et al. [32], can be further explored to better constrain the model parameters and compare future simulation outputs.

5.3 Limitations and future developments

If up until now special attention was given to the relevant outputs of this work, there are also some relevant limitations that should be properly attended in future works.

Firstly, it was clear that although most approaches used to characterise the numerical simulations output were compatible with one another, specially when referring to the decay or growth rates of the different parameters, and the qualitative behaviour of the network was similar to some of the previously identified analytical solutions, the details were not. The source of these deviations could not be completely identified and further simulations, possibly with different estimators, are required to provide a definite answer.

On the other hand, these deviations can also be read in the opposite way and actually be a smoking gun of inadequate model assumptions in the construction of the analytical model itself. In particular, it is important to understand if the momentum parameter may carry some relation to the characteristic charge of the network, and not only to the velocity. Another possibility was already hidden in the comparisons with the solutions studied by Oliveira et al. [17], where an additional model parameter, s, was used to characterise the charge gradient and that is absent here.

Finally, some solutions with distinct features were found by imposing $F' = 0$. Although there is nothing fundamentally wrong with such imposition, the analytical model relating the total energy, correlation length and charge relation may be extended to account for higher order derivatives.

Appendix A

Mathematical solutions

A.1 Introduction

The solutions that have been presented in Chapter 3 have systematically left out some possible branches for physical reasons, namely by requiring the network velocity to be strictly lower than 1 at all times, or by making the implicit assumption that for an expanding universe it is not expected that the momentum parameter may vanish. Here, these assumptions will be relaxed and a new set of solutions listed that may be natural extensions of their physical counterpart, or completely different. Firstly, the ultra-relativistic regime will be explored by explicitly setting $v_0 = 1$, implying $C = \beta = 0$, and only after that the momentum parameter will be set to $k_v = 0$. In each of these analysis, it will be assumed that only one of the physical interpretations is modified, and so this chapter ends with the analysis of the cases where both $v_0 = 1$ and $k_v = 0$.

A.2 Vanishing momentum parameter

Firstly, if the momentum parameter is allowed to vanish, even for expanding universes, the equations reduce to:

$$\alpha = \lambda\left[v_0^2\tau^{2\beta} - C\frac{L_0^2\mathcal{J}_0^2}{\xi_0^2}F'\tau^{2(\alpha-\varepsilon)+\eta}\right] + \frac{g\tilde{c}}{2}\frac{v_0}{\xi_0}\tau^{1+\beta-\varepsilon} \tag{A.1a}$$

$$\beta = -2C\lambda\left(1 + \frac{L_0^2\mathcal{J}_0^2}{\xi_0^2}F'\tau^{2(\alpha-\varepsilon)+\eta}\right) \tag{A.1b}$$

$$\gamma = -2\lambda - \rho\tilde{c}\frac{v_0\xi_0}{J_0^2L_0^2}\frac{1-g}{F' - 2Q_0^2\tau^\delta F''}\tau^{1+\beta+\varepsilon-2\alpha-\gamma} \tag{A.1c}$$

$$\delta = -2\lambda\frac{F' + 2J_0^2\tau^\gamma F''}{F' + 2Q_0^2\tau^\delta F''} - (1-\rho)\tilde{c}\frac{v_0\xi_0}{Q_0^2L_0^2}\frac{1-g}{F' + 2Q_0^2\tau^\delta F''}\tau^{1+\beta+\varepsilon-2\alpha-\delta} \tag{A.1d}$$

$$\varepsilon = \lambda v_0^2\tau^{2\beta}\left(1 + \frac{L_0^2\mathcal{J}_0^2}{\xi_0^2}F'\tau^{2(\alpha-\varepsilon)+\eta}\right) + \frac{\tilde{c}}{2}\frac{v_0}{\xi_0}\tau^{1+\beta-\varepsilon} \tag{A.1e}$$

In particular, it should be noted that the, physical, solutions for a non-expanding universe are contained within this class of solutions, by making $\lambda \to 0$. It should be noted that for these solutions it will always be that $\beta = 0$, while the remaining equations are:

$$\alpha = \frac{g\tilde{c}}{2}\frac{v_0}{\xi_0}\tau^{1-\varepsilon} \tag{A.2a}$$

$$\gamma = -\rho\tilde{c}\frac{v_0\xi_0}{J_0^2L_0^2}\frac{1-g}{F' - 2Q_0^2\tau^\delta F''}\tau^{1+\varepsilon-2\alpha-\gamma} \tag{A.2b}$$

$$\delta = -(1-\rho)\tilde{c}\frac{v_0\xi_0}{Q_0^2L_0^2}\frac{1-g}{F' + 2Q_0^2\tau^\delta F''}\tau^{1+\varepsilon-2\alpha-\delta} \tag{A.2c}$$

$$\varepsilon = \frac{\tilde{c}}{2}\frac{v_0}{\xi_0}\tau^{1-\varepsilon} \tag{A.2d}$$

It should be clear that without any loss mechanism ($\tilde{c} = 0$), every single quantity of interest will remaining constant. Additionally, if $\tilde{c} \not\emptyset$, but $g = 1$, then $\alpha = \varepsilon$, but $\delta = \gamma = 0$.

A.2.1 No losses

If all loss mechanism are neglected, by setting $\tilde{c} = 0$, it immediately follows that the current will always decay as -2λ. Two solutions emerge that where both length scales are kept constant, while the velocity decays, as given by V1 and V2. Once more, the difference between them is on the charge behaviour. Additionally, there are also solutions with constant velocities, as given by V3, but these may only happen for $\mathcal{K} = -1$ and hence $F' \neq 0$. This case is the adequate limit for a non expanding universe.

Solution V1:

1. Scaling solutions:

$$L_c = L_0 \quad , \quad \xi_c = \xi_0 \quad , \quad J^2 = J_0^2 \tau^{-2\lambda} \quad , \quad v = v_0 \tau^{-2\lambda}$$
$$L = L_0 \tau^{\lambda} \quad , \quad \xi = \xi_0 \tau^{\lambda} \quad , \quad Q^2 = Q_0^2 \tau^{-2\lambda}$$

2. Additional constraints:

$$\left(Q_0^2 = J_0^2\right)^*$$

Only for $F' = 0$

Solution V2:

1. Scaling solutions:

$$L_c = L_0 \quad , \quad \xi_c = \xi_0 \quad , \quad J^2 = J_0^2 \tau^{-2\lambda} \quad , \quad v = v_0 \tau^{-2\lambda}$$
$$L = L_0 \tau^{\lambda} \quad , \quad \xi = \xi_0 \tau^{\lambda} \quad , \quad Q^2 = Q_0^2$$

2. Additional constraints:

$$F' = 0$$

Solution V3:

1. Scaling solutions:

$$L_c = L_0 \tau^{\lambda} \quad , \quad \xi_c = \xi_0 \quad , \quad J^2 = J_0^2 \tau^{-2\lambda} \quad , \quad v = v_0$$
$$L = L_0 \tau^{2\lambda} \quad , \quad \xi = \xi_0 \tau^{\lambda} \quad , \quad Q^2 = Q_0^2 \tau^{-2\lambda}$$

2. Additional constraints:

$$\mathcal{K} = -1$$

A.2.2 No charge losses

If one now set $g = 1$, the current will still decay as -2λ. The remaining equations to be solved are:

$$\alpha = \lambda\left[v_0^2\tau^{2\beta} - C\frac{L_0^2\mathcal{J}_0^2}{\xi_0^2}F'\tau^{2(\alpha-\varepsilon)+\eta}\right] + \frac{\tilde{c}}{2}\frac{v_0}{\xi_0}\tau^{1+\beta-\varepsilon} \tag{A.3a}$$

$$\beta = -2C\lambda\left(1 + \frac{L_0^2\mathcal{J}_0^2}{\xi_0^2}F'\tau^{2(\alpha-\varepsilon)+\eta}\right) \tag{A.3b}$$

$$\gamma = -2\lambda \tag{A.3c}$$

$$\delta = -2\lambda\frac{F' + 2J_0^2\tau^\gamma F''}{F' + 2Q_0^2\tau^\delta F''} \tag{A.3d}$$

$$\varepsilon = \lambda v_0^2\tau^{2\beta}\left(1 + \frac{L_0^2\mathcal{J}_0^2}{\xi_0^2}F'\tau^{2(\alpha-\varepsilon)+\eta}\right) + \frac{\tilde{c}}{2}\frac{v_0}{\xi_0}\tau^{1+\beta-\varepsilon} \tag{A.3e}$$

Here, one may still find the decaying velocity solutions previously defined by V1 and V2 to be generalised to V4 and V5. Additionally, one may still find two additional solutions, V6 and V7, depending on the value of the expansion rate and the energy loss parameter. Finally, one may still find a constant velocity solution, given by V8, which is once more the adequate limit for a non expanding universe.

Solution V4:

1. Scaling solutions:

$$L_c = L_0 \quad , \quad \xi_c = \xi_0 \quad , \quad J^2 = J_0^2\tau^{-2\lambda} \quad , \quad v = v_0\tau^{-2\lambda}$$
$$L = L_0\tau^\lambda \quad , \quad \xi = \xi_0\tau^\lambda \quad , \quad Q^2 = Q_0^2\tau^{-2\lambda}$$

2. Additional constraints:

$$\lambda > \frac{1}{2} \quad , \quad \left(Q_0^2 = J_0^2\right)^*$$

Only for $F' = 0$

Solution V5:

1. Scaling solutions:

$$L_c = L_0 \quad , \quad \xi_c = \xi_0 \quad , \quad J^2 = J_0^2 \tau^{-2\lambda} \quad , \quad v = v_0 \tau^{-2\lambda}$$
$$L = L_0 \tau^{\lambda} \quad , \quad \xi = \xi_0 \tau^{\lambda} \quad , \quad Q^2 = Q_0^2$$

2. Additional constraints:

$$\lambda > \frac{1}{2} \quad , \quad F' = 0$$

Solution V6:

1. Scaling solutions:

$$L_c = L_0 \tau^{1-2\lambda} \quad , \quad \xi_c = \xi_0 \tau^{1-2\lambda} \quad , \quad J^2 = J_0^2 \tau^{-2\lambda} \quad , \quad v = v_0 \tau^{-2\lambda}$$
$$L = L_0 \tau^{1-\lambda} \quad , \quad \xi = \xi_0 \tau^{1-\lambda} \quad , \quad Q^2 = Q_0^2 \tau^{-2\lambda}$$

2. Additional constraints:

$$\lambda = \frac{\tilde{c} v_0}{2\xi_0} \leq \frac{1}{2} \quad , \quad \left(Q_0^2 = J_0^2\right)^* \quad , \quad ,$$

Only for $F' = 0$

Solution V7:

1. Scaling solutions:

$$L_c = L_0 \tau^{1-2\lambda} \quad , \quad \xi_c = \xi_0 \tau^{1-2\lambda} \quad , \quad J^2 = J_0^2 \tau^{-2\lambda} \quad , \quad v = v_0 \tau^{-2\lambda}$$
$$L = L_0 \tau^{1-\lambda} \quad , \quad \xi = \xi_0 \tau^{1-\lambda} \quad , \quad Q^2 = Q_0^2$$

2. Additional constraints:

$$\lambda = \frac{\tilde{c} v_0}{2\xi_0} \leq \frac{1}{2} \quad , \quad F' = 0 \quad , \quad ,$$

Solution V8:

1. Scaling solutions:

$$L_c = L_0\tau^{1+\lambda} \quad , \quad \xi_c = \xi_0\tau \quad , \quad J^2 = J_0^2\tau^{-2\lambda} \quad , \quad v = v_0$$
$$L = L_0\tau^{1+2\lambda} \quad , \quad \xi = \xi_0 t \quad , \quad Q^2 = Q_0^2\tau^{-2\lambda}$$

2. Additional constraints:

$$\mathcal{K} = -1 \quad , \quad \tilde{c} = \frac{2\xi_0}{v_0} \quad , \quad ,$$

A.2.3 With charge losses

Finally, the most general case should now be analysed. Starting once again with the decaying velocity solutions, we find solutions with constant charge and constant length scales and $\beta < -1$, given by V9, for $\rho \neq 0$, or V10, for $\rho = 0$.

Solution V9:

1. Scaling solutions:

$$L_c = L_0 \quad , \quad \xi_c = \xi_0 \quad , \quad J^2 = J_0^2\tau^{1-2\lambda} \quad , \quad v = v_0\tau^{-2\lambda}$$
$$L = L_0\tau^{\lambda} \quad , \quad \xi = \xi_0\tau^{\lambda} \quad , \quad Q^2 = Q_0^2$$

2. Additional constraints:

$$\beta < -1 \quad , \quad \rho\tilde{c}\frac{v_0\xi_0}{J_0^2L_0^2}\frac{1-g}{2Q_0^2F''} = 1 \quad , \quad \rho \neq 0 \quad ,$$

Solution V10:

1. Scaling solutions:

$$L_c = L_0 \quad , \quad \xi_c = \xi_0 \quad , \quad J^2 = J_0^2\tau^{-2\lambda} \quad , \quad v = v_0\tau^{-2\lambda}$$
$$L = L_0\tau^{\lambda} \quad , \quad \xi = \xi_0\tau^{\lambda} \quad , \quad Q^2 = Q_0^2$$

2. Additional constraints:

$$\beta < -1 \quad , \quad \rho = 0 \quad , \quad ,$$

There are also solutions with decaying velocities, but also decaying charges, as given by V11 and V12, for $F' = 0$. If, however, we have $F' \neq 0$, we may have solutions V13, for $\rho = 0$, V14, for $\rho = 1$, or V15, for any other value of ρ.

Solution V11:

1. Scaling solutions:

$$L_c = L_0 \quad , \quad \xi_c = \xi_0 \quad , \quad J^2 = J_0^2 \tau^{1/2-\lambda} \quad , \quad v = v_0 \tau^{-2\lambda}$$
$$L = L_0 \tau^{\lambda} \quad , \quad \xi = \xi_0 \tau^{\lambda} \quad , \quad Q^2 = Q_0^2 \tau^{1/2-\lambda}$$

2. Additional constraints:

$$\beta < -1 \quad , \quad F' = 0 \quad , \quad ,$$
$$2\lambda - \rho\tilde{c}\frac{v_0\xi_0}{J_0^2 L_0^2}\frac{1-g}{2Q_0^2 F''} = 2\lambda\frac{J_0^2}{Q_0^2} + (1-\rho)\tilde{c}\frac{v_0\xi_0}{Q_0^2 L_0^2}\frac{1-g}{2Q_0^2 F''}$$
$$\lambda = \rho\tilde{c}\frac{v_0\xi_0}{J_0^2 L_0^2}\frac{1-g}{2Q_0^2 F''} - \frac{1}{2}$$

Solution V12:

1. Scaling solutions:

$$L_c = L_0 \quad , \quad \xi_c = \xi_0 \quad , \quad J^2 = J_0^2 \tau^{-2\lambda} \quad , \quad v = v_0 \tau^{-2\lambda}$$
$$L = L_0 \tau^{\lambda} \quad , \quad \xi = \xi_0 \tau^{\lambda} \quad , \quad Q^2 = Q_0^2 \tau^{1/2-\lambda}$$

2. Additional constraints:

$$\beta < -1 \quad , \quad F' = 0 \quad , \quad \rho = 0 \quad ,$$
$$\lambda = \frac{1}{2} + (1-\rho)\tilde{c}\frac{v_0\xi_0}{Q_0^2 L_0^2}\frac{1-g}{2Q_0^2 F''} < \frac{1}{2}$$

Solution V13:

1. Scaling solutions:

$$L_c = L_0 \quad , \quad \xi_c = \xi_0 \quad , \quad J^2 = J_0^2 \tau^{-2\lambda} \quad , \quad v = v_0 \tau^{-2\lambda}$$
$$L = L_0 \tau^{\lambda} \quad , \quad \xi = \xi_0 \tau^{\lambda} \quad , \quad Q^2 = Q_0^2 \tau^{1-2\lambda}$$

2. Additional constraints:

$$\beta < -1 \quad , \quad F' \neq 0 \quad , \quad \rho = 0 \quad ,$$
$$\tilde{c} \frac{v_0 \xi_0}{Q_0^2 L_0^2} \frac{1-g}{F'} = -1$$

Solution V14:

1. Scaling solutions:

$$L_c = L_0 \quad , \quad \xi_c = \xi_0 \quad , \quad J^2 = J_0^2 \tau^{1-2\lambda} \quad , \quad v = v_0 \tau^{-2\lambda}$$
$$L = L_0 \tau^{\lambda} \quad , \quad \xi = \xi_0 \tau^{\lambda} \quad , \quad Q^2 = Q_0^2 \tau^{-2\lambda}$$

2. Additional constraints:

$$\beta < -1 \quad , \quad F' \neq 0 \quad , \quad \rho = 1 \quad ,$$
$$\tilde{c} \frac{v_0 \xi_0}{J_0^2 L_0^2} \frac{1-g}{F'} = -1$$

Solution V15:

1. Scaling solutions:

$$L_c = L_0 \quad , \quad \xi_c = \xi_0 \quad , \quad J^2 = J_0^2 \tau^{1-2\lambda} \quad , \quad v = v_0 \tau^{-2\lambda}$$
$$L = L_0 \tau^{\lambda} \quad , \quad \xi = \xi_0 \tau^{\lambda} \quad , \quad Q^2 = Q_0^2 \tau^{1-2\lambda}$$

2. Additional constraints:

$$\beta < -1 \quad , \quad F' \neq 0 \quad , \quad ,$$
$$(1-\rho) \tilde{c} \frac{v_0 \xi_0}{Q_0^2 L_0^2} \frac{1-g}{F'} = -1 \quad , \quad \frac{1-\rho}{\rho} = \frac{J_0^2}{Q_0^2}$$

There is another branch with decaying velocities, but where it is always verified that $2(\alpha-\varepsilon)+\eta=0$. The different solutions come with different charge behaviour. Growing charge solutions, as given by V16 and V17, are only possible if $F''\neq 0$. On the other hand, solutions with constant charge are given by V18 and V19, where the current is also kept constant or decays. The decaying charge solutions within this sub-branch are only found by $\rho=1$ and are given by V20, where the current is now kept constant.

Solution V16:

1. Scaling solutions:

$$L_c=L_0\tau^{\alpha} \quad , \quad \xi_c=\xi_0\tau^{1+\beta} \quad , \quad J^2=J_0^2\tau^{\eta} \quad , \quad v=v_0\tau^{-2\lambda(1+\mathcal{K})}$$
$$L=L_0\tau^{\alpha+\lambda} \quad , \quad \xi=\xi_0\tau^{1-\lambda(1+2\mathcal{K})} \quad , \quad Q^2=Q_0^2\tau^{\eta}$$

2. Additional constraints:

$$\eta=-2\lambda-\rho\tilde{c}\frac{v_0\xi_0}{J_0^2L_0^2}\frac{1-g}{F'}>0 \quad , \quad F'\neq 0 \quad , \quad \frac{1-\rho}{\rho}=\frac{J_0^2}{Q_0^2}$$
$$\alpha=-\lambda\mathcal{K}+\frac{g\tilde{c}}{2}\frac{v_0}{\xi_0} \quad , \quad F''=0$$

Solution V17:

1. Scaling solutions:

$$L_c=L_0\tau^{\alpha} \quad , \quad \xi_c=\xi_0\tau^{1+\beta} \quad , \quad J^2=J_0^2\tau^{-2\lambda} \quad , \quad v=v_0\tau^{-2\lambda(1+\mathcal{K})}$$
$$L=L_0\tau^{\lambda} \quad , \quad \xi=\xi_0\tau^{1-\lambda(1+2\mathcal{K})} \quad , \quad Q^2=Q_0^2\tau^{\delta}$$

2. Additional constraints:

$$\delta=-2\lambda-\rho\tilde{c}\frac{v_0\xi_0}{J_0^2L_0^2}\frac{1-g}{F'}>0 \quad , \quad F'\neq 0 \quad , \quad \rho=0$$
$$\alpha=-\lambda\mathcal{K}+\frac{g\tilde{c}}{2}\frac{v_0}{\xi_0} \quad , \quad F''=0$$

Solution V18:

1. Scaling solutions:

$$L_c = L_0\tau^{\alpha} \quad , \quad \xi_c = \xi_0\tau^{1+\beta} \quad , \quad J^2 = J_0^2 \quad , \quad v = v_0\tau^{-2\lambda(1+\mathcal{K})}$$
$$L = L_0\tau^{\lambda} \quad , \quad \xi = \xi_0\tau^{1-\lambda(1+2\mathcal{K})} \quad , \quad Q^2 = Q_0^2$$

2. Additional constraints:

$$\lambda = -\frac{\rho\tilde{c}}{2}\frac{v_0\xi_0}{J_0^2L_0^2}\frac{1-g}{F' - 2Q_0^2F''} \quad , \quad F' \neq 0 \quad , \quad \alpha = -\lambda\mathcal{K} + \frac{g\tilde{c}}{2}\frac{v_0}{\xi_0}$$

$$4\lambda\left(Q_0^2 - J_0^2\right) = \tilde{c}\frac{v_0\xi_0}{Q_0^2L_0^2}(1-g)\left[1-\rho\left(1+\frac{Q_0^2}{J_0^2}\frac{F'+2Q_0^2F''}{F'-2Q_0^2F''}\right)\right]$$

Solution V19:

1. Scaling solutions:

$$L_c = L_0\tau^{\alpha} \quad , \quad \xi_c = \xi_0\tau^{1+\beta} \quad , \quad J^2 = J_0^2\tau^{-2\lambda} \quad , \quad v = v_0\tau^{-2\lambda(1+\mathcal{K})}$$
$$L = L_0\tau^{\lambda} \quad , \quad \xi = \xi_0\tau^{1-\lambda(1+2\mathcal{K})} \quad , \quad Q^2 = Q_0^2$$

2. Additional constraints:

$$\lambda = -\frac{\tilde{c}}{2}\frac{v_0\xi_0}{Q_0^2L_0^2}\frac{1-g}{F'} \quad , \quad F' \neq 0 \quad , \quad \alpha = -\lambda\mathcal{K} + \frac{g\tilde{c}}{2}\frac{v_0}{\xi_0} \quad , \quad \rho = 0$$

Solution V20:

1. Scaling solutions:

$$L_c = L_0\tau^{\alpha} \quad , \quad \xi_c = \xi_0\tau^{1+\beta} \quad , \quad J^2 = J_0^2 \quad , \quad v = v_0\tau^{-2\lambda(1+\mathcal{K})}$$
$$L = L_0\tau^{\lambda} \quad , \quad \xi = \xi_0\tau^{1-\lambda(1+2\mathcal{K})} \quad , \quad Q^2 = Q_0^2\tau^{\delta}$$

2. Additional constraints:

$$F' \neq 0 \quad , \quad \alpha = -\lambda\mathcal{K} + \frac{g\tilde{c}}{2}\frac{v_0}{\xi_0} \quad , \quad F' = 0$$
$$\rho = 1 \quad , \quad \lambda = -\frac{\tilde{c}}{2}\frac{v_0\xi_0}{J_0^2L_0^2}\frac{1-g}{F'} \quad , \quad \delta = -2\lambda\frac{F'+2J_0^2F''}{F'}$$

Finally, there is another sub-branch of constant velocity solutions, but where it is needed $\mathcal{K} = -1$, implying $F' \neq 0$. These cases are only possible if the correlation length scales linearly. Once more, we may have decaying charge solutions, as given by V21, in which case the characteristic length also scales linearly. For constant charges, we may once more have constant currents, as given by V22, or decaying ones, as given by V23. It is still possible to have growing charges, as long as $F'' = 0$, as given by solution V24 and V25. Only the last two are possible for a non expanding universe.

Solution V21:

1. Scaling solutions:

$$L_c = L_0\tau \quad , \quad \xi_c = \xi_0\tau \quad , \quad J^2 = J_0^2 \quad , \quad v = v_0$$
$$L = L_0 t \quad , \quad \xi = \xi_0 t \quad , \quad Q^2 = Q_0^2\tau^\delta$$

2. Additional constraints:

$$\mathcal{K} = -1 \quad , \quad \rho = 1 \quad , \quad \lambda = 1 - g$$
$$\delta = -2\lambda\frac{F' + 2J_0^2F''}{F'} \quad , \quad \lambda = -\frac{\tilde{c}}{2}\frac{v_0\xi_0}{J_0^2L_0^2}\frac{1-g}{F'}$$

Solution V22:

1. Scaling solutions:

$$L_c = L_0\tau \quad , \quad \xi_c = \xi_0\tau \quad , \quad J^2 = J_0^2 \quad , \quad v = v_0$$
$$L = L_0 t \quad , \quad \xi = \xi_0 t \quad , \quad Q^2 = Q_0^2$$

2. Additional constraints:

$$F' \neq 0 \quad , \quad \lambda = -\frac{\rho\tilde{c}}{2}\frac{v_0\xi_0}{J_0^2L_0^2}\frac{1-g}{F' - 2Q_0^2F''} \quad , \quad \lambda = 1 - g$$

$$2\lambda\left(\frac{2Q_0^2 - 2J_0^2}{F' + 2Q_0^2F''}\right) = (1-\rho)\tilde{c}\frac{v_0\xi_0}{Q_0^2L_0^2}\frac{1-g}{F' + 2Q_0^2F''} - \rho\tilde{c}\frac{v_0\xi_0}{J_0^2L_0^2}\frac{1-g}{F' - 2Q_0^2F''}$$

Solution V23:

1. Scaling solutions:

$$L_c = L_0\tau \quad , \quad \xi_c = \xi_0\tau \quad , \quad J^2 = J_0^2\tau^{-2\lambda} \quad , \quad v = v_0$$
$$L = L_0 t \quad , \quad \xi = \xi_0 t \quad , \quad Q^2 = Q_0^2$$

2. Additional constraints:

$$F' \neq 0 \quad , \quad \alpha = -\lambda\mathcal{K} + \frac{g\tilde{c}}{2}\frac{v_0}{\xi_0} \quad , \quad \lambda = 1-g \quad , \quad \rho = 0$$
$$\lambda = -\frac{\tilde{c}}{2}\frac{v_0\xi_0}{Q_0^2L_0^2}\frac{1-g}{F'}$$

Solution V24:

1. Scaling solutions:

$$L_c = L_0\tau^{\lambda+g} \quad , \quad \xi_c = \xi_0\tau \quad , \quad J^2 = J_0^2\tau^{\eta} \quad , \quad v = v_0$$
$$L = L_0\tau^{2\lambda+g} \quad , \quad \xi = \xi_0 t \quad , \quad Q^2 = Q_0^2\tau^{\eta}$$

2. Additional constraints:

$$\eta = -2\lambda - \rho\tilde{c}\frac{v_0\xi_0}{J_0^2L_0^2}\frac{1-g}{F'} > 0 \quad , \quad F' \neq 0 \quad , \quad \frac{1-\rho}{\rho} = \frac{J_0^2}{Q_0^2}$$
$$\eta = 2-2(\lambda+g) \quad , \quad F'' = 0 \quad , \quad \lambda < 1-g$$

Solution V25:

1. Scaling solutions:

$$L_c = L_0\tau^{\lambda+g} \quad , \quad \xi_c = \xi_0\tau \quad , \quad J^2 = J_0^2\tau^{-2\lambda} \quad , \quad v = v_0$$
$$L = L_0\tau^{2\lambda+g} \quad , \quad \xi = \xi_0 t \quad , \quad Q^2 = Q_0^2\tau^{\delta}$$

2. Additional constraints:

$$\delta = -2\lambda - \rho\tilde{c}\frac{v_0\xi_0}{J_0^2L_0^2}\frac{1-g}{F'} > 0 \quad , \quad F' \neq 0 \quad , \quad \rho = 0$$
$$\delta = 2-2(\lambda+g) \quad , \quad F'' = 0 \quad , \quad \lambda < 1-g$$

A.3 Ultra-relativistic solutions

Having studied the cases where the moment the momentum parameter is allowed to vanish, even for expanding universes, it is now time to analyse the cases where the network velocity is such that $v_0 = 1$. In these cases, it immediately follows that $\beta = C = 0$, hence simplifying significantly the equations to be solved:

$$\alpha = \lambda + \frac{g\tilde{c}}{2}\frac{1}{\xi_0}\tau^{1-\varepsilon} \tag{A.4a}$$

$$\gamma = 2\left(\frac{k_v}{\xi_0}\tau^{1-\varepsilon} - \lambda\right) - \rho\tilde{c}\frac{1}{\xi_0}\frac{\xi_0^2}{J_0^2 L_0^2}\frac{1-g}{F' - 2Q_0^2\tau^\delta F''}\tau^{1+\varepsilon-2\alpha-\gamma} \tag{A.4b}$$

$$\delta = 2\frac{F' + 2J_0^2\tau^\gamma F''}{F' + 2Q_0^2\tau^\delta F''}\left(\frac{k_v}{\xi_0}\tau^{1-\varepsilon} - \lambda\right) - \frac{\tilde{c}}{\xi_0}\frac{\xi_0^2}{Q_0^2 L_0^2}\frac{(1-\rho)(1-g)}{F' + 2Q_0^2\tau^\delta F''}\tau^{1+\varepsilon-2\alpha-\delta} \tag{A.4c}$$

$$\varepsilon = \lambda\left(1 + \mathcal{K}\tau^{2(\alpha-\varepsilon)+\eta}\right) - \frac{k_v}{\xi_0}\mathcal{K}\tau^{2(\alpha-\varepsilon)+\eta+1-\varepsilon} + \frac{\tilde{c}}{2}\frac{1}{\xi_0}\tau^{1-\varepsilon} \tag{A.4d}$$

where the velocity equation is not presented anymore as it is trivially respected. A particular distinct feature of these solutions is that one may find cases where $1 + \beta - \varepsilon = 1 - \varepsilon < 0$, since the velocity equation does not place any additional constraints anymore, but it is true that solutions with $\varepsilon < 1$ are excluded.

A.3.1 No losses

Once more, the analysis starts neglecting all loss mechanisms by setting $\tilde{c} = 0$. This hypothesis as the immediate consequence of fixing $\alpha = \lambda$, while the remaining equations reduce to:

$$\gamma = 2\left(\frac{k_v}{\xi_0}\tau^{1-\varepsilon} - \lambda\right) \tag{A.5a}$$

$$\delta = 2\frac{F' + 2J_0^2\tau^\gamma F''}{F' + 2Q_0^2\tau^\delta F''}\left(\frac{k_v}{\xi_0}\tau^{1-\varepsilon} - \lambda\right) \tag{A.5b}$$

$$\varepsilon = \lambda + \mathcal{K}\tau^{2(\alpha-\varepsilon)+\eta}\left(\lambda - \frac{k_v}{\xi_0}\tau^{1-\varepsilon}\right) \tag{A.5c}$$

Once more it is clear that solutions where $\varepsilon < 1$ are not possible. The cases where both characteristic and correlation length scale at the same rate, either by imposing $F' = 0$ or having decaying charge solutions, as in solution U1, while constant charge solutions are still possible within the $F' = 0$ sub-branch, as given by solution U2. Both these solutions are possible for expansion rates higher than the radiation epoch value, $\lambda > 1$.

Solution U1:

1. Scaling solutions:

$$L_c = L_0\tau^{\lambda} \quad , \quad \xi_c = \xi_0\tau^{\lambda} \quad , \quad J^2 = J_0^2\tau^{-2\lambda} \quad , \quad v = 1$$
$$L = L_0\tau^{2\lambda} \quad , \quad \xi = \xi_0\tau^{2\lambda} \quad , \quad Q^2 = Q_0^2\tau^{-2\lambda}$$

2. Additional constraints:

$$\lambda > 1 \quad , \quad \left(Q_0^2 = J_0^2\right)^* \quad ,$$

* Only for $F' = 0$.

Solution U2:

1. Scaling solutions:

$$L_c = L_0\tau^{\lambda} \quad , \quad \xi_c = \xi_0\tau^{\lambda} \quad , \quad J^2 = J_0^2\tau^{-2\lambda} \quad , \quad v = 1$$
$$L = L_0\tau^{2\lambda} \quad , \quad \xi = \xi_0\tau^{2\lambda} \quad , \quad Q^2 = Q_0^2$$

2. Additional constraints:

$$\lambda > 1 \quad , \quad F' = 0 \quad ,$$

It should be noted that the solutions above are only possible for expansion rates such that $\lambda > 1$. On the other hand, for $\lambda = 1$, solutions where the charge and current may exhibit any type of behaviour, depending on the relation between k_v and λ may still be found, as given by U3, or solutions where the current decays, but the charge is conserved, as given by U4. The solutions for $F' \neq 0$ are given by U5, but in this case charge and current must decay.

Solution U3:

1. Scaling solutions:

$$L_c = L_0\tau \quad , \quad \xi_c = \xi_0\tau \quad , \quad J^2 = J_0^2\tau^\eta \quad , \quad v = 1$$
$$L = L_0 t \quad , \quad \xi = \xi_0 t \quad , \quad Q^2 = Q_0^2\tau^\eta$$

2. Additional constraints:

$$\lambda = 1 \quad , \quad F' = 0 \quad , \quad \eta = 2\left(\frac{k_v}{\xi_0} - 1\right) \quad , \quad Q_0^2 = J_0^2$$

Solution U4:

1. Scaling solutions:

$$L_c = L_0\tau \quad , \quad \xi_c = \xi_0\tau \quad , \quad J^2 = J_0^2\tau^\eta \quad , \quad v = 1$$
$$L = L_0 t \quad , \quad \xi = \xi_0 t \quad , \quad Q^2 = Q_0^2$$

2. Additional constraints:

$$\lambda = 1 \quad , \quad F' = 0 \quad , \quad \eta = 2\left(\frac{k_v}{\xi_0} - 1\right) < 0$$

Solution U5:

1. Scaling solutions:

$$L_c = L_0\tau \quad , \quad \xi_c = \xi_0\tau \quad , \quad J^2 = J_0^2\tau^\eta \quad , \quad v = 1$$
$$L = L_0 t \quad , \quad \xi = \xi_0 t \quad , \quad Q^2 = Q_0^2\tau^\eta$$

2. Additional constraints:

$$\lambda = 1 \quad , \quad F' \neq 0 \quad , \quad \eta = 2\left(\frac{k_v}{\xi_0} - 1\right) \leq 0 \quad ,$$

Finally, and for low expansion rates such that $\lambda < 1$, only growing charge and current solutions are possible, as given by U6.

Solution U6:

1. Scaling solutions:

$$\boldsymbol{L_c = L_0\tau^{\lambda}} \quad , \quad \boldsymbol{\xi_c = \xi_0\tau} \quad , \quad \boldsymbol{J^2 = J_0^2\tau^{2(1-\lambda)}} \quad , \quad \boldsymbol{v = 1}$$
$$\boldsymbol{L = L_0\tau^{2\lambda}} \quad , \quad \boldsymbol{\xi = \xi_0 t} \quad , \quad \boldsymbol{Q^2 = Q_0^2\tau^{2(1-\lambda)}}$$

2. Additional constraints:

$$\boldsymbol{\lambda < \frac{k_v}{\xi_0} = 1} \quad , \quad \boldsymbol{F' \neq 0} \quad , \quad \boldsymbol{\mathcal{K} = -1} \quad , \quad \boldsymbol{\left(Q_0^2 = J_0^2\right)^*}$$

Only for $F'' \neq 0$

A.3.2 No charge losses

Having presented the solutions in the absence on any energy or loss mechanism, it is now time to turn to the cases where energy losses are explicitly considered, by setting $g = 1$. In this case, the system of equations reads:

$$\alpha = \lambda + \frac{\tilde{c}}{2}\frac{1}{\xi_0}\tau^{1-\varepsilon} \tag{A.6a}$$
$$\gamma = 2\left(\frac{v_0 k_v}{\xi_0}\tau^{1-\varepsilon} - \lambda\right) \tag{A.6b}$$
$$\delta = 2\frac{F' + 2J_0^2\tau^{\gamma}F''}{F' + 2Q_0^2\tau^{\delta}F''}\left(\frac{v_0 k_v}{\xi_0}\tau^{1-\varepsilon} - \lambda\right) \tag{A.6c}$$
$$\varepsilon = \lambda\left(1 + \mathcal{K}\tau^{2(\alpha-\varepsilon)+\eta}\right) - \frac{k_v}{\xi_0}\mathcal{K}\tau^{2(\alpha-\varepsilon)+\eta+1-\varepsilon} + \frac{\tilde{c}}{2}\frac{1}{\xi_0}\tau^{1-\varepsilon} \tag{A.6d}$$

from where it is clear that $\varepsilon < 1$ solutions are not possible once more. Additionally, solutions U1 and U2, that share the common feature $\varepsilon = \lambda > 1$, are still a possible solution here. The linearly scaling solutions, though, are now found for a lower expansion rate, as given by U7 and U8, that can be seen to extend solutions U3 and U4, respectively, and reduce to them for $\tilde{c} = 0$. On the other hand, the proper generalisation of solutions U5 and U6 is given by U9 and U10.

Solution U7:

1. Scaling solutions:

$$L_c = L_0\tau \quad , \quad \xi_c = \xi_0\tau \quad , \quad J^2 = J_0^2\tau^\eta \quad , \quad v = 1$$
$$L = L_0 t \quad , \quad \xi = \xi_0 t \quad , \quad Q^2 = Q_0^2\tau^\eta$$

2. Additional constraints:

$$\lambda = 1 - \frac{\tilde{c}}{2\xi_0} \quad , \quad F' = 0 \quad , \quad \eta = 2\left(\frac{k_v}{\xi_0} - \lambda\right) \quad , \quad Q_0^2 = J_0^2$$

Solution U8:

1. Scaling solutions:

$$L_c = L_0\tau \quad , \quad \xi_c = \xi_0\tau \quad , \quad J^2 = J_0^2\tau^\eta \quad , \quad v = 1$$
$$L = L_0 t \quad , \quad \xi = \xi_0 t \quad , \quad Q^2 = Q_0^2$$

2. Additional constraints:

$$\lambda = 1 - \frac{\tilde{c}}{2\xi_0} \quad , \quad F' = 0 \quad , \quad \eta = 2\left(\frac{k_v}{\xi_0} - \lambda\right) < 0$$

Solution U9:

1. Scaling solutions:

$$L_c = L_0\tau \quad , \quad \xi_c = \xi_0\tau \quad , \quad J^2 = J_0^2\tau^\eta \quad , \quad v = 1$$
$$L = L_0 t \quad , \quad \xi = \xi_0 t \quad , \quad Q^2 = Q_0^2\tau^\eta$$

2. Additional constraints:

$$\lambda = 1 - \frac{\tilde{c}}{2\xi_0} \quad , \quad F' \neq 0 \quad , \quad \eta = 2\left(\frac{k_v}{\xi_0} - \lambda\right) \leq 0 \quad ,$$

Solution U10:

1. Scaling solutions:

$$L_c = L_0\tau^{\alpha} \quad , \quad \xi_c = \xi_0\tau \quad , \quad J^2 = J_0^2\tau^{2(1-\alpha)} \quad , \quad v = 1$$
$$L = L_0\tau^{\alpha+\lambda} \quad , \quad \xi = \xi_0 t \quad , \quad Q^2 = Q_0^2\tau^{2(1-\alpha)}$$

2. Additional constraints:

$$\lambda < \frac{k_v}{\xi_0} = 1 - \frac{\tilde{c}}{2\xi_0} \quad , \quad F' \neq 0 \quad , \quad \mathcal{K} = -1 \quad , \quad \left(Q_0^2 = J_0^2\right)^*$$
$$\alpha = \lambda + \frac{\tilde{c}}{2\xi_0} \quad , \quad 1 = \frac{\tilde{c}}{2\xi_0} + \frac{k_v}{\xi_0}$$

Only for $F'' \neq 0$

A.3.3 With charge losses

Finally, it is important to identify the solutions with arbitrary energy and charge loss, by setting $g \neq 1$. Here, it is convenient to decouple once more between solutions where the correlation length is allowed to grow faster than the linear scaling and the ones where it scales linearly. For the first ones, we have solutions for both $F' = 0$ and $F' \neq 0$, while the latter ones are only compatible with $F' \neq 0$.

Starting by assuming $F' = 0$ and $\varepsilon > 1$, we find solutions where both charge and current decay and solutions where the current decays, but not the charge, as given by solutions U11 and U12. For the particular case where $\rho = 0$, solution U13 is possible, which is similar to U11, but with different additional constraints.

Solution U11:

1. Scaling solutions:

$$L_c = L_0\tau^{\lambda} \quad , \quad \xi_c = \xi_0\tau^{\lambda} \quad , \quad J^2 = J_0^2\tau^{\eta} \quad , \quad v = 1$$
$$L = L_0\tau^{2\lambda} \quad , \quad \xi = \xi_0\tau^{2\lambda} \quad , \quad Q^2 = Q_0^2\tau^{\eta}$$

2. Additional constraints:

$$\lambda > 1 \quad , \quad F' = 0 \quad , \quad \eta = -2\lambda + \frac{\rho\tilde{c}}{\xi_0}\frac{\xi_0^2}{J_0^2L_0^2}\frac{1-g}{2Q_0^2F''} < 0$$
$$\lambda > \frac{\rho\tilde{c}}{\xi_0}\frac{\xi_0^2}{J_0^2L_0^2}\frac{1-g}{4Q_0^2F''}$$

$$4\lambda\left(Q_0^2 - J_0^2\right)F''\frac{L_0^2}{\xi_0} = \frac{\tilde{c}}{Q_0^2}\left[1+\rho\left(\frac{Q_0^2-J_0^2}{J_0^2}\right)\right](1-g)$$

Solution U12:

1. Scaling solutions:

$$L_c = L_0\tau^{\lambda} \quad , \quad \xi_c = \xi_0\tau^{\lambda} \quad , \quad J^2 = J_0^2\tau^{\eta} \quad , \quad v = 1$$
$$L = L_0\tau^{2\lambda} \quad , \quad \xi = \xi_0\tau^{2\lambda} \quad , \quad Q^2 = Q_0^2$$

2. Additional constraints:

$$\lambda > 1 \quad , \quad F' = 0 \quad , \quad \eta = -2\lambda + \frac{\rho\tilde{c}}{\xi_0}\frac{\xi_0^2}{J_0^2L_0^2}\frac{1-g}{2Q_0^2F''} < 0$$
$$\lambda > \frac{\rho\tilde{c}}{\xi_0}\frac{\xi_0^2}{J_0^2L_0^2}\frac{1-g}{4Q_0^2F''}$$

Solution U13:

1. Scaling solutions:

$$L_c = L_0\tau^{\lambda} \quad , \quad \xi_c = \xi_0\tau^{\lambda} \quad , \quad J^2 = J_0^2\tau^{-2\lambda} \quad , \quad v = 1$$
$$L = L_0\tau^{2\lambda} \quad , \quad \xi = \xi_0\tau^{2\lambda} \quad , \quad Q^2 = Q_0^2\tau^{1/2-\lambda/2}$$

2. Additional constraints:

$$\lambda = 1 + \frac{\tilde{c}}{\xi_0}\frac{\xi_0^2}{Q_0^2L_0^2}\frac{1-g}{Q_0^2F''} > 1 \quad , \quad F' = 0 \quad , \quad \rho = 0$$

On the other hand, solutions where $F' \neq 0$ are also possible. For arbitrary ρ, we must have $\lambda > 1$ and both current and charge decaying as $1-\lambda$, as given by solutions U14. There is another possibility, however, that is only possible $\rho = 0$ and that is given by U15, where the current always decays as -2λ and the charge must decay as $1-\lambda$

Solution U14:

1. Scaling solutions:

$$L_c = L_0\tau^{\lambda} \quad , \quad \xi_c = \xi_0\tau^{\lambda} \quad , \quad J^2 = J_0^2\tau^{1-\lambda} \quad , \quad v = 1$$
$$L = L_0\tau^{2\lambda} \quad , \quad \xi = \xi_0\tau^{2\lambda} \quad , \quad Q^2 = Q_0^2\tau^{1-\lambda}$$

2. Additional constraints:

$$\lambda = -\frac{\rho\tilde{c}}{\xi_0}\frac{\xi_0^2}{J_0^2L_0^2}\frac{1-g}{F'} - 1 > 1 \quad , \quad F' \neq 0 \quad , \quad \frac{1-\rho}{\rho} = \frac{Q_0^2}{J_0^2}$$

Solution U15:

1. Scaling solutions:

$$L_c = L_0\tau^{\lambda} \quad , \quad \xi_c = \xi_0\tau^{\lambda} \quad , \quad J^2 = J_0^2\tau^{-2\lambda} \quad , \quad v = 1$$
$$L = L_0\tau^{2\lambda} \quad , \quad \xi = \xi_0\tau^{2\lambda} \quad , \quad Q^2 = Q_0^2\tau^{1-\lambda}$$

2. Additional constraints:

$$\lambda = -\frac{\tilde{c}}{\xi_0}\frac{\xi_0^2}{Q_0^2L_0^2}\frac{1-g}{F'} - 1 > 1 \quad , \quad F' \neq 0 \quad , \quad \rho = 0$$

Finally, one may also have solutions where causality could still be satisfied, implying that the correlation length scales as fast as possible, $\varepsilon = 1$. In these cases, it must be that $F' \neq 0$, which places additional constraints on the relation between α, ε and δ. In fact, for non growing charges and arbitrary values of ρ, it will always be that $\delta = \gamma = 0$, as given by U16. There are, however, some particular solutions, given by U17 and U18, for the limit values of $\rho = 0$ or $\rho = 1$, respectively, where only one of them decays, while the other is kept constant.

Solution U16:

1. Scaling solutions:

$$L_c = L_0\tau \quad , \quad \xi_c = \xi_0\tau \quad , \quad J^2 = J_0^2 \quad , \quad v = 1$$
$$L = L_0 t \quad , \quad \xi = \xi_0 t \quad , \quad Q^2 = Q_0^2$$

2. Additional constraints:

$$\lambda = \frac{k_v}{\xi_0} - (1-g)\frac{\tilde{c}}{2\xi_0\mathcal{K}} = 1 - \frac{g\tilde{c}}{2\xi_0} < 1$$
$$\left(\frac{k_v}{\xi_0} - \lambda\right)\left(Q_0^2 - J_0^2\right) = \frac{\tilde{c}}{\xi_0}\frac{\xi_0^2}{J_0^2 L_0^2}\frac{1-g}{4F''}\left(\rho\frac{F' + 2Q_0^2F''}{F' - 2Q_0^2F''} - (1-\rho)\frac{J_0^2}{Q_0^2}\right)$$

Solution U17:

1. Scaling solutions:

$$L_c = L_0\tau \quad , \quad \xi_c = \xi_0\tau \quad , \quad J^2 = J_0^2\tau^\gamma \quad , \quad v = 1$$
$$L = L_0 t \quad , \quad \xi = \xi_0 t \quad , \quad Q^2 = Q_0^2$$

2. Additional constraints:

$$\lambda = 1 - \frac{g\tilde{c}}{2\xi_0} < 1 \quad , \quad \gamma = 2\left(\frac{k_v}{\xi_0} - \lambda\right) \quad , \quad \rho = 0$$
$$\lambda = \frac{k_v}{\xi_0} - \frac{\tilde{c}}{\xi_0}\frac{\xi_0^2}{Q_0^2 L_0^2}\frac{1-g}{2F'} > \frac{k_v}{\xi_0}$$

Solution U18:

1. Scaling solutions:

$$L_c = L_0\tau \quad , \quad \xi_c = \xi_0\tau \quad , \quad J^2 = J_0^2 \quad , \quad v = 1$$
$$L = L_0 t \quad , \quad \xi = \xi_0 t \quad , \quad Q^2 = Q_0^2\tau^\delta$$

2. Additional constraints:

$$\lambda = 1 - \frac{g\tilde{c}}{2\xi_0} < 1 \quad , \quad \lambda = \frac{k_v}{\xi_0} - \frac{\tilde{c}}{\xi_0}\frac{\xi_0^2}{J_0^2 L_0^2}\frac{1-g}{2F'}$$
$$\delta = 2\frac{F' + 2J_0^2F''}{F'}\left(\frac{k_v}{\xi_0} - \lambda\right) < 0 \quad , \quad \rho = 1$$

Finally, we may have growing charge solutions, for low expansion rates, $\lambda < 1 - \frac{g\tilde{c}}{2\xi_0}$. However, here F'' plays an important role. If $F'' = 0$, we may have solutions U19 and U20, where charge and current exhibit similar behaviour, or where charge grows slower than the current, respectively. There are also two particular solutions, for an expansion rate that is given by $\lambda = k_v/\xi_0$, where U21 should replace U20, and for $\rho = 0$, given by U22. There are also solutions where F'' vanishes. These cases are only possible if $\delta = \gamma > 0$, as given by U23.

Solution U19:

1. Scaling solutions:

$$L_c = L_0\tau^{\alpha} \quad , \quad \xi_c = \xi_0\tau \quad , \quad J^2 = J_0^2\tau^{\eta} \quad , \quad v = 1$$
$$L = L_0\tau^{\alpha+\lambda} \quad , \quad \xi = \xi_0 t \quad , \quad Q^2 = Q_0^2\tau^{\eta}$$

2. Additional constraints:

$$\lambda < 1 - \frac{g\tilde{c}}{2\xi_0} < 1 \quad , \quad \eta = 2\left(\frac{k_v}{\xi_0} - \lambda\right) - \frac{\rho\tilde{c}}{\xi_0}\frac{\xi_0^2}{J_0^2 L_0^2}\frac{1-g}{F'}$$
$$\frac{1-\rho}{\rho} = \frac{Q_0^2}{J_0^2} \quad , \quad \alpha = \lambda + \frac{g\tilde{c}}{2\xi_0} = 1 - \frac{\eta}{2}$$

Solution U20:

1. Scaling solutions:

$$L_c = L_0\tau^{\alpha} \quad , \quad \xi_c = \xi_0\tau \quad , \quad J^2 = J_0^2\tau^{\gamma} \quad , \quad v = 1$$
$$L = L_0\tau^{\alpha+\lambda} \quad , \quad \xi = \xi_0 t \quad , \quad Q^2 = Q_0^2\tau^{\delta}$$

2. Additional constraints:

$$\lambda < 1 - \frac{g\tilde{c}}{2\xi_0} < 1 \quad , \quad \gamma = 2\left(\frac{k_v}{\xi_0} - \lambda\right) \quad ,$$
$$\alpha = \lambda + \frac{g\tilde{c}}{2\xi_0} = 1 - \frac{\eta}{2} \quad , \quad \lambda \neq \frac{k_v}{\xi_0}$$
$$\delta = 2\left(\frac{k_v}{\xi_0} - \lambda\right) - (1-\rho)\tilde{c}\frac{1}{\xi_0}\frac{\xi_0^2}{Q_0^2 L_0^2}\frac{1-g}{F'}$$

Solution U21:

1. Scaling solutions:

$$L_c = L_0\tau^{\alpha} \quad , \quad \xi_c = \xi_0\tau \quad , \quad J^2 = J_0^2 \quad , \quad v = 1$$
$$L = L_0\tau^{\alpha+\lambda} \quad , \quad \xi = \xi_0 t \quad , \quad Q^2 = Q_0^2\tau^{\delta}$$

2. Additional constraints:

$$\lambda = \frac{k_v}{\xi_0} = 1 - \frac{\tilde{c}}{2\xi_0} < 1 - \frac{g\tilde{c}}{2\xi_0} < 1 \quad , \quad g < 1$$
$$\delta = -(1-\rho)\tilde{c}\frac{1}{\xi_0}\frac{\xi_0^2}{Q_0^2 L_0^2}\frac{1-g}{F'} > 0 \quad , \quad \alpha = \lambda + \frac{g\tilde{c}}{2\xi_0} = 1 - \frac{\eta}{2}$$

Solution U22:

1. Scaling solutions:

$$L_c = L_0\tau^{\alpha} \quad , \quad \xi_c = \xi_0\tau \quad , \quad J^2 = J_0^2\tau^{\gamma} \quad , \quad v = 1$$
$$L = L_0\tau^{\alpha+\lambda} \quad , \quad \xi = \xi_0 t \quad , \quad Q^2 = Q_0^2\tau^{\delta}$$

2. Additional constraints:

$$\lambda < 1 - \frac{g\tilde{c}}{2\xi_0} < 1 \quad , \quad \eta = 2\left(\frac{k_v}{\xi_0} - \lambda\right)$$
$$\delta = 2\left(\frac{k_v}{\xi_0} - \lambda\right) + \frac{\tilde{c}}{\xi_0}\frac{\xi_0^2}{Q_0^2 L_0^2}\frac{1-g}{F'} \quad , \quad \alpha = \lambda + \frac{g\tilde{c}}{2\xi_0} = 1 - \frac{\eta}{2}$$

Solution U23:

1. Scaling solutions:

$$L_c = L_0\tau^{\alpha} \quad , \quad \xi_c = \xi_0\tau \quad , \quad J^2 = J_0^2\tau^{\eta} \quad , \quad v = 1$$
$$L = L_0\tau^{\alpha+\lambda} \quad , \quad \xi = \xi_0 t \quad , \quad Q^2 = Q_0^2\tau^{\eta}$$

2. Additional constraints:

$$\lambda < 1 - \frac{g\tilde{c}}{2\xi_0} < 1 \quad , \quad \eta = 2\left(\frac{k_v}{\xi_0} - \lambda\right) \quad , \quad \alpha = \lambda + \frac{g\tilde{c}}{2\xi_0} = 1 - \frac{\eta}{2}$$
$$\lambda < \frac{k_v}{\xi_0} \quad , \quad J_0^2 = Q_0^2$$

A.4 Ultra-relativistic solutions with vanishing momentum parameter

Having studied the cases where $v_0 = 1$ or $k_v = 0$, it is now time to analyse the cases where both conditions hold. In these cases, it will always be that $\beta = C = 0$ and the equations reduce to:

$$\alpha = \lambda + \frac{g\tilde{c}}{2}\frac{1}{\xi_0}\tau^{1-\varepsilon} \tag{A.7a}$$

$$\gamma = -2\lambda - \rho\tilde{c}\frac{1}{\xi_0}\frac{\xi_0^2}{J_0^2 L_0^2}\frac{1-g}{F' - 2Q_0^2\tau^\delta F''}\tau^{1+\varepsilon-2\alpha-\gamma} \tag{A.7b}$$

$$\delta = -2\lambda\frac{F' + 2J_0^2\tau^\gamma F''}{F' + 2Q_0^2\tau^\delta F''} - (1-\rho)\tilde{c}\frac{1}{\xi_0}\frac{\xi_0^2}{Q_0^2 L_0^2}\frac{1-g}{F' + 2Q_0^2\tau^\delta F''}\tau^{1+\varepsilon-2\alpha-\delta} \tag{A.7c}$$

$$\varepsilon = \lambda\left(1 + \mathcal{K}\tau^{2(\alpha-\varepsilon)+\eta}\right) + \frac{\tilde{c}}{2}\frac{1}{\xi_0}\tau^{1-\varepsilon} \tag{A.7d}$$

A.4.1 No losses

Starting once more by the no loss scenario ($\tilde{c} = 0$), it may easily be seen that the characteristic length will always scale with the expansion rate, while the current will decay twice as fast. The charge behaviour, however, may be identical to the current, or, in the particular case where $F' = 0$, may persist over time, as given by solutions UV1 and UV2. In any case, it will always be that $\varepsilon = \alpha = \lambda$

Solution UV1:

1. Scaling solutions:

$$\boldsymbol{L_c = L_0\tau^\lambda} \quad , \quad \boldsymbol{\xi_c = \xi_0\tau^\lambda} \quad , \quad \boldsymbol{J^2 = J_0^2\tau^{-2\lambda}} \quad , \quad \boldsymbol{v = 1}$$
$$\boldsymbol{L = L_0\tau^{2\lambda}} \quad , \quad \boldsymbol{\xi = \xi_0\tau^{2\lambda}} \quad , \quad \boldsymbol{Q^2 = Q_0^2\tau^{-2\lambda}}$$

2. Additional constraints:

$$\left(\boldsymbol{Q_0^2 = J_0^2}\right)^* \quad , \quad ,$$

Only for $F' = 0$

Solution UV2:

1. Scaling solutions:

$$L_c = L_0\tau^{\lambda} \quad , \quad \xi_c = \xi_0\tau^{\lambda} \quad , \quad J^2 = J_0^2\tau^{-2\lambda} \quad , \quad v = 1$$
$$L = L_0\tau^{2\lambda} \quad , \quad \xi = \xi_0\tau^{2\lambda} \quad , \quad Q^2 = Q_0^2$$

2. Additional constraints:

$$F' = 0 \quad , \quad ,$$

A.4.2 No charge losses

Proceeding now for the no charge losses by setting $g = 1$, the system of equations is given by:

$$\alpha = \lambda + \frac{\tilde{c}}{2}\frac{1}{\xi_0}\tau^{1-\varepsilon} \tag{A.8a}$$
$$\delta = -2\lambda\frac{F'}{F' + 2Q_0^2\tau^{\delta}F''} \tag{A.8b}$$
$$\varepsilon = \lambda\left(1 + \mathcal{K}\tau^{\eta}\right) + \frac{\tilde{c}}{2}\frac{1}{\xi_0}\tau^{1-\varepsilon} \tag{A.8c}$$

Since growing charge solutions are clearly excluded, it will always be that $\alpha = \varepsilon$, and the current will always decay as -2λ. If the correlation length scales faster than linearly, then solutions UV1 and UV2 are recovered. However, there are two additional solutions where both characteristic lengths scales linearly, as given by UV3 and UV4, once more depending on the charge behaviour. These solutions only happen for a specific expansion rate.

Solution UV3:

1. Scaling solutions:

$$L_c = L_0\tau \quad , \quad \xi_c = \xi_0\tau \quad , \quad J^2 = J_0^2\tau^{-2\lambda} \quad , \quad v = 1$$
$$L = L_0 t \quad , \quad \xi = \xi_0 t \quad , \quad Q^2 = Q_0^2\tau^{-2\lambda}$$

2. Additional constraints:

$$\lambda = 1 - \frac{\tilde{c}}{2\xi_0} \quad , \quad \left(Q_0^2 = J_0^2\right)^* \quad , \quad ,$$

Only for $F' = 0$

Solution UV4:

1. Scaling solutions:

$$L_c = L_0\tau \quad , \quad \xi_c = \xi_0\tau \quad , \quad J^2 = J_0^2\tau^{-2\lambda} \quad , \quad v = 1$$
$$L = L_0 t \quad , \quad \xi = \xi_0 t \quad , \quad Q^2 = Q_0^2$$

2. Additional constraints:

$$\lambda = 1 - \frac{\tilde{c}}{2\xi_0} \quad , \quad F' = 0 \quad , \quad ,$$

A.4.3 With losses

The last cases to be analysed are the general loss cases, where $g \neq 1$, with the full system of equations:

$$\alpha = \lambda + \frac{g\tilde{c}}{2}\frac{1}{\xi_0}\tau^{1-\varepsilon} \tag{A.9a}$$
$$\gamma = -2\lambda - \rho\tilde{c}\frac{1}{\xi_0}\frac{\xi_0^2}{J_0^2L_0^2}\frac{1-g}{F' - 2Q_0^2\tau^\delta F''}\tau^{1+\varepsilon-2\alpha-\gamma} \tag{A.9b}$$
$$\delta = -2\lambda\frac{F' + 2J_0^2\tau^\gamma F''}{F' + 2Q_0^2\tau^\delta F''} - (1-\rho)\tilde{c}\frac{1}{\xi_0}\frac{\xi_0^2}{Q_0^2L_0^2}\frac{1-g}{F' + 2Q_0^2\tau^\delta F''}\tau^{1+\varepsilon-2\alpha-\delta} \tag{A.9c}$$
$$\varepsilon = \lambda\left(1 + \mathcal{K}\tau^{2(\alpha-\varepsilon)+\eta}\right) + \frac{\tilde{c}}{2}\frac{1}{\xi_0}\tau^{1-\varepsilon} \tag{A.9d}$$

where one may once more decouple between $\varepsilon > 1$ and $\varepsilon = 1$ solutions. If the correlation length scales linearly, there is a branch of solutions with $F'' = 0$ where charge and current may exhibit the same behaviour, as given by UV5, or where charge or current dominate, given by UV6 and UV7, respectively, depending on the value of ρ.

Solution UV5:

1. Scaling solutions:

$$L_c = L_0\tau^{\alpha} \quad , \quad \xi_c = \xi_0\tau \quad , \quad J^2 = J_0^2\tau^{2(1-\alpha)} \quad , \quad v = 1$$
$$L = L_0\tau^{\alpha+\lambda} \quad , \quad \xi = \xi_0 t \quad , \quad Q^2 = Q_0^2\tau^{2(1-\alpha)}$$

2. Additional constraints:

$$\lambda = \frac{2\xi_0 - \tilde{c}}{2\xi_0\,(1+\mathcal{K})} \quad , \quad F' \neq 0$$
$$\alpha = \lambda + \frac{g\tilde{c}}{2\xi_0} = \frac{\tilde{c}}{2\xi_0}\left(\frac{2\xi_0/\tilde{c} - 1}{1+\mathcal{K}} + g\right) \quad , \quad F'' = 0$$
$$\gamma = -2\lambda - \rho\tilde{c}\frac{1}{\xi_0}\frac{\xi_0^2}{J_0^2 L_0^2}\frac{1-g}{F'} \quad , \quad \frac{1-\rho}{\rho} = \frac{Q_0^2}{J_0^2}$$

Solution UV6:

1. Scaling solutions:

$$L_c = L_0\tau^{\alpha} \quad , \quad \xi_c = \xi_0\tau \quad , \quad J^2 = J_0^2\tau^{-2\lambda} \quad , \quad v = 1$$
$$L = L_0\tau^{\alpha+\lambda} \quad , \quad \xi = \xi_0 t \quad , \quad Q^2 = Q_0^2\tau^{2(1-\alpha)}$$

2. Additional constraints:

$$\lambda = \frac{2\xi_0 - \tilde{c}}{2\xi_0\,(1+\mathcal{K})} \quad , \quad \rho = 0 \quad , \quad F' \neq 0$$
$$\alpha = \lambda + \frac{g\tilde{c}}{2\xi_0} = \frac{\tilde{c}}{2\xi_0}\left(\frac{2\xi_0/\tilde{c} - 1}{1+\mathcal{K}} + g\right) \quad , \quad F'' = 0$$
$$\delta = -2\lambda - \tilde{c}\frac{1}{\xi_0}\frac{\xi_0^2}{Q_0^2 L_0^2}\frac{1-g}{F'} > -2\lambda \quad , \quad \tilde{c}\frac{1-g}{F'} < 0$$

Solution UV7:

1. Scaling solutions:

$$L_c = L_0\tau^{\alpha} \quad , \quad \xi_c = \xi_0\tau \quad , \quad J^2 = J_0^2 \quad , \quad v = 1$$
$$L = L_0\tau^{\alpha+\lambda} \quad , \quad \xi = \xi_0 t \quad , \quad Q^2 = Q_0^2\tau^{-2\lambda}$$

2. Additional constraints:

$$\lambda = \frac{2\xi_0 - \tilde{c}}{2\xi_0\,(1+\mathcal{K})} = -\frac{\tilde{c}}{\xi_0}\frac{\xi_0^2}{J_0^2L_0^2}\frac{1-g}{2F'} \quad , \quad \rho = 1 \quad , \quad F' \neq 0$$
$$\alpha = \lambda + \frac{g\tilde{c}}{2\xi_0} = \frac{\tilde{c}}{2\xi_0}\left(\frac{2\xi_0/\tilde{c} - 1}{1+\mathcal{K}} + g\right) \quad , \quad F'' = 0$$

There is also another set of solutions, with $F'' \neq 0$ where charge cannot grow. If it is constant, then solutions UV8 or UV9 are possible, where the current length scales linearly but present distinct current behaviour. If the charge decays, then only solution UV10 is possible, where the current is constant.

Solution UV8:

1. Scaling solutions:

$$L_c = L_0\tau \quad , \quad \xi_c = \xi_0\tau \quad , \quad J^2 = J_0^2 \quad , \quad v = 1$$
$$L = L_0 t \quad , \quad \xi = \xi_0 t \quad , \quad Q^2 = Q_0^2$$

2. Additional constraints:

$$\lambda = \frac{2\xi_0 - \tilde{c}}{2\xi_0\,(1+\mathcal{K})} = 1 - \frac{g\tilde{c}}{2\xi_0} = -\frac{\rho\tilde{c}}{2\xi_0}\frac{\xi_0^2}{J_0^2L_0^2}\frac{1-g}{F' - 2Q_0^2F''} \quad , \quad F' \neq 0$$
$$4\lambda F''\left(Q_0^2 - J_0^2\right) = \tilde{c}\frac{1-g}{\xi_0}\frac{\xi_0^2}{Q_0^2L_0^2}\left[1 - \rho\frac{2F'}{F' - 2Q_0^2F''}\right] \quad , \quad F'' \neq 0$$

Solution UV9:

1. Scaling solutions:

$$L_c = L_0\tau \quad , \quad \xi_c = \xi_0\tau \quad , \quad J^2 = J_0^2\tau^{-2\lambda} \quad , \quad v = 1$$
$$L = L_0 t \quad , \quad \xi = \xi_0 t \quad , \quad Q^2 = Q_0^2$$

2. Additional constraints:

$$\lambda = \frac{2\xi_0 - \tilde{c}}{2\xi_0\,(1+\mathcal{K})} = 1 - \frac{g\tilde{c}}{2\xi_0} = -\frac{\tilde{c}}{2\xi_0}\frac{\xi_0^2}{Q_0^2 L_0^2}\frac{1-g}{F'} \quad , \quad F'' \neq 0$$
$$\rho = 0 \quad , \quad F' \neq 0$$

Solution UV10:

1. Scaling solutions:

$$L_c = L_0\tau \quad , \quad \xi_c = \xi_0\tau \quad , \quad J^2 = J_0^2 \quad , \quad v = 1$$
$$L = L_0 t \quad , \quad \xi = \xi_0 t \quad , \quad Q^2 = Q_0^2\tau^{\delta}$$

2. Additional constraints:

$$\lambda = \frac{2\xi_0 - \tilde{c}}{2\xi_0\,(1+\mathcal{K})} = 1 - \frac{g\tilde{c}}{2\xi_0} = -\frac{\tilde{c}}{2\xi_0}\frac{\xi_0^2}{J_0^2 L_0^2}\frac{1-g}{F'} \quad , \quad F'' \neq 0$$
$$\delta = -2\lambda\frac{F' + 2J_0^2 F''}{F'} \quad , \quad F' \neq 0 \quad , \quad \rho = 1$$

Finally, there is still a branch of solutions where the correlation length scales faster then allowed by causality, in which case it will always be that $\alpha = \lambda$, meaning the current length will scale with the expansion rate. If $F' = 0$, then so will the correlation length, and so in these cases $\lambda > 1$. Here, current and charge may behave similarly, as given by UV11, or solutions where the charge is preserved, but the current decays, as given by UV12. On the other hand, if $F' \neq 0$ the only possible solution is given by UV13, where both charge and current decay away.

Solution UV11:

1. Scaling solutions:

$$L_c = L_0\tau^{\lambda} \quad , \quad \xi_c = \xi_0\tau^{\lambda} \quad , \quad J^2 = J_0^2\tau^{\eta} \quad , \quad v = 1$$
$$L = L_0\tau^{2\lambda} \quad , \quad \xi = \xi_0\tau^{2\lambda} \quad , \quad Q^2 = Q_0^2\tau^{\eta}$$

2. Additional constraints:

$$\eta = \frac{1-\lambda}{2} = -2\lambda + \frac{\rho\tilde{c}}{\xi_0}\frac{\xi_0^2}{J_0^2L_0^2}\frac{1-g}{2Q_0^2F''} < 0 \quad , \quad F' = 0$$
$$\lambda = \frac{\rho\tilde{c}}{3\xi_0}\frac{\xi_0^2}{J_0^2L_0^2}\frac{1-g}{Q_0^2F''} - \frac{1}{3}$$
$$\lambda\left(Q_0^2 + J_0^2\right) = \frac{1-g}{4F''}\frac{\xi_0^2}{Q_0^2L_0^2}\frac{\tilde{c}}{\xi_0}\left(1 + \rho\frac{Q_0^2 - J_0^2}{J_0^2}\right)$$

Solution UV12:

1. Scaling solutions:

$$L_c = L_0\tau^{\lambda} \quad , \quad \xi_c = \xi_0\tau^{\lambda} \quad , \quad J^2 = J_0^2\tau^{\gamma} \quad , \quad v = 1$$
$$L = L_0\tau^{2\lambda} \quad , \quad \xi = \xi_0\tau^{2\lambda} \quad , \quad Q^2 = Q_0^2$$

2. Additional constraints:

$$\gamma = -2\lambda + \frac{\rho\tilde{c}}{\xi_0}\frac{\xi_0^2}{J_0^2L_0^2}\frac{1-g}{2Q_0^2F''} = 1 - \lambda < 0 \quad , \quad F' = 0$$
$$\lambda = \frac{\rho\tilde{c}}{\xi_0}\frac{\xi_0^2}{J_0^2L_0^2}\frac{1-g}{2Q_0^2F''} - 1$$

Solution UV13:

1. Scaling solutions:

$$L_c = L_0\tau^{\lambda} \quad , \quad \xi_c = \xi_0\tau^{\lambda} \quad , \quad J^2 = J_0^2\tau^{1-\lambda} \quad , \quad v = 1$$
$$L = L_0\tau^{2\lambda} \quad , \quad \xi = \xi_0\tau^{2\lambda} \quad , \quad Q^2 = Q_0^2\tau^{1-\lambda}$$

2. Additional constraints:

$$\lambda = -\rho\tilde{c}\frac{1}{\xi_0}\frac{\xi_0^2}{J_0^2L_0^2}\frac{1-g}{F'} - 1 \quad , \quad F' \neq 0 \quad , \quad \frac{Q_0^2}{J_0^2} = \frac{1-\rho}{\rho}$$

Appendix B

Numerical simulation details

Simulations from Figure 3.1

TABLE B.1: Network properties for the simulations in Figure 3.1.

	λ	F	F'	F''	k_v	$\tilde{c}$	g	ρ
S_1	1.5							
S_2	2	1	0	0.1	0.25	0	-	-
S_3	3							
S_4	3							

TABLE B.2: Time series properties for the simulations in Figure 3.1 (all the amplitude values have been multiplied by 100).

	L			ξ			Q			J			v		
	L_i	L_0	α	ξ_i	ξ_0	ε	Q_i	Q_0	γ	J_i	J_0	δ	v_i	v_0	β
S_1		5.1	1.00		10.2	1.00	20	15.5	1.00		15.5	1.00		81.6	0.00
S_2	10	4.4	1.00	20	8.8	1.00	20	10.6	0.00	10	0.6	0.00	50	70.7	0.00
S_3		3.6	1.00		7.2	1.00	20	10.0	-2.17		0.2	0.00		57.7	0.00
S_4		3.6	1.00		7.2	1.00	10	0.2	-2.17		0.2	-2.17		57.7	0.00

Simulations from Figure 3.2

TABLE B.3: Network properties for the simulations in Figure 3.2.

	λ	F	F'	F''	k_v	$\tilde{c}$	g	ρ
S_1	2/3							
S_2	2	1	-0.5	0	0.10	0.0	-	-
S_3	3							

TABLE B.4: Time series properties for the simulations in Figure 3.2 (all the amplitude values have been multiplied by 100).

	L			ξ			Q			J			v		
	L_i	L_0	α	ξ_i	ξ_0	ε	Q_i	Q_0	γ	J_i	J_0	δ	v_i	v_0	β
S_1		5.5	0.33		9.6	0.33		200	0.00		100	0.00		64.0	-0.67
S_2	5	2.8	1.00	8.7	3.5	1.00	200	6.7	0.00	100	3.3	0.00	57.7	69.5	0.00
S_3		2.4	1.00		2.9	1.00		2.4	-2.01		1.2	-2.01		57.7	0.00

Simulations from Figure 3.3

TABLE B.5: Network properties for the simulations in Figure 3.3.

	λ	F	F'	F''	k_v	$\tilde{c}$	g	ρ
S_1	1.5							
S_2	1.67	1	0	0.1	0.25	0.05	1	-
S_3	2							
S_4	2							

TABLE B.6: Time series properties for the simulations in Figure 3.3.

	L			ξ			Q			J			v		
	L_i	L_0	α	ξ_i	ξ_0	ε	Q_i	Q_0	γ	J_i	J_0	δ	v_i	v_0	β
S_1		5.6	1.00		11.2	0.97	20	2.8	0.33		2.2	0.33		74.5	0.00
S_2	10	5.3	1.00	20	10.6	0.97	20	11.7	0.00	10	1.7	0.00	50	70.7	0.00
S_3		4.8	1.00		9.7	0.97	20	10.0	-0.66		1.1	0.00		64.5	0.00
S_4		4.8	1.00		9.7	0.97	10	1.1	-0.66		1.1	-0.66		64.5	0.00

Simulations from Figure 3.5

TABLE B.7: Network properties for the simulations in Figure 3.5.

	λ	F	F'	F''	k_v	$\tilde{c}$	g	ρ
S_1	0.57							
S_2	2	1	-0.5	0	0.10	0.05	1	-
S_3	3							

TABLE B.8: Time series properties for the simulations in Figure 3.5.

	L			ξ			Q			J			v		
	L_i	L_0	α	ξ_i	ξ_0	ε	Q_i	Q_0	γ	J_i	J_0	δ	v_i	v_0	β
S_1		5.4	0.43		9.3	0.43		200	0.0		100	0.0		53.2	-0.57
S_2	5	3.5	1.00	8.7	4.3	1.00	200	34.1	-1.33	100	17.0	-1.33	50	57.7	0.00
S_3		2.9	1.00		3.5	1.00		17.6	-3.33		8.8	-3.33		47.1	0.00

Simulations from Figure 3.6

TABLE B.9: Network properties for the simulations in Figure 3.6.

	λ	F	F'	F''	k_v	$\tilde{c}$	g	ρ
S_1								0
S_2	0.66	1	-0.5	0.0	0.10	0.1	0.1	0.5
S_3								1

TABLE B.10: Time series properties for the simulations in Figure 3.6.

	L			ξ			Q			J			v		
	L_i	L_0	α	ξ_i	ξ_0	ε	Q_i	Q_0	γ	J_i	J_0	δ	v_i	v_0	β
S_1								99.0	0.00		208.8	-0.62			
S_2	20	9.05	0.34	20	9.05	0.34	50	50.0	0.00	50	208.8	0.00	7	31.2	-0.66
S_3								50.0	-0.62		99.0	0.00			

Simulations from Figure 3.7

TABLE B.11: Network properties for the simulations in Figure 3.7.

	λ	F	F'	F''	k_v	$\tilde{c}$	g	ρ
S_1								0
S_2	0.65	1	-0.5	0.0	0.10	0.5	0.9	0.5
S_3								1

TABLE B.12: Time series properties for the simulations in Figure 3.7.

	L			ξ			Q			J			v		
	L_i	L_0	α	ξ_i	ξ_0	ε	Q_i	Q_0	γ	J_i	J_0	δ	v_i	v_0	β
S_1								63.4	0.00		11.9	-0.63			
S_2	10	11.1	1.00	10	12.2	1.00	10	31.7	0.00	10	31.7	0.00	10	40.8	0.00
S_3								11.9	-0.63		63.4	0.00			

Simulations from Figure 3.8

TABLE B.13: Network properties for the simulations in Figure 3.8.

	λ	F	F'	F''	k_v	$\tilde{c}$	g	ρ
S_1	0.66	1	-0.5	0.0	0.10	0.1	0.1	0.5
S_2						0.3	0.9	

TABLE B.14: Time series properties for the simulations in Figure 3.8.

	L			ξ			Q			J			v		
	L_i	L_0	α	ξ_i	ξ_0	ε	Q_i	Q_0	γ	J_i	J_0	δ	v_i	v_0	β
S_1	20	9.1	0.34	20	9.1	0.34	50	50.0	0.00	50	50.0	0.00	7	31.2	-0.66
S_2		1.9	1.00		1.9	1.00		48.8			48.8			9.7	0.00

Bibliography

[1] L. Susskind and G. Hrabovsky, *Classical mechanics: the theoretical minimum*. Penguin UK, 2020. [Cited on page 1.]

[2] Planck Collaboration, "Planck 2015 results - xiii. cosmological parameters," *A&A*, vol. 594, p. A13, 2016. [Online]. Available: https://doi.org/10.1051/0004-6361/201525830 [Cited on page 4.]

[3] D. Clowe, A. Gonzalez, and M. Markevitch, "Weak-lensing mass reconstruction of the interacting cluster 1e 0657–558: Direct evidence for the existence of dark matter*," *The Astrophysical Journal*, vol. 604, no. 2, p. 596, apr 2004. [Online]. Available: https://dx.doi.org/10.1086/381970 [Cited on page 4.]

[4] M. Markevitch, A. H. Gonzalez, D. Clowe, A. Vikhlinin, W. Forman, C. Jones, S. Murray, and W. Tucker, "Direct constraints on the dark matter self-interaction cross section from the merging galaxy cluster 1e 0657–56," *The Astrophysical Journal*, vol. 606, no. 2, p. 819, may 2004. [Online]. Available: https://dx.doi.org/10.1086/383178 [Cited on page 4.]

[5] J. Goldstone, "Field theories with «superconductor» solutions," *Il Nuovo Cimento (1955-1965)*, vol. 19, pp. 154–164, 1961. [Cited on page 10.]

[6] P. W. Higgs, "Broken symmetries and the masses of gauge bosons," *Physical review letters*, vol. 13, no. 16, p. 508, 1964. [Cited on page 12.]

[7] E. Witten, "Superconducting Strings," *Nucl. Phys. B*, vol. 249, pp. 557–592, 1985. [Cited on page 12.]

[8] F. London, H. London, and F. A. Lindemann, "The electromagnetic equations of the supraconductor," *Proceedings of the Royal Society of London. Series A - Mathematical and Physical Sciences*, vol. 149, no. 866, pp. 71–88, 1935. [Online].

Available: https://royalsocietypublishing.org/doi/abs/10.1098/rspa.1935.0048 [Cited on page 14.]

[9] M. Tinkham, *Introduction to superconductivity*. Courier Corporation, 2004. [Cited on page 14.]

[10] S. Weinberg, "Gauge and global symmetries at high temperature," *Physical Review D*, vol. 9, no. 12, p. 3357, 1974. [Cited on page 14.]

[11] N. Turok and P. Bhattacharjee, "Stretching cosmic strings," *Phys. Rev. D*, vol. 29, pp. 1557–1562, Apr 1984. [Online]. Available: https://link.aps.org/doi/10.1103/PhysRevD.29.1557 [Cited on page 17.]

[12] E. J. Copeland and T. W. B. Kibble, "Cosmic strings and superstrings," *Proceedings of the Royal Society A: Mathematical, Physical and Engineering Sciences*, vol. 466, no. 2115, pp. 623–657, 2010. [Online]. Available: https://royalsocietypublishing.org/doi/abs/10.1098/rspa.2009.0591 [Cited on page 19.]

[13] C. Martins, *Defect Evolution in Cosmology and Condensed Matter: Quantitative Analysis with the Velocity-Dependent One-Scale Model*, 1st ed. Springer Cham, 2016. [Cited on page 20.]

[14] A. R. R. Almeida and C. J. A. P. Martins, "Scaling solutions of wiggly cosmic strings," *Phys. Rev. D*, vol. 104, p. 043524, Aug 2021. [Online]. Available: https://link.aps.org/doi/10.1103/PhysRevD.104.043524 [Cited on pages 21, 34, 79, 80, 81, and 82.]

[15] A. Almeida and C. J. A. P. Martins, "Scaling solutions of wiggly cosmic strings. ii. time-varying coarse-graining scale solutions," *Phys. Rev. D*, vol. 106, p. 083525, Oct 2022. [Online]. Available: https://link.aps.org/doi/10.1103/PhysRevD.106.083525 [Cited on pages 21 and 79.]

[16] J. R. C. C. C. Correia and C. J. A. P. Martins, "Extending and calibrating the velocity dependent one-scale model for cosmic strings with one thousand field theory simulations," *Phys. Rev. D*, vol. 100, p. 103517, Nov 2019. [Online]. Available: https://link.aps.org/doi/10.1103/PhysRevD.100.103517 [Cited on pages 21 and 52.]

[17] M. F. Oliveira, A. Avgoustidis, and C. J. A. P. Martins, "Cosmic string evolution with a conserved charge," *Physical Review D*, vol. 85, p. 083515, 2012. [Cited on pages 21, 31, 32, 34, 36, 79, 80, 81, 82, and 83.]

[18] C. J. A. P. Martins, P. Peter, I. Y. Rybak, and E. P. S. Shellard, "Generalized velocity-dependent one-scale model for current-carrying strings," *Physical Review D*, vol. 103, p. 043538, 2021. [Cited on page 21.]

[19] I. Y. Rybak, A. Avgoustidis, and C. J. A. P. Martins, "Semianalytic calculation of cosmic microwave background anisotropies from wiggly and superconducting cosmic strings," *Phys. Rev. D*, vol. 96, p. 103535, Nov 2017. [Online]. Available: https://link.aps.org/doi/10.1103/PhysRevD.96.103535 [Cited on page 22.]

[20] I. Y. Rybak, C. J. A. P. Martins, P. Peter, and E. P. S. Shellard, "Cosmological evolution of witten superconducting string networks," 2023. [Cited on pages 23 and 81.]

[21] J. R. C. C. C. Correia and C. J. A. P. Martins, "Multitension strings in high-resolution $\mathrm{U}(1) \times \mathrm{U}(1)$ simulations," *Phys. Rev. D*, vol. 106, p. 043521, Aug 2022. [Online]. Available: https://link.aps.org/doi/10.1103/PhysRevD.106.043521 [Cited on pages 51 and 52.]

[22] J. R. C. Correia, *A New Generation of Cosmic Superstring Simulations*, ser. Springer Theses. Springer Nature, 2023. [Cited on page 51.]

[23] D. P. Bennett and F. m. c. R. Bouchet, "High-resolution simulations of cosmic-string evolution. i. network evolution," *Phys. Rev. D*, vol. 41, pp. 2408–2433, Apr 1990. [Online]. Available: https://link.aps.org/doi/10.1103/PhysRevD.41.2408 [Cited on page 51.]

[24] B. Allen and E. P. S. Shellard, "Cosmic-string evolution: A numerical simulation," *Phys. Rev. Lett.*, vol. 64, pp. 119–122, Jan 1990. [Online]. Available: https://link.aps.org/doi/10.1103/PhysRevLett.64.119

[25] C. J. A. P. Martins and E. P. S. Shellard, "Fractal properties and small-scale structure of cosmic string networks," *Phys. Rev. D*, vol. 73, p. 043515, Feb 2006. [Online]. Available: https://link.aps.org/doi/10.1103/PhysRevD.73.043515

[26] K. D. Olum and V. Vanchurin, "Cosmic string loops in the expanding universe," *Phys. Rev. D*, vol. 75, p. 063521, Mar 2007. [Online]. Available: https://link.aps.org/doi/10.1103/PhysRevD.75.063521

[27] J. J. Blanco-Pillado, K. D. Olum, and B. Shlaer, "Large parallel cosmic string simulations: New results on loop production," *Phys. Rev. D*, vol. 83, p. 083514, Apr 2011. [Online]. Available: https://link.aps.org/doi/10.1103/PhysRevD.83.083514 [Cited on page 51.]

[28] J. Correia and C. Martins, "Abelian–higgs cosmic string evolution with multiple gpus," *Astronomy and Computing*, vol. 34, p. 100438, 2021. [Online]. Available: https://www.sciencedirect.com/science/article/pii/S2213133720300925 [Cited on page 52.]

[29] N. Bevis, M. Hindmarsh, M. Kunz, and J. Urrestilla, "Cmb power spectrum contribution from cosmic strings using field-evolution simulations of the abelian higgs model," *Phys. Rev. D*, vol. 75, p. 065015, Mar 2007. [Online]. Available: https://link.aps.org/doi/10.1103/PhysRevD.75.065015 [Cited on page 52.]

[30] J. Correia and C. Martins, "Abelian-higgs cosmic string evolution with cuda," *Astronomy and Computing*, vol. 32, p. 100388, 2020. [Online]. Available: https://www.sciencedirect.com/science/article/pii/S2213133720300421 [Cited on page 53.]

[31] J. Urrestilla and A. Vilenkin, "Evolution of cosmic superstring networks: a numerical simulation," *Journal of High Energy Physics*, vol. 2008, no. 02, p. 037, feb 2008. [Online]. Available: https://dx.doi.org/10.1088/1126-6708/2008/02/037 [Cited on page 53.]

[32] F. Pimenta, J. Pacheco, S. Pereira, and F. Magalhães, "Reconstructing the bending moments time history of wind turbine tower from acceleration measurements using gaussian processes," *Journal of Physics: Conference Series*, vol. 2265, no. 3, p. 032080, may 2022. [Online]. Available: https://dx.doi.org/10.1088/1742-6596/2265/3/032080 [Cited on pages 62 and 83.]

[33] N. Metropolis, A. W. Rosenbluth, M. N. Rosenbluth, A. H. Teller, and E. Teller, "Equation of state calculations by fast computing machines," *The journal of chemical physics*, vol. 21, no. 6, pp. 1087–1092, 1953. [Cited on page 63.]

[34] W. K. Hastings, "Monte carlo sampling methods using markov chains and their applications," 1970. [Cited on page 63.]

[35] P. Gregory, *Bayesian logical data analysis for the physical sciences: a comparative approach with mathematica® support.* Cambridge University Press, 2005. [Cited on page 64.]

[36] A. Gelman, W. R. Gilks, and G. O. Roberts, "Weak convergence and optimal scaling of random walk metropolis algorithms," *The annals of applied probability*, vol. 7, no. 1, pp. 110–120, 1997. [Cited on page 64.]

[37] A. Gelman and D. B. Rubin, "Inference from iterative simulation using multiple sequences," *Statistical science*, vol. 7, no. 4, pp. 457–472, 1992. [Cited on page 64.]

[38] T. Brinckmann and J. Lesgourgues, "Montepython 3: boosted mcmc sampler and other features," *Physics of the Dark Universe*, vol. 24, p. 100260, 2019. [Cited on page 64.]

[39] C. J. A. P. Martins and E. P. S. Shellard, "Extending the velocity-dependent one-scale string evolution model," *Phys. Rev. D*, vol. 65, p. 043514, Jan 2002. [Online]. Available: https://link.aps.org/doi/10.1103/PhysRevD.65.043514 [Cited on page 75.]